

https://dspace.org/

Development of a VIGS vector based on SACMV for genomic studies in tobacco and cassava

Mwaba, Imanu Immaculee

2011-03-29
http://hdl.handle.net/10539/9265

Downloaded from a DSpace repository. https://dspace.org/

Development of a VIGS vector based on SACMV for genomic studies in tobacco and cassava

Imanu Immaculée Mwaba

A dissertation submitted to the Faculty of Science, University of the Witwatersrand, in fulfillment of the requirements for the degree of Master of Science in the School of Molecular and Cell Biology.

Johannesburg 2010

DECLARATION

I declare that this research report entitled "Development of a VIGS vector based on SACMV for genomic studies in tobacco and cassava" is my own, unaided work. It is being submitted for the degree of Master of Science at the University of the Witwatersrand, Johannesburg. It has not been submitted for any other degree or examination at any other University.

Imanu Mwaba

13th October 2010

ABSTRACT

Cassava is a major food crop in sub-Saharan Africa where it is mostly cultivated by small scale farmers. Cassava mosaic disease (CMD) is a major cause of pathogen-associated yield loss in Africa and it is caused by cassava mosaic geminiviruses (CMGs). The genomic structure of CMGs consists of two genomic molecules, DNA-A and DNA-B, enclosed in a twinned icosahedral capsid. *South African cassava mosaic virus* (SACMV) is a CMG endemic to South Africa. SACMV infection in a plant triggers post transcriptional gene silencing (PTGS), a resistance mechanism intended to target viral mRNA post transcriptionally and to prevent viral proteins translation. SACMV and CMGs, in general, encode silencing suppressors that allow them to escape PTGS from the host. Using the ability of viruses to induce PTGS against their own mRNA, the virus-induced gene silencing (VIGS) technology was developed. It involves using viruses as silencing vectors for functional genomics. In this study, SACMV-A partial dimer infectious clones were constructed to contain one copy of the coat protein (AV1) and was used to construct a SACMV-A VIGS vector and used to silence *NbNOA*1 in *N. benthamiana,* the model plant system for geminivirus infection studies. SACMV-A VIGS vector was constructed by replacing a portion of AV1 from SACMV-A infectious partial dimer with a multiple cloning site (MCS). A 403 bp of *N. tabacum su*-gene was introduced to silence the *su* gene in *N. benthamiana* and cassava. Silencing of *su*-gene in *N. benthamiana* and cassava resulted in bleaching of leaves, a phenotype observed in *su*-gene null mutations. SACMV-A VIGS vector was also used to silence *NbNOA*1 in *N. benthamiana*, a gene involved in disease resistance in *N. benthamiana* against the fungi *Colletotrichum lagenarium* and whose homolog in *Arabidopsis, AtNOA*1, is involved in disease resistance against *Pseudomonas aeruginosa*. Attempts to amplify *NbNOA*1 homolog from cassava were unsuccessful, using *AtNOA*1 specific primers, and as a result NOA1 silencing experiments were not carried out in cassava. Positive silencing of *NbNOA*1 was quantified using quantitative real-time PCR at 14, 21 and 28 dpi. SACMV viral load in silenced plants was quantified at 14, 21 and 28 dpi using absolute quantitative PCR and was found to be elevated in plants infected with the silencing SACMV-A VIGS vector bearing the *NbNOA*1 than in plants infected with an empty VIGS vector. These results suggest a possible role of *NbNOA*1 in SACMV disease resistance in *N. benthamiana*.

This work is dedicated to my parents Pierre and Elise, for their support, for having inspired me and without whom this would not be possible. To my husband, Patrick, thank you for your love, understanding, patience and encouragements. To my brothers, Chrys, Charly, Gloire and Pierre Junior.

ACKNOWLEDGEMENTS

I owe my deepest gratitude to my supervisor Prof Chrissie Rey, for valuable advice, guidance and for providing an environment where this research could be carried out.

I acknowledge financial support from the National Research Foundation and the University of the Witwatersrand post graduate Merit Award.

Special thanks go to the members of the Cassava Biotechnology Program at the University of the Witwatersrand for the encouragement and advice from the beginning to the completion of this project.

Finally and most importantly, I thank God for allowing me to see this project to completion.

TABLE OF CONTENTS

DECLARATION ..... **i**

ABSTRACT ..... **ii**

ACKNOWLEDGEMENTS ..... **iv**

TABLE OF CONTENTS ..... **v**

LIST OF TABLES ..... **ix**

LIST OF FIGURES ..... **x**

ABBREVIATIONS ..... **xii**

Chapter 1. LITTERATURE REVIEW **1**

1.1 CASSAVA 1

1.1.1 Statistics on cassava 3

1.1.2 Improvement of cassava 3

1.1.3 Diseases of cassava 3

1.2 CASSAVA MOSAIC DISEASE 4

1.3 GEMINIVIRUSES AND RNA SILENCING 9

1.3.1 Post-transcriptional gene silencing 9

1.3.1.1 siRNA pathway 10

1.3.1.2 miRNA pathway 12

1.3.2 RNA-mediated DNA Methylation 12

1.3.3 RNA silencing movement 13

1.4 GEMINIVIRUS-INDUCED GENE SILENCING 14

1.4.1 Mechanism of VIGS 16

1.4.2 VIGS vector design 16

1.4.3 VIGS for functional characterization of defense response genes 20

1.4.4 Hypersensitive response and nitric oxide 20

1.4.4.1 *In planta* nitric oxide production 23

1.4.4.2 AtNOA1/cGTPase and disease 24

1.5 AIMS AND OBJECTIVES 25

CHAPTER 2. DETECTION OF AtNOA1 HOMOLOGS IN CASSAVA.....27

2.1 INTRODUCTION 27

2.2 MATERIALS AND METHODS 29

2.2.1 PCR isolation of AtNOA1 and homologs 29

2.2.1.1 DNA extraction 29

2.2.1.2 RNA extraction 30

2.2.1.3 PCR amplification 31

2.2.2 Nucleotide sequence similarity searches 32

2.2.3 Southern Blot hybridization 33

2.2.3.1 Probe design 33

2.2.3.2 DNA extraction 33

2.2.3.3 Hybridization 34

2.2.3.4 Detection 34

2.3 RESULTS 36

2.3.1 Amplification of AtNOA1 CDS and genomic sequences 36

2.3.2 Southern Analysis 37

2.3.3 BLAST searches and protein alignments 39

2.4 DISCUSSION 43

CHAPTER 3. CONSTRUCTION OF SACMV-VIGS VECTOR.....46

3.1 INTRODUCTION 46

3.2 MATERIALS AND METHODS 49

3.2.1 Isolation of SACMV-DNA A 49

3.2.2 Construction of SACMV-A partial dimer 49

3.2.2.1 Preparation of DH5α competent cells 49

3.2.2.2 Construction of SACMV-A partial dimer infectious clone 50

3.2.3 Construction of SACMV-A VIGS vector 53

3.2.4 Cloning of the Su gene 54
3.2.5 Infection of N. benthamiana and Cassava 56
3.2.5.1 Preparation of *Agrobacterium tumefaciens* competent cells 56
3.2.5.2 Transformation into *A. tumefaciens* 57
3.2.5.3 Infiltration of *N. benthamiana* 57
3.3 RESULTS 60
3.3.1 Isolation of SACMV-A and B 60
3.3.2 Construction of SACMV-A partial dimer 61
3.3.3 Construction of SACMV-AΔCP (SACMV-A VIGS) 65
3.3.4 Insertion of Su-fragment 68
3.3.5 Silencing of su-gene in N. benthamiana and cassava 70
3.4 DISCUSSION 74

CHAPTER 4. FUNCTIONAL CHARACTERISATION OF NbNOA1 USING VIGS 80

4.1 INTRODUCTION 80
4.2 MATERIALS AND METHODS 82
4.2.1 Cloning of NbNOA1 fragment into SACMV-AΔCP 82
4.2.2 Silencing of NbNOA1 in N. benthamiana 83
4.2.3 Quantitative Real-time PCR amplification 84
4.2.3.1 RNA and DNA extraction from silenced plants 84
4.2.3.2 Construction of plasmid standard 85
4.2.3.3 Quantification of gene expression 87
4.2.4 Quantification of viral load using Real-time PCR 88
4.2.5 Statistical analysis 90
4.3 RESULTS 91
4.3.1 Cloning of NbNOA1 91
4.3.2 Silencing of NbNOA1 93
4.3.3 Virus quantification 98
4.3.4 Symptom evaluation 100

4.4 DISCUSSION 103

CHAPTER 5. CONCLUSIONS 110

CHAPTER 6. REFERENCES 114

LIST OF TABLES

Table 1-1: Virus disease of cassava 4

Table 1-2: Geminiviruses used as VIGS vector 19

Table 2-1: Sequences producing significant alignments between AtNOA1 vs cassava ESTS (Genbank) 40

Table 3-1: Primers used to replace AV1 (CP) from SACMV-A with the *su* gene in *N. benthamiana* 66

Table 4-1: *siRNA scan* results showing predicted siRNA found on the 308 bp sequence of NbNOA1. 91

Table 4-2: Rating of leaf symptoms 101

LIST OF FIGURES

Figure 1-1: A. Cassava Tree; B. Cassava roots. Chalk-white flesh surrounded by brown coarse skin; C. Cassava leaf 1

Figure 1-2: cassava leaf infected with SACMV AJ575560.1 5

Figure 1-3: DNA-A and DNA-B molecules of begomoviruses SACMV. 7

Figure 1-4: Geminivirus-induced RNA silencing 15

Figure 2-1: Amplification of AtNOA1 genomic sequence from *Arabidopsis* 36

Figure 2-2: Amplification of *AtNOA*1 and *NbNOA*1 CDS 37

Figure 2-3: PCR amplification of the DIG probe. 38

Figure 2-4: Southern blot hybridization using AtNOA1-specific probe 39

Figure 2-5: Sequences of DB926445 (A) and DB944551 (C) including translated sequence (B and D) 41

Figure 2-6: Sequence alignment of AtNOA1, NbNOA1 and translated putative NOA1 in cassava 42

Figure 3-1: Map showing cassava production and the location of occurrence of cassava mosaic virus in Africa 47

Figure 3-2: Restriction digestion of SACMV-A and SACMV-B 60

Figure 3-3: Diagrammatic representation of constructs designed in steps leading to SACMV-A vector 62

Figure 3-4: Screening of pTZA 63

Figure 3-5: Maps of the different plasmids used for VIGS vector design 64

Figure 3-6: Screening of SACMV-A partial dimer 65

Figure 3-7: Amplification of fragments SAA/F-SAA/R using assembly PCR 66

Figure 3-8: Screening of pTZAΔCP and SACMV-AΔCP 67

Figure 3-**9**: Amplification of SAA/F-SAA/R fragment of SACMV-A::su 69

Figure 3-10: Restriction digestion of the SAA/F-SAA/R fragment of SACMV-A::su with EcoRI and AflII..... 69

Figure 3-11: Diagrammatic representation of amplicons bearing the *su* gene insertion in different orientation. 70

Figure 3-12: Silencing of *su*-gene from *N. Benthamiana* 71

Figure 3-13: Silencing of su-gene from cassava T200 73

Figure 4-1: Amplification of a 308 bp fragment from *NbNOA*1 92

Figure 4-2: Plasmid map of SACMV-A::NbNOA1 93

Figure 4-3: Colony PCR to identify a positive SACMV-A::*NbNOA*1. 93

Figure 4-4: standard curve for serial dilutions of qRT-Nb1 plasmid standard 94

Figure 4-5: standard curve for serial dilutions of pTZEF1 plasmid standard..... 95

Figure 4-6: Relative expression of *NbNOA*1 in healthy untreated *N. benthamiana* and in SACMV-A::*NbNOA*1 96

Figure 4-7: Relative expression of *NbNOA*1 in healthy untreated *N. benthamiana* and in SACMV-A::*NbNOA*1. 97

Figure 4-8: Analysis of viral load of SACMV in *N. benthamiana* infected with SACMV-A and B, SACMV-AΔCP, SACMV-A::*NbNOA*1, dSACMV-AΔCP and dSACMV-A::*NbNOA*1..... 98

Figure 4-9: Symptoms development at 12 and 28 dpi. 102

ABBREVIATIONS

ACMV	*African cassava mosaic virus*
AGO	ARGONAUTE
Avr	Avirulence gene product
BCTV	*Beet curly top virus*
Bp	Base pair
CabLCuV	*Cabbage leaf curl virus*
CDK	Cyclin dependent kinase
ChlH	Chelatase H subunit
CHS	Chalcone synthase
CMD	Cassava mosaic disease
CMG	Cassava mosaic geminivirus
CP	Coat protein
Cq	Quantification cycle
CR	Common region
CTAB	Cetyl trimethylammonium bromide
dbEST	EST database
DCL	DICER LIKE
DEPC	diethyl pyrocarbonate
DI	Defecctive interfering
DMS	DEFECTIVE IN MERISTEM SILENCING
DMSO	dimethyl sulfoxide
dNTPs	Deoxynucleotide Triphosphate.
DRD	DEFECTIVE IN RNA DIRECTED DNA METHYLATION
DRM	DOMAINS REARRANGED METHYLTRANSFERASE
dsDNA	Double stranded DNA
dsRBD	Double stranded RNA binding domain
DUF	DOMAIN OF UNKNOWN FUNCTION

EACMCV	*East African cassava mosaic Cameroon virus*
EACMKV	*East African cassava mosaic Kenya virus*
EACMMV	*East African cassava mosaic Malawi virus*
EACMV	*East African cassava mosaic virus*
EACMZV	*East African cassava mosaic Zanzibar virus*
EDTA	Ethylenediaminetetraacetic acid
EF1-α	Elongation Factor 1 Alpha
EST	Expressed sequence tag
FAO	Food and agriculture organization of the United Nations
FAOSTAT	Food and Agriculture Organization Corporate Statistical Database
GFP	Green fluorescent protein
GTP/GDP	Guanosine triphosphate/Guanosine diphosphate
GTPase	GTP hydrolase
HEN	HUA ENHANCER
HR	Hypersensitive response
HYL	HYPONASTIC LEAVES
ICMV	*Indian cassava mosaic virus*
IPTG	isopropyl-β-D-thiogalactopyranoside
LB	Luria Bertani
MAPK	Mitogen-activated kinase
Mb	Megabases
MCS	Multiple cloning site
MID	MIDDLE domain
miRNA	Micro RNA
MP	Movement protein
MW	Molecular weight marker
NADPH	nicotinamide adenine dinucleotide phosphate
natsiRNA	Natural cis-antisense siRNA
NO	Nitric oxide

NOA1	Nitric oxide associated 1
NRPD	NUCLEAR RNA POLYMERASE D
NSP	Nuclear shuttle protein
NW	New world
ORF	Open reading frame
OW	Old world
PAMP	pathogens associated molecules pattern
PAZ	PIWI ARGONAUTE ZWILLE domain
PCD	Programmed cell death
PCNA	Proliferating cell nuclear antigen
PCR	Polymerase chain reaction
PDR	Pathogen derived resistance
PIWI	*P* ELEMENT-INDUCED WIMPY TEST domain
POL	RNA polymerase
PR1	Pathogenesis related 1
pRBR	Retinoblastoma-related protein
PTGS	Post transcriptional gene silencing
PVPP	Polyvinylpolypyrrolidone
PVX	*Potato virus X*
R	Resistance gene product
rbcS	ribulose bisphosphate carboxylase small subunit
RCA	Rolling circle amplification
RdRP/RDR	RNA directed RNA polymerase
REn	Replication enhancer protein
Rep	Replication associated protein
RISC	RNA-induced silencing complex
RNAi	RNA interference
RNase	Ribonuclease
ROS	Reactive oxygen species

RT-PCR	Reverse transcriptase PCR
SACMV	South African cassava mosaic virus
SAR	Systemic acquired resistance
SCR	Satellite conserved region
SDS	Sodium dodecyl sulfate
SE	SERRATE
SGS	SUPPRESSOR OF GENE SILENCING
siRNA	Small interfering RNA
SLCMV	*Sri Lankan cassava mosaic virus*
ssDNA	Single stranded DNA
tasiRNA	*Trans*-acting siRNA
TGMV	*Tomato golden mosaic virus*
TGS	Transcriptional gene silencing
TMV	*Tobacco mosaic virus*
TNA	Total nucleic acid
ToLCJV-A	Tomato leaf curl Java virus-A
ToLCNDV	Tomato leaf curl New Delhi virus
ToLCV	Tomato leaf curl
TrAP	Transcription activator protein
Tris	Tris-hydroxymethyl aminomethane
TRV	*Tobacco rattle virus*
TYLCCNV	Tomato yellow leaf curl china virus
UV	Ultraviolet
VIGS	Virus induced gene silencing
X-gal	5-bromo-4-chloro-3-indolyl-beta-D-galacto-pyranoside

Chapter 1. LITTERATURE REVIEW

1.1 CASSAVA

Cassava (*Manihot esculenta Crantz*), *manioc* (French), *mandioca* (Portuguese) or *yuca* (Latin America Spanish) is a woody shrub (Figure 1-1A) belonging to the family of *Euphorbiaceae* with edible roots and green leaves (Figure 1-1B, C). Cassava originated from South America and was introduced by European settlers in West Africa in the 16th century and later in 18th century to South-Eastern Asia (Fauquet and Fargette 1990) and its production has since then spread inland in both continents. Cassava easily grows in areas of low rainfall and poor soil fertility, hence requiring minimal financial input for cultivation, resulting in cassava being a cheap crop to grow and an affordable staple food to resource-poor populations.

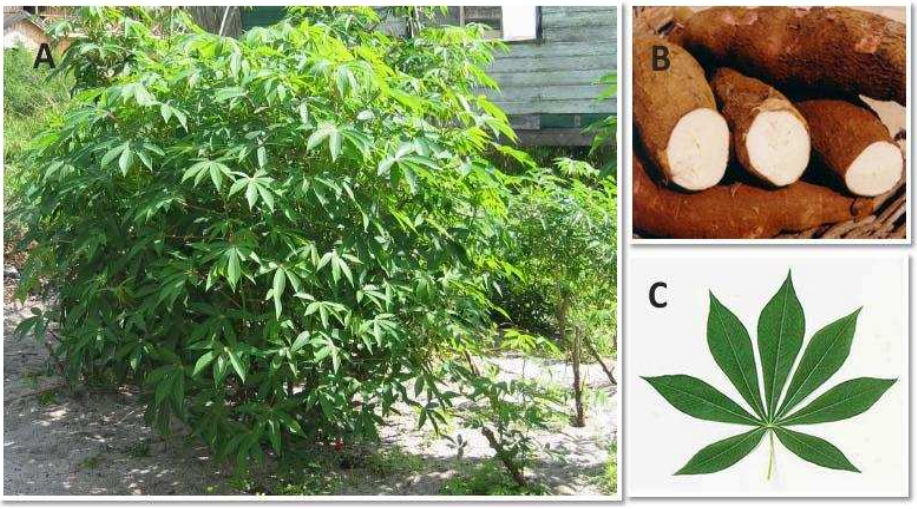

Figure 1-1: A. Cassava Tree; B. Cassava roots. Chalk-white flesh surrounded by brown coarse skin; C. Cassava leaf

Cassava's tuberous roots and leaves are mainly made up of water: dry weight content varies from 28-30% in roots (Okigbo 1980) and 10-20% in leaves, depending on the cultivar and maturity (Ravindran and Ravindran 1988). Cassava roots are constituted of 18-20% carbohydrate, 0.5% protein and less than 0.01% fats (Okigbo 1980). Cassava leaves contain less carbohydrate (5-

7.8%) but are however richer in protein, on average 4%, and in lipids, varying from 0.5 to 1.5% (Ravindran and Ravindran 1988).

In Sub-Saharan Africa, cassava is cultivated by small farmers mainly for the consumption of its leaves, roots and derived products such as *fufu,* chips and bread. Unlike the rest of sub-Saharan African countries, cassava is not a well-known crop in South Africa. It is cultivated in Limpopo, Mpumalanga and KwaZulu-Natal. The yield per hectare obtained in South Africa surpasses that of any other African country, setting an example for modernization methods of cassava cultivation (Tewe 2004). Globally, cassava is gaining importance as animal feed and in different industries where it can be used as a cheaper alternative to starch substrates. Up to the year 2006, only 10% of the world starch production came from cassava (Food and Agriculture Organization 2006). Many industries would benefit from cassava as it is not only relatively cheaper to produce but is more resilient to unfavorable climate conditions and pests, the high starch content of its roots makes cassava an ideal candidate for biofuel production. Cassava starch is already being used in the textile, paper and adhesive industry. Its high amylopectin content increases its strength and flexibility, which is a benefit for the paper, textile and dextrin-related industry (Nestel 1973; Food and Agriculture Organization 2006).

Despite the higher nutritional value of leaves compared to that of roots, consumption of cassava leaves does not equate that of its roots as cassava leaves contain 3-20 times more cyanogenic glycoside compared with roots depending on the cultivar (Siritunga and Sayre 2004; White et al. 1998). Harvesting of cassava roots and leaves causes an enzymatic production by linamarase of acetone cyanohydrins from linamarin. Acetone cyanohydrin can be broken down spontaneously at pH above 5 and temperature above 35°C or enzymatically by hydroxynitrile lyase to acetone and cyanide (Siritunga and Sayre 2004; White et al. 1998). Once ingested, cyanide binds to the mitochondria, inhibiting the use of oxygen in the blood, resulting in hypoxia (Luttrell 2009). Cyanide poisoning in humans causes glucose intolerance, Konzo or spastic paraparesis (Montagnac et al. 2009; Tylleskär et al. 1992) , tropical ataxic neuropathy (Osuntokun 1973), goiter (Ekpechi 1973) and cretinism (Montagnac et al. 2009). These conditions are exacerbated in malnourished individuals. To avoid cyanide poisoning during consumption, cassava leaves

and roots are processed post-harvest by either fermentation, desiccation, boiling or pounding, which results in the release of the volatile produced cyanide (Siritunga and Sayre 2004).

1.1.1 Statistics on cassava

Cassava is recognized to be the third most important food crop in tropical regions after maize and rice. In Africa, according to FAOSTAT (http://faostat.fao.org/), cassava was the number one produced commodity in 2007, while in South America and South-Eastern Asia, it ranked 5th and 3rd respectively. These values do not reflect the revenues made from cassava yield as it only ranked second in Africa, twentieth in South America and sixth in South-Eastern Asia. In 2007, Africa contributed to approximately 49%, South America 16.3%, and South-Eastern Asia 28% of the world cassava production.

1.1.2 Improvement of cassava

Traditional breeding methods have been used to improve different traits of cassava. Cassava has been crossed with its wild relative to increase its nutritional content and improve resistance against bacterial blight and cassava mosaic disease (Hahn et al. 1980; Hahn et al. 1980). More recently, cassava research has moved toward a transgenic-based approach, where the desired gene is transformed into the plant via *A. tumefaciens*-mediated transformation, where a single desired genetic trait is inserted into a cultivar (Taylor et al. 2004).

1.1.3 Diseases of cassava

Different pathogens have been reported to infect cassava. Cassava is vegetatively propagated through stem cuttings; this mode of propagation promotes the spread of infection. Some of the pathogens reported to infect cassava result in mild or no symptoms and others cause diseases of no economic importance. In Africa, different bacterial and fungal pathogens have been identified as the main causes in the rotting of stems and roots (Hillocks and Wydra 2002). A list of viruses that infect cassava is shown in Table 1-1. Of the viruses reported to infect cassava in Africa, cassava mosaic geminivirus are the most devastating and they result in loss of yield of up to 95% (Fauquet and Fargette 1990).

Table 1-1: Virus disease of cassava (Calvert and Thresh 2002)

Geographic region	Virus	Genus
Africa	Cassava Ivorian bacilliform virus[#]	*Alfamovirus*[1]
	Cassava mosaic geminivirus	*Begomovirus*
	Cassava brown streak virus	*Ipomovirus*
	Cassava Kumi viruses A and B[#]	unassigned
	Cassava "Q" virus[#]	unassigned
Africa **South/Central America** **Asia/Pacific**	Cassava common mosaic virus[#]	*Potexvirus*
Asia/Pacific	Cassava green mottle virus[#]	*Nepovirus*
South/Central America	Cassava vein mosaic virus	*Cavemovirus*
	Cassava America latent virus[#]	*Nepovirus*
	Cassava virus X[#]	*Potexvirus*
	Cassava Colombian symptomless virus[#]	*Potexvirus*
	Cassava frogskin "virus"	*Reoviridae*[2]

[1] this virus was tentatively classified under the specified genus (Fargette et al. 1991)
[2] the genus to which this virus belongs has not yet been specified, thus the virus family is given (Calvert et al. 2008)
[#] Viruses with localized distributions or not of economic significance.

1.2 CASSAVA MOSAIC DISEASE

Cassava mosaic disease (CMD) is the major cause of yield loss in Africa (Wydra and Verdier 2002), accounting for 20-95% of loss in cassava production in various CMD-affected areas around the world (Fauquet and Fargette 1990). Cassava mosaic disease is caused by infection with cassava mosaic geminiviruses (CMGs), belonging to the single-stranded DNA (ssDNA) *begomoviruses* genus, of the family *Geminiviridae*.

Geminiviruses are classified into 4 genera: *Begomovirus*, *Mastrevirus*, *Topocurvirus*, and *Curtovirus*; based on their genomic organization, host range and insect vector (Fauquet and Stanley 2003; Nawaz-ul-rehman and Fauquet 2009). Begomoviruses are mainly bipartite (with some monopartite) ambisense ssDNA viruses; encapsidated in two twinned (geminate) icosahedral capsids, and transmitted in a circulative persistent manner by the whitefly species,

Bemisia tabaci Gennadius to dicotyledonous plants. Phylogenetically, geminiviruses cluster based on their geographic origin and distribution and have been split in 2 groups: New World (NW) for viruses from the Americas and Old World (OW) for the rest of the world (Rybicki 1994).



Figure 1-2: Cassava leaf infected with SACMV AJ575560.1

Based on the number of species constituted in each genus of the geminiviruses family, *Begomovirus* is the largest (Fauquet et al. 2008; Florentino et al. 2008) and most diverse (Nawaz-ul-rehman and Fauquet 2009). Begomoviruses enclose in their icosahedral capsid 2 genomic molecules, DNA-A and DNA-B (Figure 1-3). However some monopartite OW begomoviruses have been reported (Nawaz-ul-rehman and Fauquet 2009). To date, 9 species and various variants of begomoviruses causing CMD have been reported (Fauquet et al. 2008). Geminivirus species are grouped according to pairwise sequence similarity in DNA-A. Sequences with a pairwise identity below 89% are grouped as species. Within a species, sequences with a pairwise identity of 85-94% correspond to a strain. Within a strain, sequences with pairwise identity of between 92-100% are considered variants (Fauquet et al. 2008).

Seven of the species identified occur in Africa, they are named according to where they were first reported geographically: *South African cassava mosaic virus* (SACMV; 3 variants), *East African cassava mosaic virus* (EACMV; 56 variants), *East African cassava mosaic Cameroon virus* (EACMCV; 6 variants), *East African cassava mosaic Kenya virus* (EACMKV; 14variants) *East African cassava mosaic Malawi virus* (EACMMV; 2 variants), *East African cassava mosaic Zanzibar virus* (EACMZV; 13 variants) and *African cassava mosaic virus* (ACMV; 12 variants).

The other 2 species were reported in India, *Indian cassava mosaic virus* (ICMV; 6 variants) and Sri Lanka, *Sri Lankan mosaic virus* (SLCMV; 11 variants). Symptoms of CMGs infection include chlorosis, mosaicism and leaf distortion (Figure 1-2). The severity of these symptoms depends on the virulence of any of the above mentioned strains.

The two genomic components of bipartite begomoviruses, DNA-A and DNA-B, have sizes ranging between 2.7-2.8 kb and share a common region (CR) of about 200 bp with a similar sequence (Bisaro 2006) that contains the origin or replication, a conserved TAATATT/AC sequence and other regulatory sequences (Lazarowitz et al. 1992). DNA-A generally encodes for 6 proteins, 2 on the virion (sense) strand and 4 on the complimentary (antisense) strand. AC1-4 are found on the complimentary strand and code for a replication associated protein (Rep/AC1), transcription activator protein (TrAP/AC2), replication enhancer protein (REn/AC3) and AC4, whose function has not yet been determined. AV1 and AV2 are found on the virion (sense) strand and encode a coat protein (CP) and a pre-CP, respectively. The DNA-B component of geminiviruses only encodes 2 genes, BV1 in the virion sense coding for a movement protein (MP) and BC1 in the complimentary sense coding for a nuclear shuttling protein (NSP).

Rep and REn are involved in viral replication with Rep being solely required for replication (Elmer et al. 1988) and REn assisting Rep by enhancing the rate of replication (Sunter et al. 1990) probably through stabilizing DNA-Rep and protein-Rep interactions (Fontes et al. 1994). TrAP is a transcription factor needed for expression of late viral genes, CP and BV1 (Rajeswaran et al. 2007), and for pathogenicity-required host genes (Trinks et al. 2005; Shivaprasad et al. 2005) TrAP contributes to establishing and maintaining infection by suppressing the hypersensitive response (HR) (Hussain et al. 2007) and post-transcriptional gene silencing (PTGS) (Bisaro 2006; Rajeswaran et al. 2007) , both of which are crucial to pathogen defense response in plants. The function of AC4 has not yet been defined. It is believed to be membrane bound and involved in symptom development and to have (similarly to TrAP) some PTGS silencing activity (Latham et al. 1997; Vanitharani et al. 2004; Fondong et al. 2007).

The CP is multi-functional. It is involved in virus-vector specificity (Roberts et al. 1984), viral encapsidation (BD Harrison 2002), targeting the virus into the nucleus and out to the cell

membrane (Unseld et al. 2001) and accumulation of ssDNA particles in the cytoplasm (Qin et al. 1998). In monopartite begomoviruses, CP serves a nuclear shuttling role (Gafni 2002); this function is carried out in bipartite begomoviruses by the DNA-B component. Pre-CP is only found in OW begomoviruses and little is known on its functions. It is thought to be involved in encapsidation (Sunter et al. 1990) and it possesses a putative kinase C motif that could be directly or indirectly involved in movement (Padidam et al. 1996) and suppression of post-transcriptional gene silencing (PTGS) (Chowda-Reddy et al. 2008). AV2 is not found in NW begomoviruses (Nawaz-ul-rehman and Fauquet 2009). The DNA-B encoded proteins NSP and MP are movement proteins. NSP is responsible for transporting newly formed ssDNA viral particles from the nucleus to the cytoplasm through nuclear pores. Through interactions with MP, the ssDNA is transported to neighboring cells through the plasmodesmata, by modifying its structure (Gafni 2002).

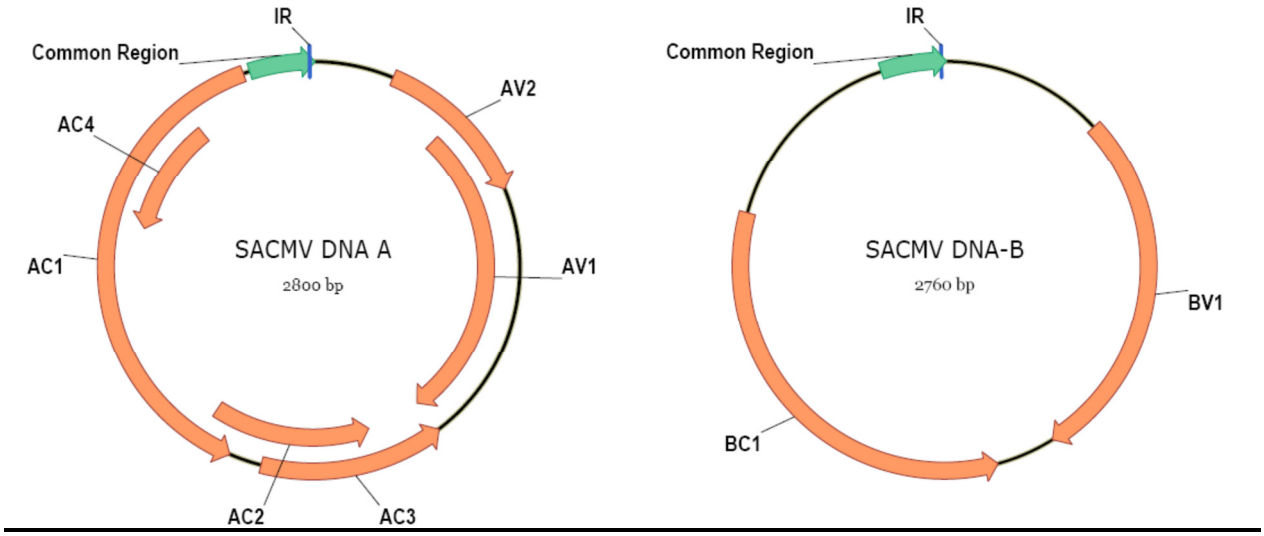

Figure 1-3: DNA-A and DNA-B molecules of begomoviruses SACMV.

In addition to the 2 genomic particles, begomoviruses are associated with 2 types of subgenomic particles, namely defective interfering (DI) molecules (Stanley and Townsend 1985) and satellites (Nawaz-ul-rehman and Fauquet 2009). DI molecules are derived from DNA-B and are approximately half the size of the molecule they are derived from. They have a truncated BV1 (deleted at the C-terminal) with no BC1 gene (Patil and Dasgupta 2006). DI molecules rely on a helper virus for replication and movement and they have been shown to delay and attenuate infection symptoms (Stanley and Townsend 1985; Frischmuth and Stanley 1991).

Satellites are only associated with OW monopartite begomoviruses (Nawaz-ul-rehman and Fauquet 2009). There are 2 types of satellites: alphasatellites also known as DNAα (Mansoor et al. 1999) and β-satellites or DNAβ (Saunders et al. 2000). The function of α-satellites is not yet known. Their genome organization consists of an adenine-rich region, and a Nanovirus-like replication associated protein and origin of replication, allowing the alphasatellites to depend on the helper virus only for movement and not replication (Nawaz-ul-rehman and Fauquet 2009). β-satellites are required by their helper virus for symptom development (Saunders et al. 2000). They share no sequence similarity with the helper virus except the conserved TAATATT/AC sequence. Their genome organization includes a satellite conserved region (SCR), an adenine rich region and a βC1 gene (Saunders et al. 2000; Mansoor et al. 1999). βC1 is a pathogenicity determinant as it is needed by helper virus for successful infection (Saunders et al. 2004) and has also been shown to be a silencer of PTGS (Gopal et al. 2007).

Because of its small genome size, geminiviruses do not encode all the genes required for replication and transcription. To alleviate this limitation, geminiviruses recruits the host machinery to its own advantage; sometimes reinitiating the cell life cycle in quiescent cells to re-enter the S-phase, thereby promoting viral DNA replication (Nagar et al. 1995). In quiescent cells, a progression out of the G_o phase into the G_1 phase is controlled by retinoblastoma related protein (pRBR). Interaction between pRBR and E2F, suppresses the transcription of genes required for the G_1 to S phase transition. Phosphorylation of pRBR by cyclin-dependent kinase (CDK) results in a release of pRBR from the pRBR-E2F complex, allowing the transition from the G_1 phase to the S phase.

Begomovirus Rep and REn proteins bind to the pRBR, disrupting it from the pRBR-E2F complex thus bypassing the need for CDK phosphorylation and allowing the cell to progress into the S phase, resulting in viral replication through a dsDNA intermediate (Hanley-Bowdoin et al. 2004). Proliferating cell nuclear antigen (PCNA) is one of the genes repressed by the pRBR-E2F complex. PCNA is one of the genes not expressed in quiescent cells, until an infection occurs (Hanley-Bowdoin et al. 2004). The conversion of viral ssDNA to a dsDNA intermediate is mediated by cellular factors, however the exact mechanism by which this occurs has not yet been clarified. The intermediate dsDNA interacts with histones, forming a supercoiled chromosome-

like structure which becomes the template for replication and transcription. Replication of the intermediate dsDNA occurs through a rolling circle mechanism and is initiated by the cleavage of the conserved TAATATT/AC sequence in the CR. The resulting ssDNA is then transported once enough movement proteins (CP, NSP, and MP) are synthesized (Gutierrez 2000; Gutierrez 2002; Hanley-Bowdoin et al. 2004).

1.3 GEMINIVIRUSES AND RNA SILENCING

To protect themselves from invading pathogens, plants have developed different mechanisms in response to viral infections, varying from restricting the entry of pathogen into their cells to preventing replication and proliferation of the invading pathogen. Remission or recovery is one such mechanism reported in response to certain virus' infections, including geminiviruses. Recovery is an antiviral response where infected plants have lower symptomatic leaves with symptomless emerging leaves that are resistant to re-infections (Van Kammen 1997; Baulcombe 2004; Ratcliff et al. 1999; Lindbo et al. 1993). Recovery has been observed in transgenic plants carrying a fragment of the viral genome. Upon infection, these transgenic plants mount resistance to the infecting virus, a process known as pathogen derived resistance (PDR) (Sanford and Johnston 1985; Carrillo-Tripp et al. 2007; Lindbo et al. 2001). Both Recovery and PDR occur through an RNA-mediated pathway known as RNA-mediated silencing or RNA silencing in short.

1.3.1 Post-transcriptional gene silencing

RNA silencing is an ensemble of RNA-mediated pathways that occurs via RNA specific interaction, resulting in suppression of gene expression (Vanitharani et al. 2005). RNA silencing is conserved across the eukarya domain; it is known as RNA interference (RNAi) in animals and quelling in fungi (Vanitharani et al. 2005). In plants, there are 2 types of RNA silencing, PTGS, and RNA-mediated DNA methylation (Baulcombe 2004)' (Vanitharani et al. 2005).

PTGS was first reported when attempts to produce petunia petals with an intense violet/pink color by overexpressing chalcone synthase (CHS) resulted in white petals, indicating a

suppression of CHS activity (van Der Krol et al. 1990; Napoli et al. 1990).This was initially named co-suppression: the presence of the transgene suppressed expression of the endogenous gene and vice-versa. “Co-suppression” was also observed in plants transformed with a fragment of tobacco etch virus (TEV), in which the virus conferred resistance to viral infection (Ratcliff et al. 1997; Lindbo et al. 1993). Lindbo and colleagues observed that even though transcriptional activity was not suppressed, viral mRNA accumulation was prevented. They hypothesized that elevated mRNA in petals overexpressing CHS in combination with increases in transcriptional activity from viruses, somehow initiated a chain of events leading to silencing. In 1997, Metzlaff et al. showed that increased transcriptional activity resulted in aberrant mRNA that could trigger the initiation of gene silencing pathway (Metzlaff et al. 1997).

Since the early studies of PTGS, more information has come to light, allowing a better understanding and description of PTGS. PTGS involves the cleavage of dsRNA, by DICER-LIKE (DCL) protein into small RNA fragments of 21-26nt in length, known as short interfering RNA (siRNA) and microRNA (miRNA) (Baulcombe 2004). The difference between these 2 small RNAs lie in the way they’re generated and the PTGS silencing pathway they participate in.

1.3.1.1 siRNA pathway

The siRNA pathway mainly regulates the expression of endogenous and exogenous genes, consequently playing a role in silencing induced by virus infection. The presence of partial dsRNA arising from overlapped, folded and aberrant mRNA that are possibly a result of abundant viral transcriptional activity, activate RNA dependent RNA polymerase (RdRP/RDR), which extends the partial dsRNA into long dsRNA. The long dsRNA is recognized by DCL and cleaved into small dsRNA with 2nt overhangs at the 3′ends of both strands (Herr and Baulcombe 2004).

Four DCL proteins have been identified in *Arabidopsis* and 2 putative DCL members in *Oryza sativa* (Schauer et al. 2002). Different domains are found across the DCL protein family: Nuclear localization signal, DExH-box RNA helicase C, Zinc finger, PAZ (PIWI/ARGONAUTE/ZWILLE), DUF283 (DOMAIN of UNKNOWN FUNCTION), a dsRNA binding domain (dsRBD) and Ribonuclease III (RNase III) (Schauer et al. 2002). The PAZ

domain has both a dsRNA and ssRNA binding activity, which can bind to 3′ ends of ssRNA and 2nt of 3′overhangs of dsRNA. The function of DUF238 is yet to be discovered; analysis have identified a putative dsRNA binding role that could, together with PAZ, assist in dsRNA binding role of DCL molecules (Dlakić 2006). These domains determine the function of the respective protein member and also the pathway they are involved with. Their function is partially redundant as, although they are involved in different sections of RNA silencing, they can substitute each other's function in mutated plants (Gasciolli et al. 2005).

The dsRNA cleaved by DCL is incorporated in the RNA-induced silencing complex (RISC) which directs the antisense strand to the target RNA. RISC is made up of different proteins, with ARGONAUTE (AGO) being the only protein that has been extensively studied in animals and plants. In *Arabidopsis,* 10 proteins have been identified as belonging to the Argonaute family; they all share a variable N-terminal, a PAZ domain, a MID (MIDDLE) domain and a PIWI (*P* ELEMENT-INDUCED WIMPY TESTS) domain (Vaucheret 2008). The MID domain binds to 5′phosphate of small RNAs and the PIWI domain has an RNase H-like fold with endonuclease activity, allowing this protein to cleave a region complimentary to the small RNA in the target (Vaucheret 2008). The antisense strand bound to the RISC leads the latter to degrade target mRNA, through specific Watson-Crick interactions. The antisense siRNA can also serve as a primer, binding alone to the target mRNA, resulting in polymerization by RdRP, leading to an amplification of the silencing signal or production of secondary siRNAs (Baulcombe 2004; Vanitharani et al. 2005).

Two other types of siRNA are present in plants. *Trans*-acting small interfering RNA (tasiRNAs) arise from both sense and antisense non-coding RNA (Kalantidis et al. 2008) and unlike conventional siRNA, their sequence does not obligatory match their target's (Vazquez et al. 2004). RDR6 and SGS3 (SUPPRESSOR OF GENE SILENCING 3), a putative RNA binding protein involved in the cosuppression pathway, DCL4 and AGO1, DCL1, HEN (HUA ENHANCER) 1 and HYL (HYPONASTIC LEAVES) 1 involved in miRNA production regulate tasiRNA biogenesis (Peragine et al. 2004; Vazquez et al. 2004; Kumakura et al. 2009; Xie et al. 2005). Natural antisense transcript derived small interfering RNA (natsiRNAs) are produced from overlapping transcripts or natural *cis*-antisense transcripts in response to abiotic and biotic

stress (Borsani et al. 2005). DCL2, RDR6, SGS3 and NRPD1A (NUCLEAR RNA POLYMERASE D1A), a subunit of DNA-dependent RNA polymerase IV, are involved in natsiRNAs biogenesis (Kalantidis et al. 2008; Borsani et al. 2005).

1.3.1.2 miRNA pathway

Unlike siRNAs that are entirely complimentary to their targets and are made from both endogenous and exogenous mRNA, miRNAs allow for mismatches with the targets and are only generated from endogenous mRNA. miRNA is transcribed in the nucleus by RNA polymerase II, from mRNA containing internal hairpins into long primary miRNA (pri-miRNA). Pri-miRNAs are cleaved by DCL1 (Park et al. 2002) into pre-miRNA of about 65nt in length and then into mature miRNA that get translocated into the cytoplasm (Zhu 2008). In the nucleus, DCL1 has been shown to interact strongly with other proteins, HYL1, and C2H2 Zn-finger SERRATE (SE) (Dong et al. 2008). HYL1 has a protein-protein domain that interacts with one of its two dsRBD domain through which it forms a multiprotein complex with DCL1 and SE (Wu et al. 2007). This interaction is important for the cleaving properties of DCL1 as it has been shown that DCL1 does not efficiently cleave without these interactions (Yang et al. 2006). Once cleaved, the mature miRNA is methylated by the methyltransferase HEN1, which adds a methyl group at the 2′ OH of the 3′ end of mature miRNA (Yang et al. 2006). The mature miRNA then translocates into the cytoplasm, where it is recruited in the RISC.

1.3.2 RNA-mediated DNA Methylation

DNA methylation was first discovered when viroid cDNA, transformed into tobacco, became methylated once replication of inoculated viroid occurred, through an RNA-RNA mechanism (Wassenegger et al. 1994). Methylation occurred only in viroid sequences, and not in the flanking T-DNA region. This was the first report of a *de novo* DNA methylation, regulated by homologous RNA sequences accounting for 30% of cytosine methylation in *Arabidopsis* (Matzke et al. 2009). Because the outcome of the *de novo* methylation is the repression of transcription, this process is sometimes called transcriptional gene silencing (TGS). RNA-mediated DNA methylation uses a similar mechanism to that of PTGS as it is uses small RNAs produced from dsRNA structures (Sijen et al. 2001).

Key players of RNA-mediated DNA methylation have been identified but, their functional characterization has not yet been completed. RNA-mediated DNA methylation is believed to be induced in the nucleus where transcriptional activity of DNA dependent RNA polymerase II (POLII) can result in sequence overlaps, leading to a dsRNA structure. The dsRNA formed is cleaved by DCL3 (Gasciolli et al. 2005) and the small RNAs produced are methylated by HEN1 and then bind to AGO4 associated with POLV, a POLII related polymerase. The AGO4/POLV complex interacts with a methylase DRM2 (DOMAINS REARRANGED METHYLTRANSFERASE2), with its co-factors, DRD1 (DEFECTIVE IN RNA DIRECTED DNA METHYLATION1) and DMS3 (DEFECTIVE IN MERISTEM SILENCING 3), leading to methylation of the target sequence (Matzke et al. 2009). In transgenic studies, it has been shown that methylation occurring in this way can be extended to promoter sequences resulting in suppression of gene expression (Mette et al. 2000; Sijen et al. 2001).

1.3.3 RNA silencing movement

RNA silencing, once induced in a cell or a group of cells, has been shown to spread, locally, to neighboring cells, as well as systemically. Systemic silencing signal spreads through the phloem; the exact nature of the signal carrier as well as the genes involved in systemic spread has not yet been deciphered (Kalantidis et al. 2008). A cocktail of genes have been identified to be involved with short range silencing spread. Short range silencing spread can be further divided in two: non-extensive and extensive. Non-extensive short range silencing involves spreading of the signal to neighboring 10-15 cells possibly through the plasmodesmata by siRNAs (Himber et al. 2003; Kalantidis et al. 2008). In extensive short range silencing, the signal spreads further than 10-15 cells, through the veins, to the entire leaf (Kalantidis et al. 2008). Beside the range of spreading, no amplification occurs in non-extensive local spread while in extensive spread, the signal is amplified as it moves from a cell to another, producing secondary siRNA along the way. Extensive short range spread has only been observed with silencing of transgenes (Smith et al. 2007); endogenous genes have developed a system not allowing for amplification of the silencing signal to take place (Kalantidis et al. 2008).

1.4 GEMINIVIRUS-INDUCED GENE SILENCING

Although geminivirus does not replicate through a dsRNA intermediate phase like plant RNA viruses, they can induce a strong PTGS response in their host (Vanitharani et al. 2005). The encoded AC2 and AC4 PTGS inhibiting activity is needed to circumvent the host silencing effect. AC2 and AC4 silencing inhibitor activity is not always successful, as observed during recovery. The mechanism by which geminivirus/virus-induced PTGS, known as "virus-induced gene silencing" (VIGS) occurs, is at this stage speculative; the early abundant transcripts produced during infection, the fold-back structure and the overlapping sequences of expressed geminiviruses genes (Figure 1-4) are all believed to play a role in virus mediated PTGS induction (Vanitharani et al. 2005)

VIGS can be adapted in laboratories as a tool for functional genomics studies. The VIGS technology involves introducing a modified virus as a vector carrying a fragment of a gene of interest, generally in the antisense orientation, into host plants (Robertson 2004). As the virus induces PTGS against its own genes, genes in host with sequence similarity to the inserted fragment will also be silenced, allowing studying the function of the target gene. Unlike other functional genomics methods such as plant transformation, VIGS can be quickly achieved, avoiding the laborious processes of plant transformation and also allowing the study of otherwise lethal mutations as would occur in null-mutation of developmental genes (Robertson 2004). VIGS also allows for functional genomics studies, when only partial sequence information is known (Lindbo et al. 2001; Senthil-Kumar et al. 2007).

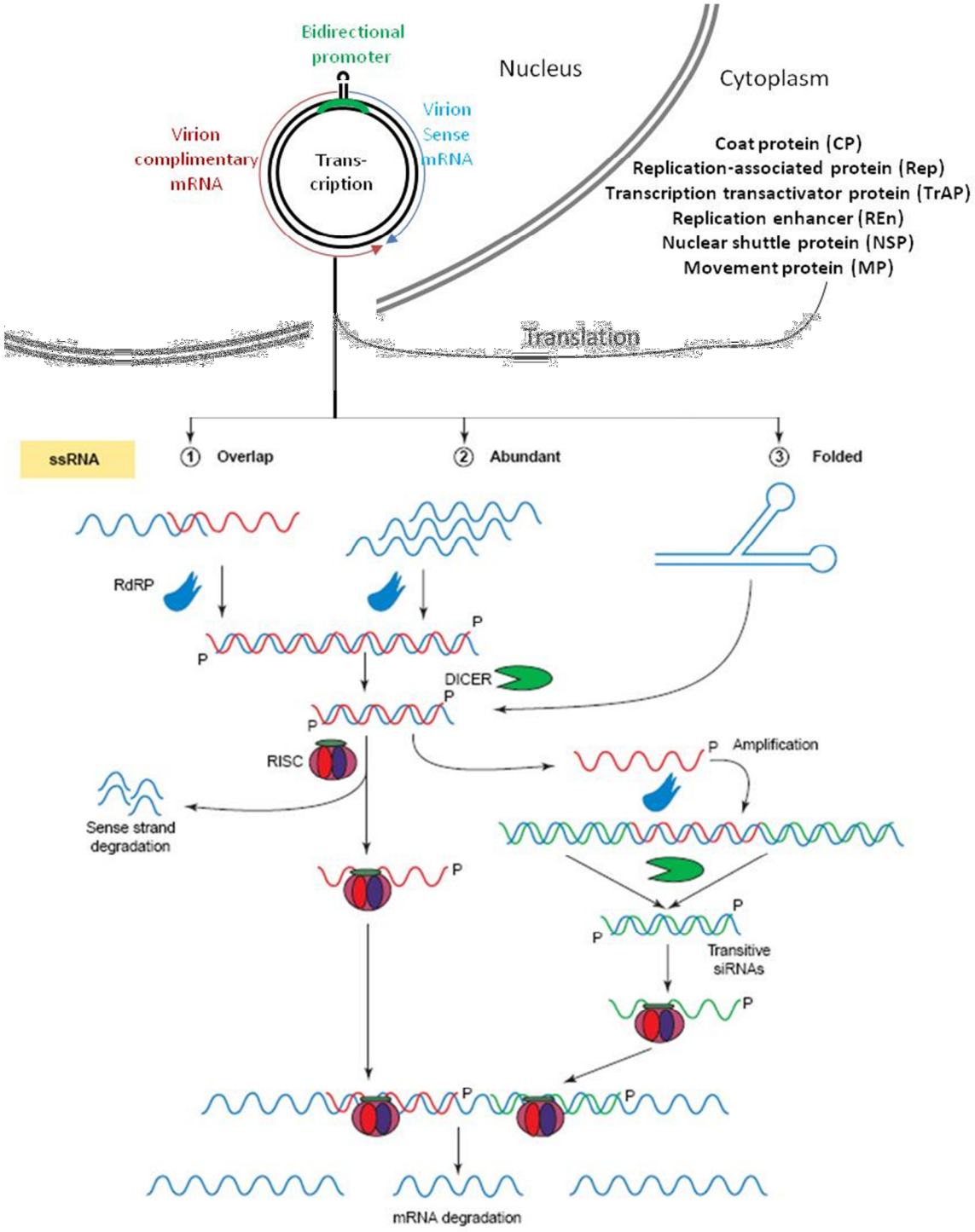

Figure 1-4: Geminivirus-induced RNA silencing

Expressed geminiviral transcripts translocate out of the nucleus into the cytoplasm for translation in the cytoplasm, RdRP produces dsRNA from overlapped, abundant and folded transcripts. DICER cleaves the dsRNAs to make siRNAs that are incorporated into the RISC. The sense strand in blue is degraded and the antisense strand in red hybridizes to matching RNA through RNA specific interaction. RdRP recognizes the hybridization of siRNAs to target RNA, extending the partial dsRNA to form long dsRNA that are cleaved by DICER to produce transitive siRNAs (in green) that are complementary to regions other than the initial siRNA (Vanitharani et al. 2005).

Initially, VIGS was used to silence endogenous phytoene desaturase (PDS) in *N. benthamiana*, using an antisense fragment of PDS in tobacco mosaic virus (TMV) (Kumagai et al. 1995). Since then, VIGS has been applied to different plants, both monocots and dicots, using both RNA and DNA viruses as vectors (Unver and Budak 2009). Amongst these vectors are geminiviral vectors that are preferred over RNA viruses as they have shown to elicit a more stable response. Since geminiviruses replicate through a dsDNA intermediate, replication cannot be targeted by RNA silencing as is the case for RNA viruses (Golenberg et al. 2009) and the viral vector with the silencing signal can still move. Furthermore the small genome size of geminiviruses makes them easier to manipulate (Carrillo-Tripp et al. 2006).

1.4.1 Mechanism of VIGS

The exact pathway of VIGS has not yet been fully characterized. Depending on the nature of silencing inducer (DNA-virus or RNA-virus), 2 pathways for VIGS have been proposed, namely DNA-virus and RNA-virus VIGS, and shown to require different players of the RNA silencing machinery (Muangsan et al. 2004; Blevins et al. 2006). All four *Arabidopsis* DCLs cleave DNA-virus induced siRNA precursors while only DCL4 was found to be important for RNA viruses (Blevins et al. 2006). Although RDR6 and SGS3 are often found working together and have been shown to interact and colocalize in the cytoplasm (Kumakura et al. 2009), only RDR6 was found to be involved in both types of VIGS (Vaistij and Jones 2009), unlike previously reported (Muangsan et al. 2004). Another pathway of VIGS was also shown in transgenic plants as transgenes targeted by VIGS are silenced through methylation (De-Jiang et al. 2004; Jones et al. 1998).

1.4.2 VIGS vector design

Two important factors considered while designing VIGS experiments are the choice of vector and the region of the target gene that could produce maximum small RNA molecules leading to an efficient silencing signal. The choice of vector is mainly determined by the plant under investigation, as successful infection has to take place before VIGS can occur. Environmental factors are also important for VIGS experiments as they have to allow for efficient silencing to occur. The optimal temperature at which VIGS experiments should be carried out is variable,

depending on the host and virus vector under investigation: lower temperature was seen to increase stability of VIGS in cotton (Tuttle et al. 2008) while in cassava and *Nicotiana,* higher temperature was more beneficial (Chellappan et al. 2005).

To date geminivirus VIGS vectors have been designed only from viruses belonging to the Genus *Begomovirus* and *Curtovirus* (Table 1-2). Begomovirus vectors have been designed from DNA-A (Kjemtrup et al. 1998), DNA-B (Peele et al. 2001; Turnage et al. 2002) and DNAβ (Tao and Zhou 2004). Modification of DNA-A for VIGS generally involves deletion of the CP region. Bipartite begomoviruses do not rely on the CP for systemic movement and thus bipartite begomoviruses lacking the CP can still propagate and move throughout the plant, allowing for the spread of the silencing signal. The deleted CP gene is replaced by a multiple cloning site (MCS) in which any fragment of up to 800 bp can be cloned (Kjemtrup et al. 1998). The fragment is inserted without a promoter or a terminator as its transcription is driven by the CP promoter in the CR.

DNA-B-based VIGS vectors are designed by inserting a MCS in the region downstream of BV1 (Peele et al. 2001; Turnage et al. 2002). Even though a *Tomato golden mosaic virus* (TGMV) DNA-B VIGS vector was shown to be more efficient than DNA-A (Peele et al. 2001), Turnage and colleagues showed that *Cabbage leaf curl virus* (CabLCuV) DNA-B VIGS vector resulted in stronger symptoms with limited silencing when compared to the DNA-A based vector (Peele et al. 2001; Turnage et al. 2002). VIGS using DNAβ is accomplished by deleting the βC1 gene required for symptom development and replacing it with a MCS (Tao and Zhou 2004; Qian et al. 2006).

Only one Curtovirus-derived VIGS vector has been designed to date (Golenberg et al. 2009). This vector was designed on the broad range *Beet curly top virus* (BCTV) by modifying CP and the pre-CP, resulting in a vector that can replicate, not move efficiently and produce symptomless silencing (Golenberg et al. 2009).

Using VIGS technology, it is possible to simultaneously silence more than one gene, if they share a degree of sequence similarity (Robertson 2004). Although this is advantageous, such as when a gene family is under investigation, it poses a problem when only one gene needs to be

silenced; hence the sequence or region of the target to be inserted into the VIGS vector needs to be carefully studied. Multiple genes, with no sequence similarity can also be simultaneously targeted by inserting more than one gene fragment (Peele et al. 2001; Turnage et al. 2002; Tao and Zhou 2004). Because the size of the fragment to be inserted in a VIGS vector is limited to about 800 bp (Kjemtrup et al. 1998), the fragment for each gene to be inserted needs to be one that will produce the maximum silencing with the least possible sequence length.

Reporter genes are used in VIGS experiments to provide a visible marker as a positive control of VIGS vector functionality. Amongst the most used reporter genes are PDS, chelatase H subunit gene (ChlH), CHS as endogenous gene and green fluorescent protein (GFP) as the most common exogenous reporter gene (Robertson 2004; Shao et al. 2008). Successful inhibition of PDS, ChlH and CHS can be confirmed by the bleaching of leaves and petals. When GFP is used as a reporter gene, suppression of its activity can be confirmed once transgenic plants appear red under ultraviolet (UV) light instead of green as transgenic plants expressing GFP should appear.

Most VIGS experiments performed to date have been achieved using RNA viruses *Tobacco rattle virus* (TRV), *Tobacco mosaic virus* (TMV) and *Potato virus X* (PVX). TRV has been the RNA virus of choice because unlike PVX and TMV, it can silence genes in the meristem and upon infection produces milder symptoms (Ratcliff et al. 2001). Other RNA vectors have been developed for silencing experiments in plants that cannot be infected by PVX, TRV or TMV (reviewed in (Purkayastha and Dasgupta 2009)). Geminivirus VIGS vectors produce stable silencing because transcription of viral genes, and not their DNA genome, is targeted by the host RNA silencing machinery. Table 1-2 shows a list of geminivirus-derived VIGS vectors. TGMV and BCTV VIGS vectors were like TRV, shown to silence genes in the meristems, although geminiviruses do not infect meristematic tissues (Peele et al. 2001; Golenberg et al. 2009). Geminiviruses silencing vectors also allow for functional studies in plants like cassava that are not infected by commonly used RNA-based VIGS vector (Fofana et al. 2004). VIGS has been used for functional studies of genes involved in development, abiotic and biotic defense responses.

Table 1-2: Geminiviruses used as VIGS vector

Virus *vector*	Silenced genes	Silenced host	Reference
ACMV	*PDS, Su*	*N. benthamiana*	(Fofana et al. 2004)
	Su, CYP79D1 and *2*	cassava	
CabLCuV DNA	*Su*[1], *PDS* *Su* and *GFP* [2]	*A. thaliana*	(Turnage et al. 2002)
	SGS1-3, AGO1	*A. thaliana*	(Muangsan et al. 2004)
TGMV	*Su, LUC*	*N. benthamiana*	(Kjemtrup et al. 1998)
	Su[1] *Su* and *GFP*[2, 3] *Su*[3], *PCNA*[3] *Su* and *PCNA*[4]	*N. benthamiana*	(Peele et al. 2001)
TYLCCNV DNAβ	*Su*	Tomato	(Cai et al. 2007)
	Su, PDS	*N. benthamiana* *N. tabacum Samsun* *N. glutinosa*	(Tao and Zhou 2004)
	Su and *PCNA* *Su* and *GFP*	*N. benthamiana*	
TbCSV DNAα	*GFP, PCNA, NbTOM1, 3* *GFP* and *Su*[2]	*N. benthamiana*	(Huang et al. 2009)
	Su	*N. tabacum* *N. glutinosa* Tomato *N. benthamiana*	
	CHS	*Petunia hybrida*	
ToLCV	*GFP, PCNA*	Tomato	(Pandey et al. 2009)
BCTV	*Su*	Tomato	(Golenberg et al. 2009)
	PI, APE, transketalase, rbcS	Spinash	

[1] Silencing vector was designed on DNA-A and DNA-B component
[2] Both genes were inserted in one vector and simultaneously silenced
[3] Silencing vector designed on DNA-B
[4] *Su* was inserted in DNA-A and *PCNA* in DNA-B and silencing was simultaneously achieved

1.4.3 VIGS for functional characterization of defense response genes

The VIGS approach used to elucidate genes involved in pathways other than disease resistance involves infecting the plant being studied with a VIGS vector carrying the candidate gene and the resultant phenotype is observed. VIGS studies for defense responses involve primarily silencing the candidate gene using the VIGS approach and subsequently infecting the plants using a second pathogen whose infectivity is under investigation.

This approach has been used to study genes involved in the *N* gene resistance against TMV (Purkayastha and Dasgupta 2009). *N. benthamiana* is susceptible to TMV infection, however transgenic plants harboring the *N* gene induce a HR response when infected with TMV. To identify possible genes involved in the *N* mediated resistance pathway, the candidate genes in transgenic tobacco are silenced using a PVX or TRV based VIGS approach. Once silencing is established, these plants are infected with TMV and observed for initiation of HR. Using this approach, members of the WRKY family of transcription factors as well as different mitogen-activated protein kinases (MAPKs) were found to be involved in *N* mediated resistance (Purkayastha and Dasgupta 2009). The same approach has revealed the involvement of BECLIN-1, an autophagy-related gene in yeast and mammals, in HR induced plant cell death (PCD) (Liu et al. 2005). Silencing of a candidate gene using the VIGS approach followed by inoculation of a pathogen to which the plants is resistant, has been used to identify genes involved in the induction of HR in response to non-host infections (Purkayastha and Dasgupta 2009; Burch-smith et al. 2004).

1.4.4 Hypersensitive response and nitric oxide

Induction of the HR in response to pathogen attack is a vital step in resistance against infection. The HR is a cascade of reactions resulting in locally restricted PCD in resistant host-pathogens interactions (Jones and Dangl 2006). PCD that occurs during the HR has certain similarities with mammalian apoptosis in that both processes involve mitochondrial membrane depolarization, ions influxes, changes in protein phosphorylation and oxidative damage (Zaninotto et al. 2006; Mur et al. 2006) and involvement of caspase-like molecules in plants (Belenghi et al. 2003) resulting in DNA fragmentation and nuclear collapse. PCD is required to prevent the spread of

the infecting pathogen to non-infected cells and tissues. HR is initiated by recognition of the pathogen's avirulence gene product (avr) by the plants resistance gene product (R). The guard hypothesis stipulates that the host R proteins monitor the effect of pathogen avr proteins on cellular processes (Jones and Dangl 2006).

For an effective response against pathogen attack, plants need to be able to recognize the infection early (Garcia-Brugger et al. 2006). Recognition of avr by plant R proteins promotes the expression of defense-related genes, activation of protein kinases and phosphatases, oxidative burst, production of salicylic acid (SA), influx of Ca^{2+}into the cytoplasm and alteration of ion pumps/channels, leading to changes in intracellular pH (Garcia-Brugger et al. 2006; Cohn et al. 2001). Together, these changes in the cellular environment, lead to oxidative-burst mediated cell death, executed by the activity of caspase-like proteases. To contain cell death elicitors in the infected cells, double membrane autophagosomes form around the dying cells (Mur et al. 2008). The induction of the production of resistance signals by SA and systemic spread of the resistance signals follows PCD. The spread of resistance signals prepares uninfected cells for a probable secondary infection and this response is known as systemic acquired resistance (SAR) (Durrant and Dong 2004).

Geminiviruses encode various inducers of HR or avirulence determinants. C2 of *Tomato yellow leaf curl China virus* (TYLCCNV) and *Tomato leaf curl* (ToLCV) was found to induce HR in Nicotiana spp. (Selth et al. 2004; Wezel et al. 2002). The N-terminus of V2 of *Tomato leaf curl Java virus*-A (ToLCJV-A) containing the PTGS-suppressing domain was shown to elicit HR in tomato (Sharma and Ikegami 2010). The NSP of *Tomato leaf curl New Delhi virus* (ToLCNDV) and BDMV induce HR in tomato and common bean, respectively (Garrido-Ramirez et al. 2000; Hussain et al. 2005; Hussain et al. 2007; Zhou et al. 2007). As well as encoding avr proteins, these viruses have evolved ways to suppress the HR. Rep of ACMV expressed using PVX expression vectors was shown to induce HR in *N. benthamiana* only in the absence of AC4 (van Wezel et al. 2002; Hong et al. 2003). The HR determinant domain (HRD) was shown to overlap with regions needed for Rep, REn and pRBR interaction. A positive and a negative modulating domain was found upstream of the HRD, and predicted to structurally constrain HRD activity. The HR response induced by NSP of ToLCNDV could only be achieved in the absence of ToLCNDV TrAP.

Nitric oxide (NO) has emerged as a key player in oxidative burst leading to PCD. Nitric oxide is a gaseous signaling molecule which participates in various processes crucial for growth and development of plants (Neill et al. 2002; Neill et al. 2003), stomatal closure, iron homeostasis and response to both abiotic and biotic stresses as well as disease resistance (Lamotte et al. 2005). Nitric oxide is highly reactive; it has a singlet electron and in a cell, NO can be found in different forms, NO radical ($NO^{\cdot}$), nitroxyl (NO^{-}) and nitrosonium (NO^{+}) ions. Once formed, NO can be metabolized or chemically altered by reaction with reactive oxygen species to form peroxynitrite ($ONOO^{-}$), S-nitrosothiols, higher oxides of nitrogen and dinitrosyl-iron, termed reactive nitrogen species (Leitner et al. 2009). Generation of reactive nitrogen species from NO can be involved with different molecules, in a wide range of signaling pathways (Mur et al. 2006).

The involvement of nitric oxide in plant defense responses was initially established when it was shown that NO scavengers and inhibitors of NO synthesis rendered a plant susceptible to attack (Zeier et al. 2004; Delledonne et al. 1998). In the case of tobacco, application of exogenous NO resulted in reduced lesions caused by TMV infection (Song and Goodman 2001). Nitric oxide production has been shown to increase during HR in response to *Pseudomonas syringae* infection in *Arabidopsis* and tobacco (Clarke et al. 2000). Increase in NO was also shown in tobacco cells challenged with the death-inducing elicitor cryptogein (Foissner et al. 2000) and, in barley, in response to mildew fungus (Prats et al. 2005). Exogenously applied NO causes DNA fragmentation during HR and the ensuing NO-mediated death is inhibited by caspase inhibitors in plants (Clarke et al. 2000). Features of PCD such as loss in mitochondrial membrane potential and release of cytochrome C, known in animals to initiate apoptosis, are initiated by NO in plants (Mur et al. 2006).

The exact mechanism by which NO brings about changes in cellular states during the HR has not yet been elucidated but based on the property of NO, it can modulate the expression of genes as well as changing protein activity post-translationally. Using microarray studies, gene products whose expression is modulated by exogenously applied NO have been identified (Besson-Bard et al. 2009; Polverari et al. 2003; Parani et al. 2004). These genes include heat shock proteins, antioxidants, genes involved in iron homeostasis, defense-related genes and MAPKs. S-nitrosylation is the most studied post-translational modifications mediated by NO in plants. S-

nitrosylation is modification of thiol groups in cysteine residues, and has been linked to gene regulation, phytohormonal signaling and cell death (Leitner et al. 2009). Other post-translational modifications by NO are nitration, the modification of tyrosine residues and metal nitrosation and the binding of NO to iron of haeme containing proteins forming iron-nitrosyl complexes (Garcia-Brugger et al. 2006; Mur et al. 2006).

1.4.4.1 *In planta* nitric oxide production

In mammals where NO was first identified, three different isoforms of NO synthase (NOS) catalyze the conversion of L-Arginine to L-Citrulline and NO (Mayer and Hemmens 1997; Wendehenne et al. 2001; Moncada et al. 1989). Nitric oxide synthases are homodimeric proteins with 2 domains: At the N-terminal, NOS contains an oxygenase with a haeme catalytic domain with binding sites for L-Arginine and tetrahydrobiopterin, and at the c terminal it contains a reductase domain with binding sites for flavin mononucleotide, flavin adenine dinucleotide and reduced nicotinamide adenine dinucleotide phosphate (NADPH) (Wendehenne et al. 2001). In plants, no mammalian NOS homologs, have yet been identified, although NOS-like activity has been observed in plants (Corpas et al. 2009) including peas (Barroso et al. 1999), maize (Ribeiro Jr et al. 1999), tobacco (Durner and Klessig 1999), soybeans (Modolo et al. 2002; Delledonne et al. 1998) and in *Arabidopsis* (Zeidler et al. 2004). However, the gene encoding a NOS or the protein responsible for the NOS activity is yet unidentified (Guo et al. 2003; Leitner et al. 2009).

In plants, enzymatic production of NO has been linked to nitrate reductase, which catalyses the reduction of nitrite to NO (Wendehenne et al. 2004; Neill et al. 2003); xanthine oxidoreductase which catalyses nitrite or nitrate reduction under anaerobic conditions to generate NO (R Harrison 2002); and nitrite-NO reductase, an enzyme bound to the plasma membrane in root cells and catalyses the reduction of nitrite to NO (Stöhr et al. 2001). Nitric oxide can also be synthesized non-enzymatically from nitrite under acidic and reducing conditions, from a reaction between ascorbate and nitrous acid and from nitrogen dioxide (Neill et al. 2003). Though all these different potential source of NO have been identified, the involvement of NO produced from these sources in NO signaling is not fully understood, and neither is the link between NO produced from these sources and plant-pathogen interactions.

In 2003, Guo et al. identified a gene that they named *AtNOS*1, related to a NO producing enzyme in *Helix pomati.* Overexpression of AtNOS1 in *Arabidopsis* resulted in an increase in NOS-like activity (Guo et al. 2003) while *atnos1* mutants show a decrease in NO production in plants and with phenotypic features that can be rescued by applying NO using an exogenous donor (Zeier et al. 2004). This enzyme was shown to have no sequence similarity to and not all co-factor requirements of mammalian NOS; it requires Ca^{2+}, camoldulin and NADPH (Guo et al. 2003). AtNOS1 was shown to produce NO from purified bacterial extracts through the conventional L-arginine dependent pathway. Homologous sequences to AtNOS1 have been identified in mammals and bacteria (Zemojtel et al. 2004). In mammals, an AtNOS1 homolog was shown to be expressed in variety of tissues and in bacteria they were identified as putative GTPase; a GTP binding domain was later found in AtNOS1 (Zemojtel et al. 2006; Zemojtel et al. 2004).

Further experiments on AtNOS1 could not be reproduced with regards to the *in vitro* NO producing activity of purified recombinant AtNOS1 (Crawford et al. 2006; Zemojtel et al. 2006). It was then concluded that although AtNOS1 did not directly produce NO, the decrease in NO production in *atnos1* mutants showed an indirect relationship between AtNOS1 and NO; AtNOS1 was thus renamed AtNOA1, for nitric oxide associated 1 (Crawford et al. 2006). In 2008, Morreau and colleagues confirmed the putative GTP hydrolysis activity of AtNOA1, showed that AtNOA1 was localized in the chloroplast. AtNOA1 was shown to be essential for ribosome assembly (Gas et al. 2009; Leitner et al. 2009). In a different study it was shown that mutations in AtNOA1 result in decrease in expression of plastome (plastid genome) proteins and this activity is independent of NO (Flores-Pérez et al. 2008).

1.4.4.2 AtNOA1/cGTPase and disease

*AtNOA*1 is homologous to YqeH from *Bacillus subtilis,* a member of the YlqF/YawG family of proteins, involved in ribosome assembly (Gas et al. 2009; Flores-Pérez et al. 2008). Although the biological link between *AtNOA*1 and NO observed in *atnoa1* plants has not yet been established, it has been speculated that defective plastids present in *atnoa1* mutants could results in elevated levels of reactive oxygen species (ROS) that readily react with NO present in cells, resulting in a decrease in the presence of free NO (Gas et al. 2009; Leitner et al. 2009). There is some evidence

that plastids may play a central role in NO homeostasis in plant cells; clarification on this relationship could provide answers on the link between NO and AtNOA1 (Gas et al. 2009).

Even though AtNOA1 is not directly involved in NO production, there is evidence linking AtNOA1 to disease resistance. The expression of AtNOS1 was found to be modulated by lipopolysaccharide and *atnos1* mutants were shown to be highly susceptible to *Pseudomonas syringae* pv. *tomato* DC3000 (Zeidler et al. 2004). In *N. benthamiana,* silencing of *NbNOA1*, a *AtNOA1* homolog, using VIGS, resulted in an increase in susceptibility to *Colletotrichum lagenarium*, and a decrease in expression of pathogenesis related 1 (PR1), a marker of defense response, when these plants were challenged with *Colletotrichum lagenarium* (Kato et al. 2007).

1.5 AIMS AND OBJECTIVES

Cassava is an important food crop and source of starch for industrial applications and biofuels. In South Africa, cassava is grown by small-scale farmers and commercially in Mpumalanga and Swaziland. CMD is endemic in SA and our laboratory is interested in genetic engineering for CMD using pathogen-derived resistance and RNA silencing, as well as looking at endogenous resistance genes that can be manipulated into providing natural resistance. Previous research in our laboratory has shown that the expression of NbNOA1 is affected in SACMV- infected *N. benthamiana* (van Schalk, unpublished), and therefore we were interested in examining this gene in light of its potential involvement in virus resistance. Therefore, the overall objective of this study was to develop a VIGS system that could be used in cassava and *N. benthamiana* for routine functional gene validation in our research group.

The specific aims for this study were:

1. *To identify a potential homolog of AtNOA1 in cassava*

AtNOA1 homologs have been found in many different plants, however with the limited sequences available on the cassava transcriptome, a homolog has not yet been identified in cassava.

2. *To design a VIGS vector of SACMV*

To test for the functionality of SACMV-VIGS vector, we aimed to use *ChlH* as a reporter gene as it has been shown to work in cassava and *N. benthamiana* using a *su*-gene from *N. tabacum*

3. To use the SACMV-based VIGS vector and attempt to silence NbNOA1 homologs in N. benthamiana

The involvement of AtNOA1 and NbNOA1 in disease resistance has been shown in response to different pathogens. In order to elucidate the potential role of NbNOA1 in response to SACMV infection, NbNOA1 was silenced in *N. benthamiana* using VIGS and the resulting effect on proliferation was studied.

CHAPTER 2. DETECTION OF AtNOA1 HOMOLOGS IN CASSAVA

2.1 INTRODUCTION

Expressed sequence tag (EST) database is an important tool for transcriptome studies. EST libraries are made up of partial random sequences, that have been read from one or both the 5′ and the 3′ ends of expressed genes. ESTs are randomly derived from cDNA libraries that were constructed from mRNA extracted from plants exposed to conditions that allow studies such as changes in gene expression in response to developmental cues, abiotic stresses, biotic stresses and organs-specific gene expression (Nagaraj et al. 2007). As costs associated with gene sequencing have decreased over the years, the number of ESTs libraries available has flourished (Nagaraj et al. 2007). Unfortunately, not all plants receive the same attention or interest, cassava being one of the less fortunate. In Sub-Saharan Africa, cassava is one of the main sources of carbohydrates and a cash crop for subsistence farmers in poor areas. In the industry the use of cassava over other starch sources has its advantages and because cassava grows easily on nutrient poor soils, it is relatively inexpensive to grow. Moreover, cassava starch has characteristics that are preferable over other starch sources in the textile, paper, adhesives and food industries (Nestel 1973).

Despite its different attributes, genome and transcriptome research on cassava is not as advanced as for other starch crops. When compared to other plant species, the genetic information available on cassava in public databases has been meager; at present there are only about 80 thousand cassava ESTs in GenBank when compared to about 350 thousand for potato, 1 million for rice and 2 million for maize. The small set of available ESTs for cassava makes homology searches challenging. In November 2009, 416 megabases (Mb) of the estimated 760Mb of the cassava genome was released. Although a large portion is yet to be sequenced, it is believed to be made up of repetitive sequences as 95% of known cassava genes, predicted using cassava UniGene, were identified in the 416Mb sequenced. The cassava sequence was obtained from a partially inbred line, AM560-2, and is publicly available at Phytozome (http://www.phytozome.net/cassava.php#).

Homology searches have assisted in functional characterization of proteins like AtNOA1. AtNOA1/AtNOS1 was initially believed to produce NO in *A. thaliana* via a NOS-like pathway even though it was found to have neither sequence similarity to NOS nor similar co-factor requirements to mammalian NOS (Guo et al. 2003). Nitric oxide production in mammals mainly occurs through the action of NOS enzymes that catalyze the conversion of L-arginine to L-citrulline and NO. There are three known mammalian NOS isoforms, of which two are constitutively active (neuronal NOS and endothelial NOS) and one is an inducible NOS (Mayer and Hemmens 1997; Moncada et al. 1989). However since the initial findings, the NOS activity of AtNOA1 could not be reproduced; further research has recently identified AtNOA1 as a member of a conserved cGTPase family, with no NO producing activity (Moreau et al. 2008; Zemojtel et al. 2004). Homologs to AtNOA1 have been identified across plants, mammals, yeast and bacteria (Sudhamsu et al. 2008). *AtNOA*1 sequence analysis has revealed a zinc-binding motif, a central GTP-binding domain, a C-terminal domain of unknown function (albeit seemingly essential for physiological function) and an N-terminal of unknown function with a putative mitochondrial targeting sequence (Moreau et al. 2008).

Although NOS-like activity has been reported in plants (Clarke et al. 2000; Foissner et al. 2000; Barroso et al. 1999; Durner et al. 1998; Delledonne et al. 1998; Neill et al. 2002; Neill et al. 2003) no NOS-like protein has yet been identified, nor have similar sequences to mammalian NOS been identified. Nevertheless, because *atnoa1* mutants in *Arabidopsis*, were shown to have a decreased NO production that could be rescued with exogenous NO application and null mutant of *atnoa1* had a decreased resistance to disease and abiotic stresses like salinity, drought and heat, *AtNOA1* homologs in plants have received much attention in the NO field and recently other orthologous sequences in plants have been identified (Kato et al. 2007; Qiao et al. 2009). The aim of this study was to use the information in public databases to identify and potentially isolate an AtNOA1 ortholog in cassava using sequence similarity searches with available cassava EST databases (dbEST).

2.2 MATERIALS AND METHODS

All nucleic acids quantification procedures were performed using the NanoDrop® ND-1000 spectrophotometer (NanoDrop Technologies, Wilmington, USA). All primers were designed using the PrimerQuest package of the Scitools online tool available at Integrated DNA Technology (http://eu.idtdna.com/Home/Home.aspx). PCR reactions were carried out using MyCycler Thermal Cycler (Bio-Rad, Hercules, USA). Table top centrifugation runs were carried out in *MiniSpin* (Eppendorf, Hamburg, Germany) and refrigerated centrifuge Mikro 200R (Andreas Hettich GmbH and Co. KG, Tuttlingen, Germany) large scale centrifugation runs were carried out in a Beckman J2-21 refrigerated high-speed centrifuge (Beckman Coulter, Brea, USA). BioDoc-It™ System, (UVP, Upland, USA) was used for agarose electrophoresis gel documentation and Microsoft PowerPoint was used to label the individual gel images.

2.2.1 PCR isolation of AtNOA1 and homologs

2.2.1.1 DNA extraction

DNA was extracted from *Arabidopsis* leaves using a modified Cetyl trimethylammonium bromide (CTAB) extraction procedure (Doyle and Doyle 1987). Approximately 50 mg of leaf tissue was ground in a microcentrifuge tube using a micropestle in the presence of liquid nitrogen. The ground material was resuspended in 0.5ml of extraction buffer, 2% w/v CTAB, 2% w/v polyvinylpolypyrrolidone (PVPP), 20 mM ethylenediaminetetraacetic acid (EDTA), pH 8.0, 1.4 M NaCl, 100 mM (hydroxymethyl aminomethane HCl (Tris-HCl)), pH 8.0, and 0.1% (v/v) β-mercaptoethanol, and incubated at 65ºC for 60 min. PVPP was included in the extraction buffer to chelate polyphenolics (Porebski et al. 1997).

A volume of 500 µl of chloroform:isoamyl alcohol (24:1) was added to the sludge to separate proteins and cell wall debris (carbohydrate) from the total nucleic acid (TNA). Addition of chloroform:isoamyl alcohol was followed by mixing by inversion and centrifuging at 12000 *g* for 10 min, in a *MiniSpin* (Eppendorf, Hamburg, Germany). The top aqueous layer containing the TNA was resuspended in an equal volume of 0.5ml chloroform:isoamyl alcohol, discarding the lower organic phase. Centrifugation was repeated at 12000 *g* for 10 min. Isopropanol (500 µl) was added to the top aqueous layer to precipitate TNA and the sample was centrifuged at 12000

g. The supernatant was discarded and the pellet was washed in 1ml of ice-cold 70% ethanol (v/v), followed by centrifugation at 7500 *g* for 5 min, then the supernatant was once again discarded. The washing step was repeated and the pellet allowed first to air dry and then resuspended in 100 µl of Tris-EDTA (TE) and RNase A buffer (10 mM Tris-HCl, pH 8, 1 mM EDTA, 200 µg/L RNase A). The extracted TNA was incubated at 37ºC for an hour to allow completion of RNase digestions and then incubated overnight at 4ºC, to allow for DNA resuspension. The extracted DNA was stored at -20ºC. To check for integrity of extracted genomic DNA and 1 µg of extracted DNA was electrophoresed on 0.8% agarose gel.

2.2.1.2 RNA extraction

RNA was extracted from cassava, *Arabidopsis* and *N. benthamiana* in an attempt to amplify *AtNOA1* from *Arabidopsis* and *AtNOA1* homologue in cassava and *N. benthamiana.* To avoid RNase A contamination that would degrade RNA, all prepared solutions that do not contain Tris were treated with diethyl pyrocarbonate (DEPC) by adding 0.1% of DEPC (v/v) and incubating the solution overnight at 37˚C. The following day these solutions were autoclaved at 121˚C, 1 bar, for 20 min to inactivate DEPC. Tris containing solutions were made using DEPC-treated H_20 as DEPC chemically renders Tris unsuitable to be used as a buffer. All glassware was baked overnight at 220˚C in an oven. All non-disposable plasticware was soaked in 0.1 M NaOH and 1 mM EDTA. RNase Away® (Molecular Bio Products Inc, San Diego, USA) was used to decontaminate gloves and laboratory benches.

Between 50 and 100 mg of plant leaves was ground into a fine powder in liquid nitrogen, using a micropestle in an eppendorf centrifuge tube. Into the eppendorf centrifuge tube, 750 µl of grinding buffer (200 mM Tris-HCl, 100 mM LiCl, 25 mM EDTA, 1% SDS (v/v), 2% PVPP were added to lyse plant cells and denature proteins. Phenol (250 µ)l equilibrated in TLE (200 mM Tris-HCl, 100 mM LiCl, 25 mM EDTA) and 250 µl of chloroform were added to the lysate. The lysate was incubated at 50˚C for 20 min. At an acidic pH, DNA is soluble in phenol. This allowed to separate the lysate in two phases, a lower protein soluble phase on top of which was an aqueous phase in which DNA and RNA was found. Following incubation, the microcentrifuge tubes were centrifuged at 8500 *g* for 15 min at 4˚C in a refrigerated centrifuge (Mikro 200R; Andreas Hettich GmbH and Co. KG, Tuttlingen, Germany). The aqueous phase

was then transferred into a new tube and the organic phase was discarded. Phenol and chloroform were once again added to the aqueous phase and the centrifugation step was repeated.

After centrifugation, the organic phase was discarded and 1/3 of 8 M LiCl was added to the aqueous phase. The samples were mixed and incubated at 4˚C overnight. LiCl was added in order to selectively precipitate RNA from DNA. The following day, the samples were centrifuged at 8500 *g* for 20 min at 4˚C to precipitate RNA. After centrifugation, the pellet was washed with 1ml 2 M LiCl. The microcentrifuge tube was slightly vortexed to dislodge the pellet and the samples were centrifuged at 8500 *g* for 3 min at 4˚C LiCl was discarded and the pellet resuspended in 800 µl nuclease-free H_2O. LiCl (300 µl of 8 M solution) was added and the samples were incubated at 4˚C for 6 hours. After this the samples were centrifuged at 8500 *g* for 20 min at 4˚C. The supernatant was discarded and the pellet was resuspended in 400 µl nuclease-free H_2O, to which 40 µl of NaAc (3 M sodium acetate) and 1ml of absolute ethanol were added. The samples were incubated overnight at -20˚C to allow for RNA precipitation and removal of salts.

The following day the samples were centrifuged at 16000 *g* at 4˚C for 20 min. The pellet was washed with 250 µl of 70% ethanol (v/v) by mild vortexing followed centrifugation at 16000 *g* for 3 min at 4˚C. Ethanol was discarded and the pellet allowed to air dry for 5 min, then resuspended in nuclease-free H_2O.

2.2.1.3 PCR amplification

AtNOA1-specific primers, 5′AtNOS (GATAAGCTTATGGCGCTACGAACACTCTCAA) and 3′AtNOS (GATGAATTCTCAAAAGTACCATTTGGGTCTTA), were designed to bind and amplify *AtNOA*1 genomic sequence and mRNA. For cloning purposes, restriction sites, *Hind*III for 5′AtNOS, and *EcoR*I for 3′AtNOS, underlined in each sequences were added to each primer. A tri-nucleotide GAT was also added to the primer sequence to allow for cleavage near the ends of PCR fragments. PCR was carried using 500 ng of extracted *A. thaliana* DNA using the MyCycler Thermal Cycler (Bio-Rad, Hercules, USA). The final reaction mix contained, 1X Phusion™ HF Buffer, 200 µM of each dNTPs, 0.5 µM of each primers and 1 U Phusion™ Hot Start DNA polymerase, in a total volume of 50 µl. PCR was run for 30 cycles; initial

denaturation at 98ºC for 30 sec, denaturation at 98ºC, 10 sec, annealing at 58ºC for 10 sec and elongation at 72ºC for 90 sec and final elongation 72ºC for 10 min.

To isolate the *AtNOA*1 mRNA, 2 step RT-PCR was carried out on 1 µg of extracted cassava, *N. benthamiana, A. thaliana* RNA using SuperScript® III Reverse Transcriptase (Invitrogen, Carlsbad, USA). The final reaction was carried out in a total volume of 20 µl and contained 1x First-Strand buffer, 10 µM DTT, 40 U RiboLock™ RNase inhibitor (Fermentas International Inc., Burlington, Canada), 50 U Superscript III (Invitrogen, Carlsbad, USA), 2.5 µM oligo$(dT)_{20}$, 0.5 mM dNTPs and 1 µg of total RNA. Before being added to the reaction, RNA together with the oligo$(dT)_{20}$ primers and dNTPs were incubated at 65˚C for 5 min, to minimize RNA secondary structures. After incubation at 65˚C, the rest of the reagents were added, the reaction mix was incubated at 50˚C for 2 h and the reaction was stopped by incubating at 85˚C for 5 min. The produced cDNA (2 µl) was used in the second step PCR using Phusion™ Hot Start High-Fidelity DNA Polymerase (Finnzymes, Espoo, Finland). PCR was carried out for 30 cycles and the following cycling conditions were applied: initial denaturation 98ºC for 30 sec, denaturation 98ºC, 10 sec, annealing 58ºC for 10 sec and elongation at 72ºC for 15 sec and final elongation 72ºC for 10 min. The PCR reaction components were used as recommended by the manufacturer without the optional addition of dimethyl sulfoxide (DMSO).

2.2.2 Nucleotide sequence similarity searches

BLAST searches were carried out in search of sequences similar to *AtNOA1* (Accession NM114613) (Guo et al. 2003), *NbNOA*1 (AB303300) (Kato et al. 2007) or *OsNOA*1 (OS02G01440) (Qiao et al. 2009). Protein sequences were aligned with translated nucleotide database (TBLASTN) in the databases cassava and leafy spurge EST Project (http://titan.biotec.uiuc.edu/cassava/) and the cassava EST project (ESTIMA; http://titan.biotec.uiuc.edu/cgi-bin/ESTWebsite/estima_start?seqSet=cassava) and eventually, GenBank. Pairwise and multiple alignments were carried out using the AlignX module of VectorNTI (Invitrogen, Carlsbad, USA).

2.2.3 Southern Blot hybridization

2.2.3.1 Probe design

Forward 5′ADIG (GAGGAGATTATTGCACGGAAAGTTG) and reverse primer 3′ADIG (ATGGTCACTTCCACAACCCAATCC) were designed to bind at 375 and 1065 bp of genomic *AtNOA*1 (gAtNOA1) respectively. These primers were used in conventional PCR, to amplify a 691 bp fragment from *gAtNOA*1 from 500 ng *A. thaliana* template DNA, using Recombinant Taq DNA polymerase (Fermentas International Inc., Burlington, Canada). The reaction mix consisted of the following: 1X Taq buffer, 200 µM of each dNTPs, 1 µM of each primer, 1.5 µM $MgCl_2$ and 0.25 U Taq DNA polymerase (Recombinant). PCR was carried out for 30 cycles and the following cycling conditions were applied: initial denaturation 94ºC for 2 min, denaturation 94ºC, 1 min, annealing 60ºC for 30 sec and elongation at 68ºC for 45 sec and final elongation 68ºC for 7 min. PCR product (5 µl) was run on a 1% agarose gel to check the results of the reaction.

A 1 µl aliquot of the above PCR was used as a template to amplify the probe, A-DIG, using PCR DIG Probe Synthesis Kit (Roche Applied Science, Penzberg, Germany). To 5 µl of PCR buffer with $MgCl_2$, 0.5 µM of each primer, 5 µl of PCR DIG mix, 0.75 µl of enzyme mix and enough nuclease-free water were added for a final volume of 50 µl (template included). PCR was carried out for 30 cycles and the following cycling conditions were applied: initial denaturation 95ºC for 2 min, denaturation 95ºC, 30 sec, annealing 60ºC for 30 sec and elongation at 72ºC for 40 sec and final elongation 72ºC for 7 min. An aliquot of 5 µl of PCR product was run on a 2% agarose gel to check the results of the reaction.

2.2.3.2 DNA extraction

DNA was extracted from *N. benthamiana* and cassava leaves using the CTAB protocol as performed in section 2.2.1.1. Approximately 30 µg of purified DNA was used for overnight digestion at 37 °C with *Hind*III. The DNA was separated by electrophoresis on a 0.8% agarose gel in 1X TAE buffer, then depurinated, denatured and transferred overnight onto Nylon membrane (Roche Applied Science, Penzberg, Germany) using capillary transfer, as

recommended by the manufacturer's manual. The transferred DNA was fixed on the nylon membrane by UV crosslinking for 3 min.

2.2.3.3 Hybridization

The PCR probe (4 µl) was denatured in 50 µl water, and added to 3.5ml of DIG Easy Hyb prepared from DIG Easy Hyb Granules (Roche Applied Science, Penzberg, Germany) according to the manufacturer's instructions. To calculate the temperature of hybridization (T_{hyb}). The following formulae were used:

$$T_m = 49.82 + 0.41\ (\%G + C) - 600/l \qquad \textbf{Equation 2-1}$$

$$T_{hyb} = T_m - 25°C \qquad \textbf{Equation 2-2}$$

Where

$T_m =$ melting point of probe-target hybrid

$(\%G + C) =$ % of G and C residues in probe sequence

$l =$ length of probe in bp

With a 37% G+C content and a 691 bp probe, T_{hyb} was calculated to be 39˚C. A temperature of 37˚C was used for hybridization as it is the minimum temperature recommended by the manufacturer, since no information was available at the time on the extent of possible similarity across the homologs. The blot was pre-hybridized at 37˚C and hybridized overnight at the same temperature. The following day, the membrane was first placed in a low stringency buffer (2× SSC containing 0.1% SDS) for 10 min, and then in 0.5× SSC + 0.1% SDS (at 60˚C) for 30 min as recommended for sequence homology of less than 80%.

2.2.3.4 Detection

After the stringency washes, the membrane was washed in washing buffer (0.1 M maleic acid, 0.15 M NaCl; pH 7.5; 0.3% (v/v) Tween 20) and incubated at room temperature for 30 min in blocking solution (0.1 M Maleic acid, 0.15 M NaCl adjusted to pH 7.5; 1% (w/v) blocking reagent). The blocking solution was discarded and the membrane was further incubated for 30

min in 20ml antibody solution (Anti-Digoxigenin-AP diluted 10 000 times in blocking solution). After washing twice with washing buffer, the membrane was incubated for 3 min in detection buffer (0.1 M Tris-HCl, 0.1 M NaCl, pH 9.5) to which 10ml of color substrate solution (200 µl NBT/BCIP in 10ml detection buffer) was added. The membrane was incubated overnight in the dark. The following day the membrane was washed in TE buffer and photographed using Nikon Coolpix S600. The image were cropped and labeled using Microsoft PowerPoint.

2.3 RESULTS

2.3.1 Amplification of AtNOA1 CDS and genomic sequences

Primers 5′and 3′ATNOS were used in an attempt to amplify the genomic sequence of *AtNOA*1 from *Arabidopsis*. *gAtNOA*1 (accession number NC003074), from the start codon, ATG, to the stop codon, TGA, is 3055 bp in length. With 18 nucleotides comprising the tail and restriction sites at both 5′and 3′end, an amplicon of 3073 bp was expected. As expected, PCR performed with 5′and 3′ATNOS primers gave a positive amplicon that matched around 3000 bp of the marker (Figure 2-1).

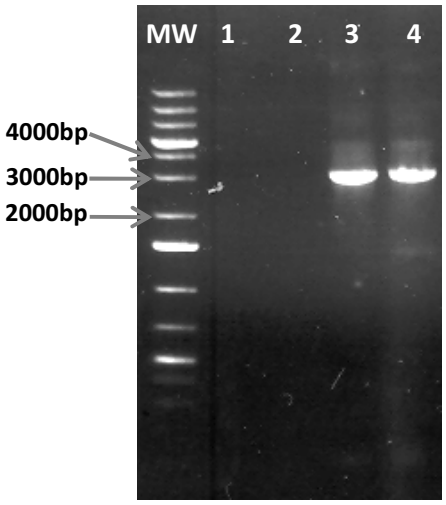

Figure 2-1: Amplification of AtNOA1 genomic sequence from *Arabidopsis*
PCR product (5 µl) was loaded in lanes 2-4. Lane 2, negative control, lane 3-4, gAtNOA1 3073 bp amplicon, run in duplicate. Molecular weight marker (MW), O'GeneRuler, DNA ladder 1KbPlus. These samples were analyzed on 1% agarose gel, with 1 µg/ml ethidium bromide

The same primers were used in a 2 step RT-PCR, to amplify *AtNOA*1 CDS from *Arabidopsis* and its homologs in cassava and *N. benthamiana*. Positive amplification was obtained for a *NbNOA*1 homolog from *N. benthamiana* (Figure 2-2). PCR using the same primers gave no amplification from cassava. The sequence of *NbNOA*1 was not yet available at the time of this experiment, nor were any EST clones with similarities to *AtNOA*1. Since then, *NbNOA*1 sequence has been published and its size revealed to be 1707 bp (Kato et al. 2007). *AtNOA*1 is 1686 bp in length, 21

bp smaller. Although slight, the difference can be seen in Figure 2-2, thereby showing that *NbNOA*1 and not *MeNOA*1 (from cassava) could be amplified using *AtNOA*1 specific primers.

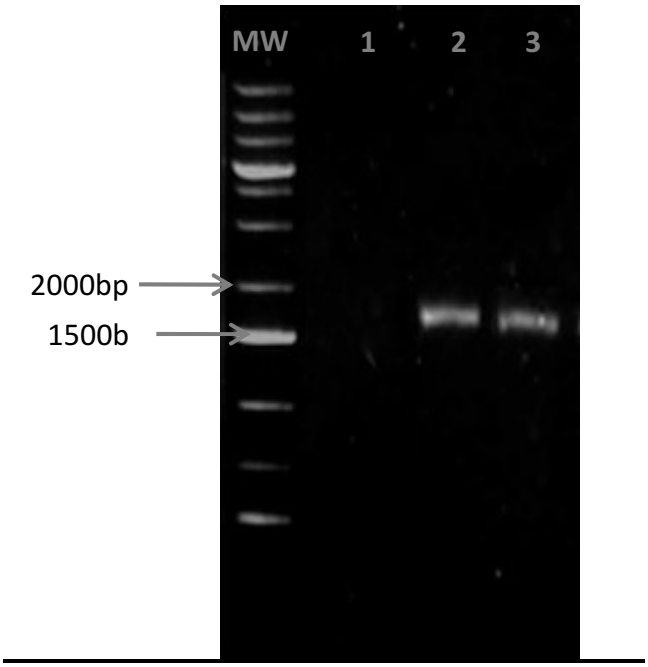

Figure 2-2: Amplification of *AtNOA*1 and *NbNOA*1 CDS
PCR product (5 µl) was loaded in lanes 1-3. Lane 1 negative control, lane 2 *N. benthamiana* 1725 bp PCR product, lane 3 *A. thaliana* 1704 bp PCR product. The amplicon sizes expected were calculated based on the length of the added tails and the publish sequence length. Using MW, O'GeneRuler, DNA ladder 1 KbPlus, bands of corresponding size were obtained. These samples were analyzed on 1% agarose gel, with 1 µg/ml ethidium bromide.

2.3.2 Southern Analysis

To confirm whether or not, there are sequences in the cassava genome, with any degree of nucleotide similarity to *AtNOA*1, Southern hybridization was performed using 30 µg of *N. benthamiana* and cassava genomic DNA. The *AtNOA1* DIG labeled probe was designed using the gAtNOA1 PCR product (Figure 2-3). The DIG labeled amplicons that were obtained, migrated slower than the non DIG-labeled amplicon because of the added DIG molecules present in DIG-labeled probes (Figure 2-3).

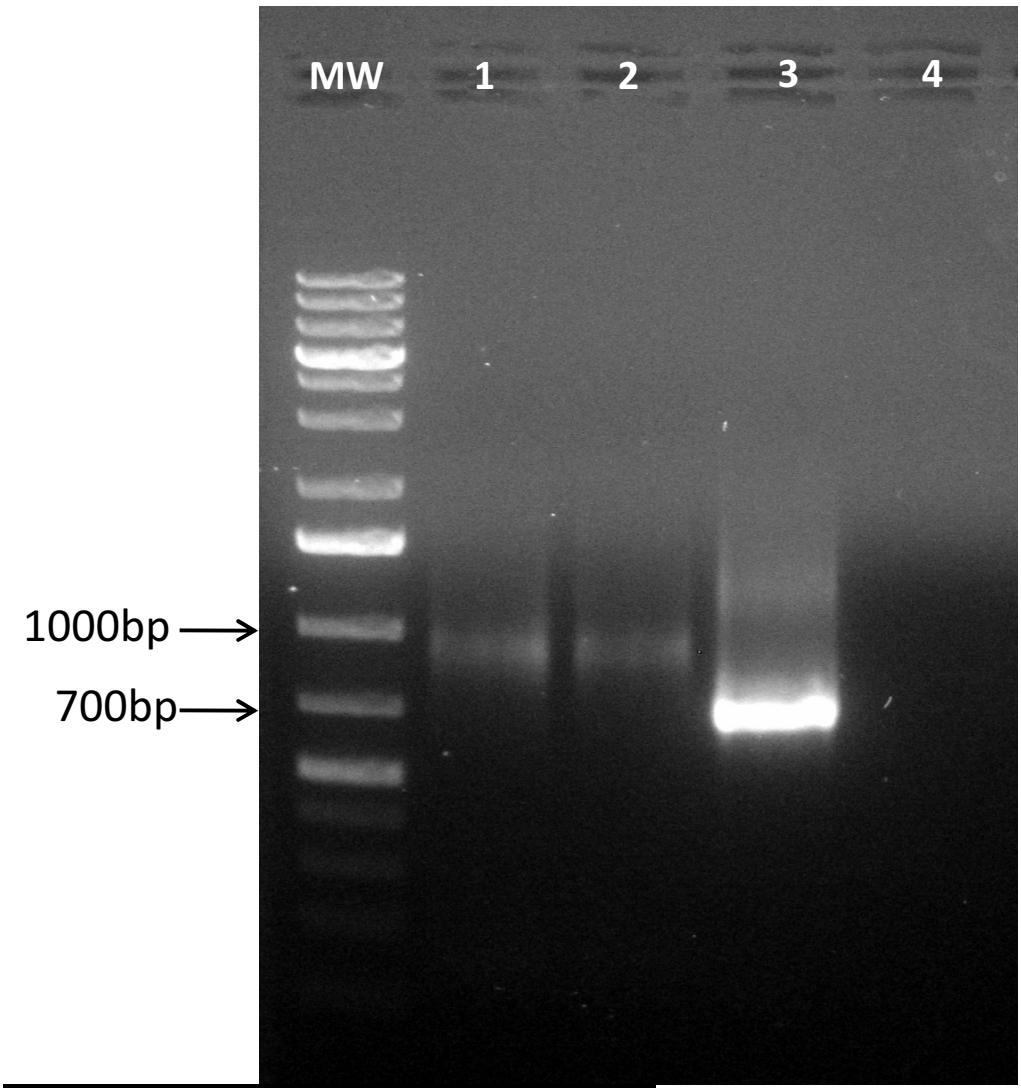

Figure 2-3: PCR amplification of the DIG probe.
PCR product (5 µl) was loaded in lanes 1-4. Lane 1-2, DIG labeled 691 bp AtNOA1 amplicon, run in duplicate, Lane 3 non-labeled AtNOA1 691 bp amplicon, lane 4 negative control. MW, O'GeneRuler, DNA ladder 1 KbPlus. These samples were analyzed on 1% agarose gel, with 1 µg/ml ethidium bromide.

The hybridization temperature and stringency of washes was decreased to allow for hybridization and a potential signal for identification of sequences with less than 80% homology. Hybridization was carried out 2˚C below the calculated T_{hyb} and the temperature at which the blot washes were lowered from 65˚C, the recommended temperature for low stringency washes, to 60˚C. Although faint, many non-specific hybridization bands were obtained for *N. benthamiana* and cassava DNA (Figure 2-4). As a positive control 100 ng of g*AtNOA1* amplicon not labeled with DIG was also loaded (Figure 2-3). The positive control showed non-specific

binding, most probably because of the smear visible in Figure 2-3 and the decrease in stringency of both the washes and hybridization temperature.

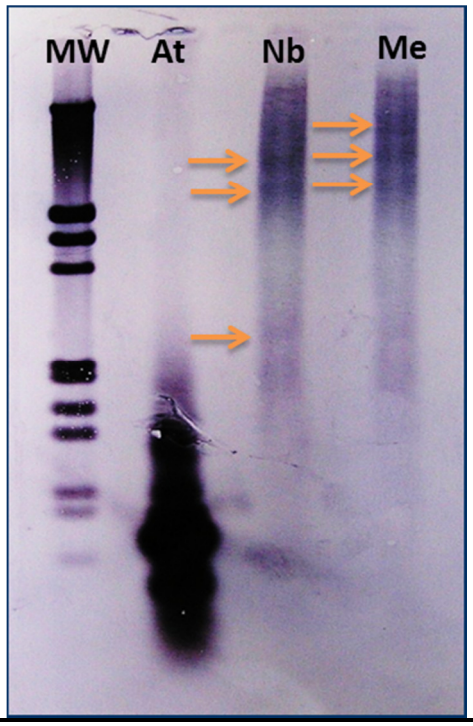

Figure 2-4: Southern blot hybridization using AtNOA1-specific probe
Southern blot analysis of *AtNOA*1 691 bp amplicon (At) and *Eco*RI digested *N. benthamiana* (Nb) and cassava (Me). 100 ng of *AtNOA*1 691 amplicon and 30 µg of *N. benthamiana* and cassava genomic DNA was loaded. MW: DNA molecular weight marker III (Roche Applied Science, Penzberg, Germany). 13 fragments: 125, 564, 831, 947, 1375, 1584, 1904, 2027, 3530, 4268, 4973, 5148, 21226 bp.

2.3.3 BLAST searches and protein alignments

Previous attempts to find cassava ESTs with sequence similarity to *AtNOA*1 sequence were unsuccessful, most probably because the number of cassava ESTs available at that point was low. However, recently, searching for *AtNOA*1 homologs in GenBank has identified a clone (CAS01018L19) from the cultivar MTAI16, with 2 ESTs bearing sequence similarity to *AtNOA*1 (Table 2-1). The 2 ESTs, accession numbers DB926445 and DB944551, when translated in the frames +3 and -3 respectively, have about 60% homology to AtNOA1 (Table 2-1). Both ESTs represent sequences from the cDNA clone CAS01 018 L19.

Table 2-1: Sequences producing significant alignments between AtNOA1 vs cassava ESTS (Genbank)

Accession	Description	Max score	Total score	Query coverage	E value	Max identity
DB944551.1	DB944551 full-length enriched cassava cDNA library Manihot esculenta cDNA clone CAS01_018_L19 3', mRNA sequence	159	159	21%	3e-39	60%
DB926445.1	DB926445 full-length enriched cassava cDNA library Manihot esculenta cDNA clone CAS01_018_L19 5', mRNA sequence	136	136	28%	2e-32	53%
FF536603.1	CASRQ24TF CASR Manihot esculenta cDNA 5', mRNA sequence	40.8	40.8	21%	0.001	23%
DB935037.1	DB935037 full-length enriched cassava cDNA library Manihot esculenta cDNA clone CAS01_042_F17 5', mRNA sequence	29.6	29.6	8%	3.1	38%
DV454505.1	CV02016A1B03.f1 CV02-normalized library Manihot esculenta cDNA clone CV02016A1B03.f1, mRNA sequence	29.6	29.6	5%	3.2	40%
FF380176.1	CASL692TF CASL Manihot esculenta cDNA 5', mRNA sequence	29.3	29.3	25%	4.5	23%
DB924576.1	DB924576 full-length enriched cassava cDNA library Manihot esculenta cDNA clone CAS01_013_J08 5', mRNA sequence	28.9	28.9	8%	5.1	38%
DB933053.1	DB933053 full-length enriched cassava cDNA library Manihot esculenta cDNA clone CAS01_036_O19 5', mRNA sequence	28.9	28.9	8%	5.1	38%
DB926092.1	DB926092 full-length enriched cassava cDNA library Manihot esculenta cDNA clone CAS01_017_L17 5', mRNA sequence	28.9	28.9	8%	5.4	38%
DB932750.1	DB932750 full-length enriched cassava cDNA library Manihot esculenta cDNA clone CAS01_036_B14 5', mRNA sequence	28.9	28.9	8%	5.8	38%

The sequence for each of the 2 matching EST clones was retrieved from GenBank and the position of the start codon ATG and the stop codon TTA was identified according to the reading frames given along with the BLAST results (Figure 2-5). Each EST was aligned using the multiple alignment algorithms in the AlignX package of VectorNTI. EST. DB926445 was found to align with the N-terminus and DB944551 with the C-terminus (Figure 2-6). These alignments revealed certain strings of amino acid sequences that are conserved across all three organisms in both termini. From the alignment, it was observed that amino acid sequences at the far-end of the N-terminus of *NbNOA*1 and *AtNOA*1 are highly similar. At the C-terminus this is true for all three sequences from cassava, *N. benthamiana* and *Arabidopsis.*

```
A      1 CAGACAATAATATGACATTTTCATTTTTCAATTTTGTAGATTAGT
      46 TATACACAAAGAATTTATCCAAAAACAAAGGTTAGAAATGCCATT
      91 TTGGTCTTAATTCCTCTTCCTTCTCAGTTAACTCCCGATACTGAT
     136 ACCACTCTGCTCCAGCTTTACCCACTGGCAATGGAGGCCGAACAA
     181 AAATCTCAACTGGCTTTGGAACATGAACAGCCAAATGCAATTCTT
     226 TAACAGTTTCTTCTAAATTCGATTCAGGCCTTCCAGGTGATCTAC
     271 TTACTGGTTCAATGGCAATCCATCCAAGACCAGATATAGCCACAT
     316 CACTTGCAGGTCTTCTGGGATCTTCGAATTTTATTTGCAGTTCAC
     361 GCATGATTTCAAGTCCTTTCCAGTCTTTTGCTTTCTTTTCTCCAG
     406 TAGGAGATGTCAATAGAACTCCGAGTTCTTTCT

B      1 KELGVLLTSPTGEKKAKDWKGLEIMRELQIKFEDPRRPASDVAIS
      46 GLGWIAIEPVSRSPGRPESNLEETVKELHLAVHVPKPVEIFVRPP
      91 LPVGKAGAEWYQYRELTEKEEELRPKWHF*PLFLDKFFVYN*STK
     136 LKNENVILLS

C      1 GGGTATACTAGTGTGTTGTACGCTGATTCTTTTCTTTCCACTCTA
      46 TCACTCGCCACCAAAAGCTAAAACCCCAGCTCTCTATCTTCTTTA
      91 ACGGTCTCTAATGGCGCCCAAAACCCTCTCCGCATTTCTCTCTCC
     136 TATATCTTCTCCCTCACCATCTTACCCAGTTTAACCCCAAATTCC
     181 TTAAAATTAACACGAAACCTACTCGCATCTTCTGTAAATCCGCAC
     226 AATCACATAAAACTCCGCTCTCGGAGACCCAATTATCAGTTTCCA
     271 TGCCGGAAGCCGGTGGTGCGGGGGCAGCTGCTCCTACCCCTGGAG
     316 AGCAGTTTCTTGAGCGCCAAAAAGCATTTGAAGCTGCGAAACTGG
     361 TTATGAAAGAGGCTAAGAAGAAAAAGAGGAGGGAGAAACAGAAGG
     406 CTTTGAAGGTGAACTCCGCAGTGGTTTGTTGTTATGGGTGCGGGG
     451 CTCCGTTGCAAACTTCGGATCAGGAAGCTCCGGGTTATGTGGACC
     496 CGGATACATATGAATTGAAGAAGAGACACCATCAGCTTAGAACTG
     541 TTCTTTGTGGGAGGTGTAGGCTGTTATCTCATGGTCATATGATAA
     586 CGGCTGTTGGTGGGAATGGAGGGTATCCTGGGGGGAAGCAGTTCG
     631 TTTCAGCT

D      1 VY*CVVR*FFSFHSITRHQKLKPQLSIFFNGL*WRPKPSPHFSLL
      46 YLLPHHLTQFNPKFLKINTKPTRIFCKSAQSHKTPLSETQLSVSM
      91 PEAGGAGAAAPTPGEQFLERQKAFEAAKLVMKEAKKKKRREKQKA
     136 LKVNSAVVCCYGCGAPLQTSDQEAPGYVDPDTYELKKRHHQLRTV
     181 LCGRCRLLSHGHMITAVGGNGGYPGGKQFVSA
```

Figure 2-5: Sequences of DB926445 (A) and DB944551 (C) including translated sequence (B and D)

(A) Sequence of DB944551 obtained from GenBank and showing highlighted in yellow, the stop codon TTA.

(B) Amino acid sequence of frame -3 translation of DB944551, highlighted in yellow, the position of the termination codon.

(C) Sequence of DB926445 obtained from GenBank; highlighted in yellow, the first ATG read in the +3 frame.

(D) amino acid sequence of frame +3 translation of DB926445 highlighted in yellow, the first methionine indicating the beginning of translation.

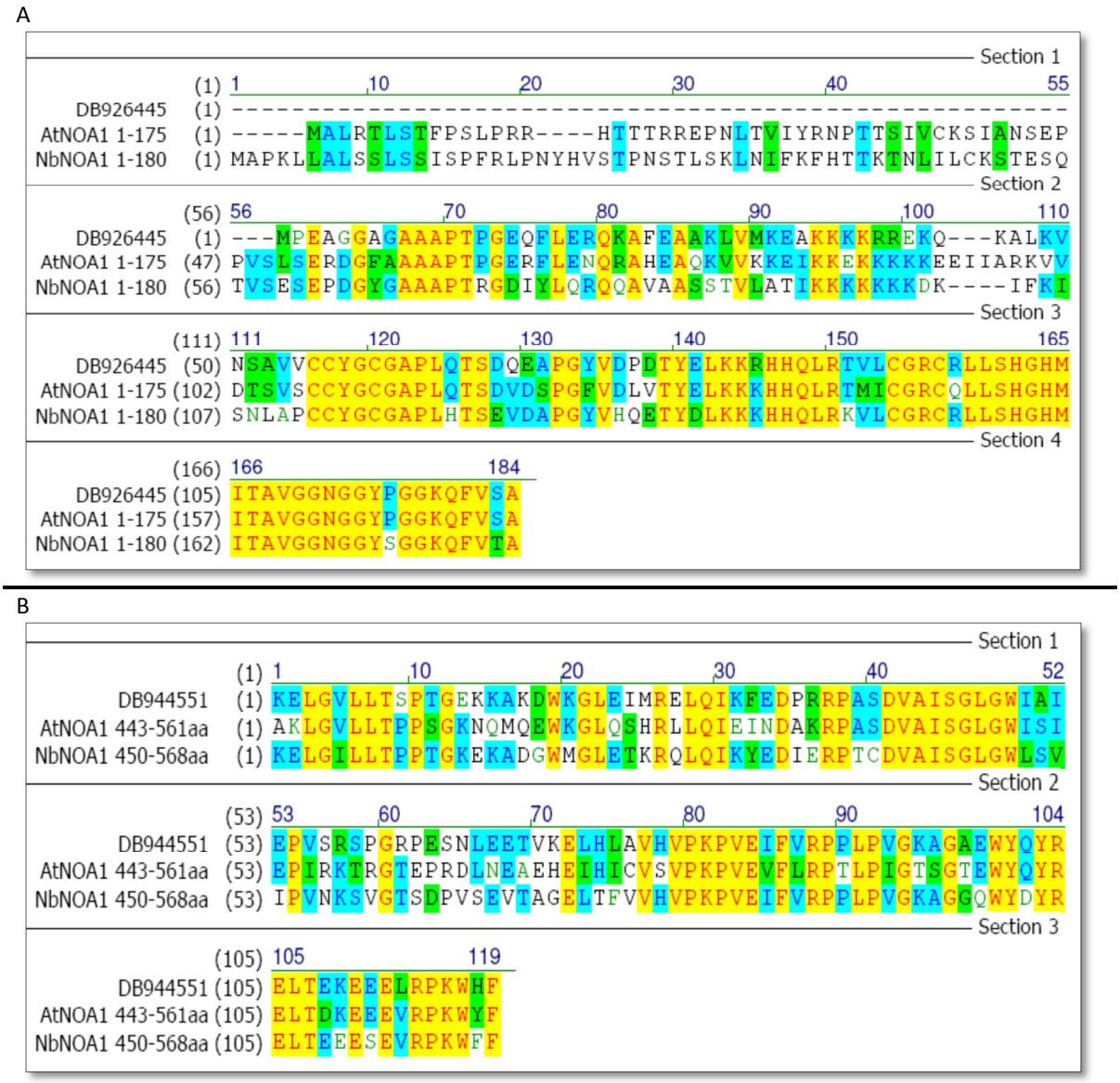

Figure 2-6: Sequence alignment of AtNOA1, NbNOA1 and translated putative NOA1 in cassava

(A) Amino acid sequences 1-175 for AtNOA1 and 1-180 for NbNOA1 were aligned with translated DB926445, from the first methionine amino acid. % amino acids identities across the species were, 70% DB944551 and AtNOA1, 63% DB944551 and NbNOA1, 50% AtNOA1 and NbNOA1. (B) Amino acid sequences 443-561 for AtNOA1, 450-568 for NbNOA1 were aligned with translated DB944551, until the last amino acid before the stop codon. % amino acid identities across the species were, 60% DB944551 and AtNOA1, 66% DB944551 and NbNOA1, 53% AtNOA1 and NbNOA1. Alignments were performed using AlignX module of VectorNTI (Invitrogen, Carlsbad, USA).

2.4 DISCUSSION

The objective in this study was to identify and possibly amplify *AtNOA*1 homolog in cassava. AtNOA1 and NbNOA1 have been associated with disease resistance. Amplifying the *NOA*1 cassava homologue would allow us to study its possible involvement in cassava responses to SACMV infection. *N. benthamiana* was chosen as a model host as it is extensively used in geminivirus research because of its susceptibility to geminiviruses (Goodin et al. 2008). Since the objective of the study was to develop a VIGS system based on SACMV-A, *N. benthamiana* was used as an experimental host for testing the VIGS vector designed in Chapter 3. At the time this research was carried out, *AtNOA*1 was the only member of this gene family to have been sequenced and published (Guo et al. 2003).

Because no phylogenetic data was available on *AtNOA*1 and the possible level of conservation of *AtNOA*1 across plant species was unknown, Southern analysis was carried out to detect potentially similar sequences in *N. benthamiana* and cassava. The hybridization and washing conditions were altered to allow for hybridization of *AtNOA*1 DIG probe to sequences with some degree of similarity in both cassava and *N. benthamiana*. Positive hybridization was obtained for both *N. benthamiana* and cassava, which confirmed the presence of genomic sequences with some degree of similarity to *AtNOA*1 in *N. benthamiana* and cassava.

After confirmation of the presence of sequences similar to *AtNOA*1 in cassava and *N. benthamiana* through Southern hybridization, *AtNOA1*-homologous sequences were searched for in ESTIMA and the cassava leafy spurge project dbESTs. AtNOA1 protein sequence (NP190329.2) was used to search each EST database using the translated nucleotide (TBLASTN) algorithm. Searching for homologs or similar sequences using protein or translated nucleotide sequence yielded no results. Homology searches using protein sequence was preferred over nucleotide sequence searches because of the redundancy of the genetic code; similarity across protein sequences would reflect probable functional homology better than nucleotides sequence similarity.

At this stage of the project, the lack of available sequences to be aligned with *AtNOA*1 from which a consensus sequence could be derived meant that no degenerate primers could be designed. Other methods such as rapid amplification of cDNA ends (RACE) PCR have been used for isolation of mRNA sequences. For RACE to work however, a partial sequence needs to be available either at the 3′ end or the 5′ end that could be used with 5′ end cap primers or oligo(dT) respectively. Using primers designed to amplify *AtNOA*1 mRNA from the start codon to the stop codon, *NbNOA*1 sequence could be amplified from *N. benthamiana.* Using the same method, no *MeNOA*1 could be amplified from cassava. Soon after *NbNOA*1 was amplified in our laboratory, a research group published the sequence of *NbNOA*1 that was identified from a cDNA library using primers designed on a partial *Solanum lycopersicum* (tomato) sequence (Kato et al. 2007).

With positive Southern hybridization results obtained, we concluded that failure to amplify *MeNOA*1 from cassava could have been due to low nucleotide sequence similarities at the annealing sites of primers designed on *AtNOA*1 nucleotide sequence. As a putative *MeNOA*1 could not be isolated from cassava, *NbNOA*1 was used in Chapter 4 for VIGS mediated silencing experiments in *N. benthamiana*. Since the completion of the research, more cassava EST sequences have been deposited in the public cassava dbEST at GenBank. Recent searches in the public dbEST have revealed 2 putative *MeNOA*1 ESTs. Both ESTs were sequenced from the clone CAS01018L19, from a cDNA library obtained from cultivar MTAI16 (Sakurai et al. 2007). Aligning translated nucleotide sequences for each EST with the NbNOA1 and AtNOA1 amino acid sequences, revealed high sequence similarity at the C-terminal across all three amino acids sequence. A stretch of sequence is missing at the N-terminal in the putative MeNOA1 amino acid sequence, validated the conclusion made here to why *MeNOA*1 could not be amplified using *AtNOA*1 specific primers.

This is the first report of identification of a putative *MeNOA*1 gene in cassava. The recent publication of the cassava genome will allow for more cassava genes to be identified and characterized. For the putative *MeNOA*1 gene in particular, the completion of the genome will reveal more about its sequence and maybe a link into the evolutionary conservation of this gene. NOA1 is evolutionary well conserved with homologs in *B. subtilis* as well as putative proteins

homologs in mammals *Drosophila, Caenorhabditis elegans* and *Fugu rubripes* (Zemojtel et al. 2006), suggesting a vital role for this gene family in gene function shared across different kingdoms. Functional characterization of the different putative homologs would contribute to a better understanding of the role of proteins from this gene family and whether they acquired novel function in plants, not found in other species. Plant NOA1 has been linked to disease resistance, only through their involvement with NO. With the discovery of the GTP hydrolysis function of NOA1, new models will need to be made on the link between GTP/GDP, NO and disease resistance. In relation to geminivirus infection, the speculations around the possible role of NOA1 are given in chapter 4.

CHAPTER 3.CONSTRUCTION OF SACMV-VIGS VECTOR

3.1 INTRODUCTION

Cassava mosaic disease (CMD) is the major threat to cassava growth and cultivation in Africa (Fauquet and Fargette 1990; Wydra and Verdier 2002). It affects mainly the leaves, causing chlorosis and mosaic pattern, eventually resulting in severely reduced foliage leading to lower yields. Cassava mosaic begomoviruses are the causative agents of CMD. They are encapsidated in 2 identical icosahedral capsids enclosing 2 ssDNA genomic molecules, DNA-A and DNA-B, of about 2.8 kb in size (Fauquet and Stanley 2003; Nawaz-ul-rehman and Fauquet 2009). DNA-A mainly encodes proteins required for replication and DNA-B, movement proteins.

SACMV is a strain of cassava mosaic begomoviruses identified in 1997 in South Africa (Berrie et al. 1997; Berrie et al. 2001). Since its identification, SACMV has been reported in cassava samples from Swaziland, Madagascar and Zimbabwe (Ndunguru et al. 2005; Briddon et al. 2004). Six other strains of *African* occurring cassava mosaic viruses have been identified: EACMV-UG, EACMV, EACMCV, EACMMV, EACMZV and ACMV. Geographically, EACMV and ACMV infections are more widely spread than SACMV and they have been shown to occur in mixed infections, resulting in an increase in symptoms severity (Figure 3-1).

Not all cassava cultivars are susceptible to CMGs; the mechanism of resistance to cassava mosaic virus is not completely understood. In some cultivars, the virus replicates within the host with no symptom development. In others, symptoms remission or recovery occurs. A plant is said to be in recovery when symptomless leaves, resistant to re-infection, emerge from an infected symptomatic plant as a result of VIGS (Van Kammen 1997; Baulcombe 2004; Ratcliff et al. 1999; Lindbo et al. 1993). Virus infection of the host results in an increase in transcriptional activity as the virus coerces the host's machinery into processing viral proteins as well as replication. Abundance in viral transcripts triggers a sequence of events leading to viral sequence-specific RNA silencing (Vanitharani et al. 2005).

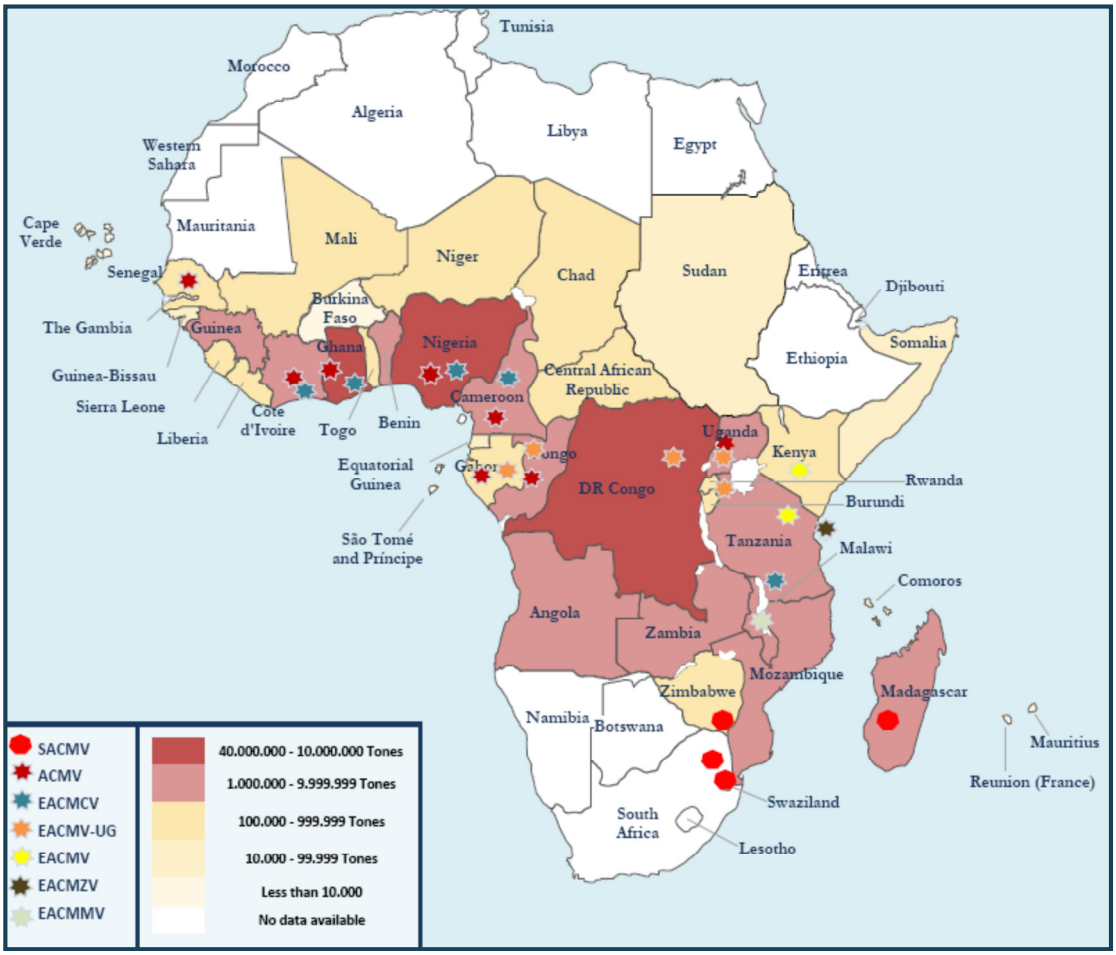

Figure 3-1: Map showing cassava production and the location of occurrence of cassava mosaic virus in Africa

Cassava productions values were obtained from Food And Agricultural Organization of United Nations: Economic And Social Department: The Statistical Division (FAO-STAT 2008). Occurrence of cassava mosaic viruses were distributed according to Ndunguru et al., 2005. The Map of Africa was drawn using SmartDraw 2010.

The ability of geminiviruses to induce RNA silencing has led researchers to develop silencing vectors with a geminivirus backbone (Huang et al. 2009; Peele et al. 2001; Golenberg et al. 2009; Fofana et al. 2004; Turnage et al. 2002; Muangsan et al. 2004; Pandey et al. 2009; Kjemtrup et al. 1998; Tao and Zhou 2004; Cai et al. 2007). These vectors are used for functional studies: a fragment of a gene of interest is inserted in the virus vector, and used to infect a host plant. As the host RNA silencing mechanism targets increasing viral transcripts arising from infection, the gene corresponding to the inserted fragment is inherently silenced. Begomoviruses silencing vectors have been designed using both the DNA-A and DNA-B components. Because of the presence of non-coding sequences in DNA-B, target gene fragments are inserted in the

non-coding region downstream of BV1 (Peele et al. 2001; Turnage et al. 2002). DNA-A based VIGS vectors are designed by replacing the CP with the target gene fragment, as the CP is dispensable for begomoviruses (Fofana et al. 2004). Begomoviruses CP is required for plants to vector transmission, encapsidation (BD Harrison 2002) and nuclear shuttling (Gafni 2002). Although a must for vector transmission, begomoviruses can replicate and spread systematically with the DNA-B encoded movement proteins, forgoing the need for the CP.

To attest to the functionality of VIGS vectors, endogenous genes have been used as visual reporter. *PDS*, *ChlH*, *sulfur gene (su)* are often used as a down-regulation of these genes results in bleaching of leaves or flowers (Robertson 2004). VIGS vector have been used for functional studies of a vast array of genes, including genes whose null mutations, established using other reverse genetics methods, are lethal (Peele et al. 2001; Qu et al. 2008). However because the virus vector retains characteristics of the non-modified vector, symptomatically, silencing genes involved in disease resistance does not always give clear results (Muangsan et al. 2004). The objective of this study was to develop a SACMV-DNA A based VIGS vector that could be used for functional studies in *N. benthamiana* and cassava, using *N. tabacum su*-gene as a reporter which has been used effectively to silence *su* in cassava (Fofana et al. 2004). Candidate genes believed to play a role in disease resistance in cassava and *N. benthamiana* like *MeNOA*1 identified previously in chapter 2 can be silenced using this approach and the effect of their silencing in response to geminivirus infection can be investigated.

3.2 MATERIALS AND METHODS

All nucleic quantification procedures were performed using the NanoDrop® ND-1000 spectrophotometer (NanoDrop Technologies, Wilmington, USA). All plasmid maps were derived using VectorNTI Advance 10. All primers were designed using the PrimerQuest package of the Scitools online tool available at Integrated DNA Technology (http://eu.idtdna.com/Home/Home.aspx) and synthesized by Inqaba Biotec (Pretoria, South Africa). PCR reactions were carried out using MyCycler Thermal Cycler (Bio-Rad, Hercules, USA). Table top centrifugation runs were carried out in *MiniSpin* (Eppendorf, Hamburg, Germany) and refrigerated centrifuge Mikro 200R (Andreas Hettich GmbH and Co. KG, Tuttlingen, Germany) large scale centrifugation runs were carried out in a Beckman J2-21 refrigerated high-speed centrifuge (Beckman Coulter, Brea, USA). BioDoc-It™ System, (UVP, Upland, USA) was used for agarose electrophoresis gel documentation and Microsoft PowerPoint was used to label the individual gel images.

3.2.1 Isolation of SACMV-DNA A

To isolate SACMV-DNA A molecules, DNA was extracted from SACMV-infected *N. benthamiana* samples using a modified CTAB extraction procedure as described in section 2.2.3.2. RCA was carried out on 50 ng template DNA extracted from infected *N. benthamiana* leaf samples using Illustra™ TempliPhi 100 Amplification Kit (GE Healthcare, Little Chalfont, UK) according to the manufacturer's instructions. The reaction was allowed to occur overnight.

3.2.2 Construction of SACMV-A partial dimer

3.2.2.1 Preparation of DH5α competent cells

To make DH5α competent cells, a inoculating loopful of DH5α glycerol stock was streaked onto a Luria Bertani agar plate (1% tryptone, 0.5% yeast extract, 1% NaCl, 1.5% agar (w/v)) and allowed to grow overnight at 37˚C. After overnight incubation, a single colony was used to inoculate 5ml of Luria Bertani (LB) medium (1% *g* tryptone, 0.5% yeast extract, 1% NaCl, w/v) and the culture was allowed to grow overnight. The following day, the 5ml overnight culture was

subcultured into 50ml of LB and allowed to grow for 90 min or until the culture reached OD_{600} of 0.3 to 0.5. The 50ml culture was centrifuged for 15 min at 3000 *g* in a Beckman J2-21 refrigerated high-speed centrifuge (Beckman Coulter, Brea, USA) at 4˚C. The supernatant was discarded and the pellet was gently resuspended in ice cold 5ml PIPES (Piperazine-1,4-bis(2-ethanesulfonic acid)) buffer (10 mmol/l $CaCl_2$, 10 mmol/l PIPES-HCl, 15% glycerol (v/v), pH 7) and incubated on ice for 20 min. The centrifugation step was repeated at 1000 *g* for 10 min at 4˚C. The supernatant was removed and the pellet resuspended gently in 2ml PIPES buffer. The competent cells were stored in 100 µl aliquots in a freezer, at -80˚C.

3.2.2.2 Construction of SACMV-A partial dimer infectious clone

To construct SACMV-A partial dimer infectious clone, the first step involved inserting a SACMV-A monomer into pTZ57R (pTZB2) and a partial SACMV-A sequence into pTZ57R (pTZBS). RCA product (5 µl) from 3.2.1 was digested using *Sal*I (Fermentas International Inc., Burlington, Canada), which cuts SACMV-A at 1857 bp, in O buffer, as recommended by the manufacturer. The restriction digestion ion product was purified using High Pure PCR Product Purification Kit (Roche Applied Science, Penzberg, Germany), eluted in 40 µl and further digested using *BamH*I (Fermentas International Inc., Burlington, Canada), in *BamH*I buffer, which cuts SACMV-A at 180 bp. pTZ57R was digested similarly. pTZ57R is a plasmid vector sold as part of the InsTAclone polymerase chain reaction (PCR) cloning kit (Fermentas International Inc., Burlington, Canada). It carries the β-lactamase gene to confer resistance against ampicillin. In a separate reaction, 5 µl of RCA product was digested using *BamH*I (Fermentas International Inc., Burlington, Canada), and pTZ57R (Fermentas International Inc., Burlington, Canada) was digested similarly.

Both RCA restriction digestion ion reactions and corresponding plasmids were run on a 1% agarose electrophoresis gel, extracted using QIAquick Gel Extraction Kit (Qiagen, Hilden, Germany) and ligated in a 1:3 ratio (vector:insert) using T4 DNA ligase (Fermentas International Inc., Burlington, Canada), according to the manufacturer's protocol. Each ligation (20 µl) reaction was transformed into 100 µl DH5α competent cells, which were plated on LB agar plates supplemented with 100 mg/L ampicillin, 100 µM isopropyl-β-D-thiogalactopyranoside (IPTG) and 20 mg/L (w/v) 5-bromo-4-chloro-3-indolyl-beta-D-galacto-pyranoside (X-gal). The

plates were incubated at 37°C for 16 h. Colonies containing presumptive positive recombinant plasmids were identified by their white color, and were used to inoculate 5ml LB supplemented with 100 mg/L ampicillin and allowed to grow overnight in a ZHWY-200D incubator (Zhicheng, Shanghai, China) set at 37°C and 200 rpm.

Recombinant pTZBS (Fragment *Sal*I-*BamH*I in pTZ57R) and pTZB2 (RCA fragment *BamH*I-*BamH*I) plasmids were extracted from overnight cultures using an alkaline lysis method based on Sambrook et al. (1989)(Sambrook et al. 1989). The culture (1.5 ml) was centrifuged in a *MiniSpin* (Eppendorf, Hamburg, Germany) at maximum speed for 1 min; unused culture was used to make a glycerol stock (15% glycerol) and stored at -70°C. The supernatant was discarded and the bacterial pellet resuspended in 250 µl of ice-cold resuspension solution/solution I (50 mM glucose, 25 mM Tris-Cl pH 8.0, 10 mM EDTA). The pellet was resuspended by brief vortexing, and 250 µl of lysis solution/solution II (0.2 M NaOH. 1% SDS) was added and the suspension was inverted gently to mix, and incubated at room temperature for 5 min. Ice-cold neutralization solution/solution III (350 µl) was added to the lysate and mixed by inversion until the formation of white cloudy flocculants containing cell debris was observed. The lysate was placed on ice for 5 min and then centrifuged in a *MiniSpin* (Eppendorf, Hamburg, Germany) at maximum speed for 10 min. To precipitate the nucleic acids, the supernatant was transferred in a new microcentrifuge tube to which 0.7 volume of isopropanol was added. The tube was mixed by inversion, then centrifuged in a *MiniSpin* (Eppendorf, Hamburg, Germany) at maximum speed for 10 min. The supernatant was discarded and the nucleic acid pellet washed in ice-cold 70% ethanol (v/v) by briefly vortexing to resuspend the pellet and centrifuging in a *MiniSpin* (Eppendorf, Hamburg, Germany) at maximum speed for 5 min. Ethanol was removed, the pellet was air dried and resuspended in 50 µl TE-RNase A buffer. The extracted pTZBS and pTZB2 plasmids were incubated at 37ºC for an hour to allow for completion of RNase digestion and plasmid resuspension.

pTZB2 was digested using the double cutter *BamH*I (Fermentas International Inc., Burlington, Canada) according to the manufacturer's protocol. pTZBS was digested similarly and dephosphorylated by adding 1 unit of shrimp alkaline phosphatase (SAP; Fermentas) in the digest reaction. Both digests were run on a 1% agarose electrophoresis gel, extracted using

QIAquick Gel Extraction Kit (Qiagen, Hilden, Germany) and ligated in a 1:3 ratio (vector:insert) using T4 DNA ligase (Fermentas International Inc., Burlington, Canada), according to the manufacturer's protocol. Each ligation reaction (20 µl) was transformed into 100 µl DH5α competent cells, which were plated on LB plates with 1.5% agar supplemented with 100 mg/L ampicillin. The plates were incubated at 37°C for no more than 16 h. Colonies were lifted off the plates and used to inoculate 5ml LB supplemented with 100 mg/L ampicillin and allowed to grow overnight in a ZHWY-200D incubator (Zhicheng, Shanghai, China) set at 37°C and 200 rpm. The presumptive recombinant plasmid was named pTZA (pTZ57R plasmid containing partial dimer of SACMV-A) and extracted from overnight cultures using alkaline lysis as described previously. To confirm recombination of pTZA, pTZA was digested with *Pst*I which has 3 restriction sites in pTZA.

pTZA was double-digested with *Hind*III (Fermentas International Inc., Burlington, Canada) and *Eco32*I (Fermentas International Inc., Burlington, Canada), and blunted using T4 DNA polymerase (Fermentas International Inc., Burlington, Canada) using the following reaction conditions: 1 µl 10X Buffer (Red), 50 µl pTZA restriction digestion ion reaction, 3 µl dNTP Mix (2.5 mM), 1 µl T4 DNA Polymerase, 5 µl sterile distilled H_2O. The reaction was incubated at 37°C for 30 min, and then stopped for 10 min at 75°C. The binary vector pCAMBIA0380 was linearized using *Sma*I (Fermentas International Inc., Burlington, Canada), a blunt end restriction enzyme, and simultaneously dephosphorylated with SAP (Fermentas International Inc., Burlington, Canada) according to the manufacturer's protocol. The blunted restriction digestion ion product from pTZA was separated by electrophoresis on 1% agarose electrophoresis gel, extracted using QIAquick Gel Extraction Kit (Qiagen, Hilden, Germany) and ligated in a 1:10 ratio (vector:insert) using T4 DNA ligase (Fermentas International Inc., Burlington, Canada), according to the manufacturer's protocol. Each ligation reaction (20 µl) was transformed into 100 µl DH5α competent cells, which were plated on LB plates with 1.5% agar supplemented with 100 mg/L kanamycin. The plates were incubated at 37°C overnight. Colonies were lifted off the plates and used to inoculate 5ml LB supplemented with 100 mg/L kanamycin and allowed to grow overnight in a ZHWY-200D incubator (Zhicheng, Shanghai, China) set at 37°C and 200 rpm. The presumptive recombinant plasmid was named pC8A and extracted from overnight cultures by alkaline lysis as described above. To confirm for recombination, pC8A was digested

with *EcoR*I (Fermentas International Inc., Burlington, Canada). In the text and result section, pC8A clone would be referred to as SACMV-A.

3.2.3 Construction of SACMV-A VIGS vector

To delete the CP and insert the multiple cloning sites (MCS), 2 sets of primers were designed; their respective sequences are listed in Table 3-1. The sequence of primers SAA/F and SAA/R were designed to match entirely on the SACMV-A sequence; primers MCS1/R and MCS2/F were designed to include restriction sites for restriction enzymes *Xba*I, *Sac*I, *Afe*I, *Acc65*I/*Kpn*I and *Xho*I (Table 3-1).

To delete the CP, conventional and assembly PCR was performed in MyCycler Thermal Cycler (Bio-Rad, Hercules, USA) using Phusion™ Hot Start High-Fidelity DNA Polymerase (Finnzymes, Espoo, Finland). Conventional PCR was carried on pTZB2 in 2 steps, using 2 sets of primers, SAA/F and MCS1/R and SAA/R and MCS2/F. The following cycling conditions were applied: initial denaturation 98ºC for 30 sec, denaturation 98ºC, 10 sec, annealing 63ºC for 10 sec and elongation at 72ºC for 15 sec and final elongation 72ºC for 10 min. The PCR reaction components were used as recommended by the manufacturer's without the optional addition of DMSO. The 2 PCR products were used as a template for the second step of PCR, using primers SAA/F and SAA/R. Similar cycling conditions as the first step was applied and reaction components were used as recommended by the manufacturer without the optional addition of DMSO.

The SAA/F-SAA/R amplicon was used to replace the fragment *Bsp1407*I and *BspT*I in pTZA. Both SAA/F-SAA/R amplicon and pTZA were digested with *Bsp1407*I (Fermentas International Inc., Burlington, Canada), purified using High Pure PCR Product Purification Kit (Roche Applied Science, Penzberg, Germany) and then digested and *BspT*I (Fermentas International Inc., Burlington, Canada), according to the manufacturer's instructions. The pTZA and SAA/F-SAA/R digestion reactions were run on a 1% agarose electrophoresis gel, extracted using QIAquick Gel Extraction Kit (Qiagen, Hilden, Germany) and ligated in a 1:3 ratio (vector:insert) using T4 DNA ligase (Fermentas International Inc., Burlington, Canada), according to the manufacturer's protocol. Each ligation reaction (20 µl) was transformed into 100 µl DH5α

competent cells, which were plated on LB plates with 1.5% agar supplemented with 100 mg/L ampicillin. The plates were incubated at 37°C for no more than 16 h. Colonies were lifted off the plates and used to inoculate 5ml LB supplemented with 100 mg/L ampicillin and allowed to grow overnight in a ZHWY-200D incubator (Zhicheng, Shanghai, China) set at 37°C and 200 rpm. The presumptive recombinant plasmid was pTZAΔCP (pTZ57R plasmid containing partial dimer of SACMV-A with no CP) and extracted from overnight cultures by alkaline lysis method as described above. To confirm correct insertion of the *BamH*I-*BamH*I fragments lacking the CP, extracted pTZAΔCP was digested with *SalI*. As with pTZA, pTZAΔCP was double-digested with *Hind*III (Fermentas International Inc., Burlington, Canada) and *Eco32*I (Fermentas International Inc., Burlington, Canada), blunted and ligated into linear pCAMBIA0380 (Figure 3-5A), transformed into DH5α as described for pTZA above. The recombinant plasmid was named SACMV-AΔCP.

3.2.4 Cloning of the Su gene

To amplify the *su*-gene from *N. tabacum, N. tabacum* seeds were grown in germination mix (Culterra, Muldersdrift, South Africa) in a seed tray, covered with cling wrap to provide moisture, at 25°C with a photoperiod of 16 h light and 8 h dark. Seedlings (3 weeks old) were transplanted in individual pots containing germination mix and allowed to acclimatize for a week. RNA was extracted using Tri Reagent (Sigma-Aldrich, St Louis, USA) from 4 week old seedlings. To avoid RNase contamination during RNA extraction, similar precautions as those stipulated in section 2.2.1.2 were taken.

Between 50 and 100 mg of leaf tissue was homogenized in a microcentrifuge tube using a micropestle in the presence of liquid nitrogen. The ground tissue was resuspended in 1ml of Tri Reagent (Sigma-Aldrich, St Louis, USA) and incubated at room temperature for 5 min. Chloroform (200 µl) was added, the sample was mixed vigorously, left to stand for 5 min at room temperature and centrifuged at 12000 g for 15 min at 4°C. The aqueous layer was transferred into a new microcentrifuge tube. To the aqueous phase 500 µl of isopropyl alcohol was added to precipitate RNA. The samples were incubated at room temperature for 10 min and centrifuged at 12000 *g* for 10 min at 4°C. The supernatant was removed and 1ml of 75% ethanol

(v/v) was added. The pellet was dislodged by brief vortexing and the sample was centrifuged at 7500 g for 5 min at 4°C. The RNA pellet was allowed to air dry for 10 min and resuspended in nuclease-free water. The extracted RNA was stored at -70°C. Extracted RNA (2 µg) was treated using RNase-free DNAse (Fermentas International Inc., Burlington, Canada) according to the manufacturer's recommendations. To prevent RNA degradation, 40 U of RNase inhibitor (Fermentas International Inc., Burlington, Canada) were included and the DNAse treatment was carried out for an hour.

N. tabacum RNA (1 µg) was reversely transcribed using SuperScript® III Reverse Transcriptase (Invitrogen, Carlsbad, USA) according to the manufacturer's protocol, using oligo(dT) as primers. The reverse transcription product (2 µl) was used for PCR, performed using Taq Polymerase (Recombinant, Fermentas International Inc., Burlington, Canada) using primers Su-Fw (CTTCTACACCCTTGTCTTCTCGCT) and Su-RV (CTCAACAACAAGTACACCCGAGTC) binding respectively at 67-90 bp and 1245 bp-1268 bp of the su-fragment. PCR was carried out in using MyCycler Thermal Cycler (Bio-Rad, Hercules, USA) and the following cycling conditions: initial denaturation 94ºC for 2 min, denaturation 94ºC, 30 sec, annealing 63ºC for 20 sec and elongation at 68ºC for 1 min and final elongation 68ºC for 10 min. The PCR reaction components were used as recommended by the manufacturer's recommendation however using a final primer concentration of 0.5 µM. The amplicon was TA-cloned into pTZ57R/T contained in the InsTAclone kit (Fermentas International Inc., Burlington, Canada) according to the manufacturer's recommendations. Each ligation reaction (20 µl) was transformed into 100 µl DH5α competent cells, which were plated on LB agar plates with 100 mg/L ampicillin, 100 µM IPTG and 20 mg/L (w/v) X-gal. The plates were incubated at 37°C for no more than 16 h. White colonies were used to inoculate 5ml LB supplemented with 100 mg/L ampicillin and allowed to grow overnight in a ZHWY-200D incubator (Zhicheng, Shanghai, China) set at 37°C and 200 rpm.

The recombinant vector was digested using *Eco32I* (Fermentas International Inc., Burlington, Canada) yielding a blunt fragment that was subcloned in *Eco47III*/*Afe*I (Fermentas International Inc., Burlington, Canada) digested and SAP (Fermentas International Inc., Burlington, Canada)-dephosphorylated SACMV-AΔCP. Both restriction digestion ion were separated on 1%

electrophoretic agarose gel, gel-extracted using QIAquick Gel Extraction kit (Qiagen, Hilden, Germany) and ligated in a 1:10 ratio (vector:insert) using T4 DNA ligase (Fermentas International Inc., Burlington, Canada), according to the manufacturer's protocol. Each ligation reaction (20 µl) was transformed into 100 µl DH5α competent cells, which were plated on LB plates with 1.5% agar supplemented with 100 mg/L kanamycin. The plates were incubated at 37°C overnight. Recombination was confirmed using colony PCR with primers SAA/F and SAA/R. Colony-PCR was performed in the MyCycler Thermal Cycler using the following cycling conditions: initial denaturation 94ºC for 2 min, denaturation 94ºC, 30 sec, annealing 63ºC for 20 sec and elongation at 68ºC for 30 sec and final elongation 68ºC for 10 min. The PCR reaction components were used as recommended by the manufacturer with final primer concentration of 0.5 µM. Positive colonies were used to inoculate 5ml LB supplemented with 100 mg/L kanamycin and allowed to grow overnight in a ZHWY-200D incubator (Zhicheng, Shanghai, China) set at 37°C and 200 rpm. The recombinant plasmid was named SACMV-A::*su* and extracted from overnight cultures by alkaline lysis as described above, then stored at -20°C. To check for orientation of the insert in the recombinant plasmid, PCR was performed on SACMV-A::*su* using primers SAA/F-SAA/R. A restriction digestion ion was performed on the amplicon using *EcoR*I (Fermentas International Inc., Burlington, Canada) and *Afl*II/*BspT*I (Fermentas International Inc., Burlington, Canada) in O buffer as per manufacturer's recommendation. 2 clones, SACMV-A::*su*1 and 2 with different insert orientation were isolated.

3.2.5 Infection of N. benthamiana and Cassava

3.2.5.1 Preparation of *Agrobacterium tumefaciens* competent cells

To prepare competent *A. tumefaciens* cells*, A. tumefaciens* C58C1 cultures were initiated by inoculating 5 ml of YEP media (10 g/L peptone, 5 g/L yeast extract, 5 g/L NaCl, 20 mM $MgSO_4$ pH 7.2) supplemented with 50 mg/L rifampicin, with some scraping of a C58C1 glycerol stock and allowing this to grow overnight, at 28°C, shaking at 220 rpm. The next day, 50ml fresh YEP media with rifampicin (50 mg/L) was inoculated using 2ml of the overnight culture and allowed to grow for about 6-8 h, until the culture reached an OD_{600} between 0.5 and 1.0. The 50ml culture was centrifuged for 10 min at 10000 *g* in a Beckman J2-21 refrigerated high-speed centrifuge (Beckman Coulter, Brea, USA). The supernatant was discarder and the pellet washed

by resuspending in 5ml of ice-cold 20 mM $CaCl_2$. The centrifugation step was repeated and the supernatant once again discarded. The pellet was resuspended in 1ml of ice-cold 20 mM $CaCl_2$ and stored at -70°C in 100 µl aliquots.

3.2.5.2 Transformation into *A. tumefaciens*

To transform the different constructs into C58C1, 500 ng of plasmids SACMV-DNA-A, SACMV-AΔCP; SACMV-DNA B and SACMV-A::*su*1 and 2 were added in 100 µl of frozen C58C1 competent cells. This was placed on ice, mixed intermittently and allowed to thaw. Once the cells had thawed, they were placed in liquid nitrogen to snap freeze for 5 min. The cells were allowed to thaw at room temperature and used to inoculate 2ml of fresh YEP media, which was incubated with moderate shaking at 28°C for 3 h to allow for the cells to express the kanamycin resistance gene found on the transformed plasmid. After 3 h, the cells were spun in a benchtop *MiniSpin* (Eppendorf, Hamburg, Germany) for 5 min at maximum speed, to collect the cells in a pellet. The supernatant was discarded, the pellet was resuspended in 50 µl YEP media supplemented with 100 mg/L kanamycin and 50 mg/L rifampicin and spread on a plate of YEP agar with 100 mg/L kanamycin and 50 mg/L rifampicin. The plate was incubated at 28°C to allow for selection of transformants. Single colonies were collected off the plates after 2 days, for colony PCR to confirm presence of positive transformants. Positive colonies were grown to saturation in 5ml YEP media supplemented with 100 mg/L kanamycin and 50 mg/L rifampicin. The culture was used to make 15% glycerol stocks and stored at -70°C.

3.2.5.3 Infiltration of *N. benthamiana*

To infect *N. benthamiana* using agroinfiltration glycerol stocks of *A. tumefaciens* C58C1 containing the different plasmid were used to inoculate 5 ml YEP media containing 100 mg/L kanamycin and 50 mg/L rifampicin and grown overnight at 28°C. The following day, 50ml of fresh YEP media supplemented with 10 mM morpholino-ethane-sulfonic acid (MES), 20 µM acetosyringone 100 mg/L kanamycin and 50 mg/L rifampicin was inoculated with the overnight culture and allowed to grow overnight. The cells were collected by centrifugation at 10000 *g* for 10 min in Beckman J2-21 refrigerated high-speed centrifuge (Beckman Coulter, Brea, USA). The pellet was resuspended in enough infiltration media (sterile distilled water containing 10 mM $MgCl_2$, 10 mM MES, and 200 µM acetosyringone) for an OD_{600} of 1. The culture was

incubated at room temperature for 3 hours to allow for the expression of the *vir* genes needed to facilitate T-DNA transfer. Unless otherwise indicated, each DNA-A equivalent plasmid (plasmids SACMV-A, SACMV-AΔCP and SACMV-A::*su*1 and 2) was mixed with an equal volume of plasmids SACMV-DNA B and the mixture was used to infiltrate the 2 source leaves (lower leaves) of *N. benthamiana* using a needleless syringe.

N. benthamiana seeds were germinated in germination mix (Culterra, Muldersdrift, South Africa) in a seed tray, covered with cling wrap to provide for moisture, at 25°C with a photoperiod of 16 h light and 8 h dark. Three week old seedlings were transplanted in individual pots containing germination mix and allowed to acclimatize for a week. At 4 weeks, the source leaves of plants that had reached the four to six leaf stage were infiltrated using *A. tumefaciens* cultures containing SACMV-A and SACMV-DNA B, SACMV-AΔCP and SACMV-B, SACMV-A::*su*1 and SACMV-DNA B, SACMV-A::*su*2 and SACMV-DNA B. Plants previously infiltrated with SACMV-A::*su* and SACMV-DNA B were re-infiltrated, 7 days later, with SACMV-A and SACMV-DNA B and 4 plants were used for infiltration with each construct. To study the effect of the development age of the plant in silencing, SACMV-A::*su*2 and SACMV-DNA B were used to infiltrate *N. benthamiana* older than 6 weeks. At 12, 21 and 35 dpi, leaf symptoms were observed and images captured using Nikon Coolpix S600, and edited in Microsoft PowerPoint.

From a culture of cassava T200 grown aseptically, T200 was propagated via nodal propagation on Murashige and Skoog (MS) medium (Murashige and Skoog 1962) supplemented with 20 g/l sucrose (MS2; Highveld Biological, Modderfontien, South Africa), solidified with 7.8 g/l agar, pH 5.8, and allowed the nodal explants to grow at 25ºC under a 16 h photoperiod until apparition of roots. The nodal explants were then transferred onto Jiffy® pellets and placed in a tray covered with a cling film, to simulate the moisture environment of the tissue culture plates in which they were previously found, and gradually creating slits in the cling film to allow for acclimatization. These plants were acclimatized in a Binder growth cabinet at 28°C/26°C with a photoperiod of 16 h light and 8 h dark until they were about 10 cm tall. The leaves were agroinfiltrated using SACMV-AΔCP and SACMV-B and SACMV-A::*su*2 and SACMV-DNA B resuspended in infiltration media supplemented with one drop of Tween-20 for every 50ml of

infiltration media. Four plants were used for infiltration with each construct. Cassava leaves were agroinfiltrated on the abaxial side of their leaves with 1ml syringe. The appearance of symptoms was captured using Nikon Coolpix S600. The images were cropped and labeled using Microsoft PowerPoint.

3.3 RESULTS

3.3.1 Isolation of SACMV-A and B

Genomic DNA was extracted from SACMV infected *N. benthamiana* plants in order to isolate circular ssDNA to be used in designing the VIGS vectors. Using φ29 DNA polymerase contained in the Illustra™ TempliPhi 100 Amplification Kit (GE Healthcare, Little Chalfont, UK), circular ssDNA-A and B were amplified from DNA extracted from infected *N. benthamiana* leaf samples through a RCA mechanism, resulting in concatemers.

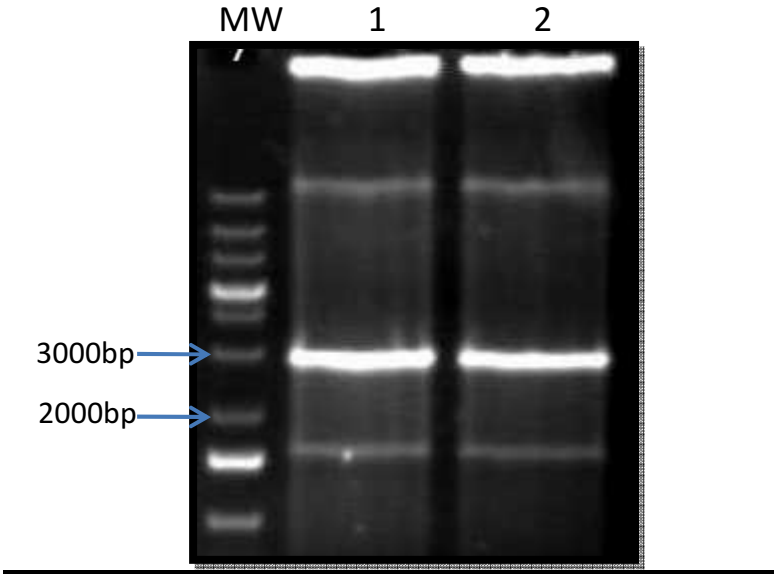

Figure 3-2: Restriction digestion of SACMV-A and SACMV-B.
RCA product (10 µl)was loaded in each lane. DNA-A shown here (Lane 1) was digested with *Sal*I and DNA-B (lane 2) with *Xho*I. The bands between the markers 2000-3000 bp represent 2800 bp for DNA-A and 2760 bp for DNA-B. O'Generuler™ 1 Kb Plus DNA ladder was used as molecular marker (MW).These samples were analyzed on 0.8% agarose gel in 1XTAE, with 1 µg/ml ethidium bromide

VectorNTI (Invitrogen, Carlsbad, USA) was used to find single cutters that selectively digest each SACMV monomer, *Sal*I and *BamH*I were identified as restriction enzymes that selectively cut SACMV-A and *Xho*I as the restriction enzyme that cuts SACMV-DNA B alone. Restriction digestion using these enzymes allowed for the isolation of monomers of SACMV-A and B (Figure 3-2).

3.3.2 Construction of SACMV-A partial dimer

In order to construct a VIGS vector that does not carry an open reading frame (ORF) coding for the CP, a partial dimer infectious clone of SACMV-A was constructed to contain only one copy of the AV1 ORF. A partial fragment flanked by restriction sites *SalI-BamH*I, representing 180-1857 bp of SACMV-A was inserted into pTZ57R giving rise to pTZBS plasmid (Figure 3-3A). The monomer that contains a full SACMV-A sequence flanked by restriction sites *BamH*I and *BamH*I is shown as inserted in pTZB2 (Figure 3-3B), representing the SACMV-A region 180 bp-2800 bp and 1 bp-180 bp, was subcloned into pTZBS and the recombinant vector was named pTZA (Figure 3-3C; Figure 3-4A). pTZA was screened by restriction digestion ion using *Pst*I. According to the plasmid map in Figure 3-4A, *Pst*I cuts pTZA three times at 1133 bp, 3933 bp and 4587 bp. Restriction digestion on pTZA should yield fragment of sizes 3342, 2800 and 654 bp, which were obtained and are shown on the electrophoretic gel in Figure 3-4B.

pTZA was made up of an entire SACMV-A monomeric sequence (from *BamH*I to *BamH*I) and a partial sequence (from *Sal*I-*BamH*I) , containing 2 CR sequence, between which exists one ORF for AC1, AC2, AC3, AC4, AV1, AV2 (Figure 3-3C; Figure 3-4A). Included in the partial dimer outside the region bordered by CR are an extra ORF for AC4 and a truncated AC1.

The partial dimer was removed from pTZA using restriction enzymes *EcoR*V and *Hind*III, shown in Figure 3-5C to cut on either side of the two CR respectively at 651 bp and 4601 bp. The fragment *EcoR*V and *Hind*III was blunted and subcloned into pCAMBIA0380 (Figure 3-5A), a binary vector that does not carry a reporter gene nor antibiotic resistance genes within the T-DNA borders, yielding a recombinant vector named pC8A or SACMV-A (Figure 3-5B). As the *EcoR*V- *Hind*III fragment was blunt end cloned, the insertion in pCAMBIA0380 could have occurred in two orientations. To confirm orientation of insertion of the partial dimer fragment *EcoR*V – *Hind*III from pTZA into pCAMBIA0380, pC8A was digested with *EcoR*I, which would give different banding pattern, depending on the orientation of the insert. Based on the banding pattern obtained (Figure 3-6), the plasmid map for pC8A was predicted to be as shown in (Figure 3-5B). pC8A was transformed into *A. tumefaciens* C58C1 and will be referred to as SACMV-A.

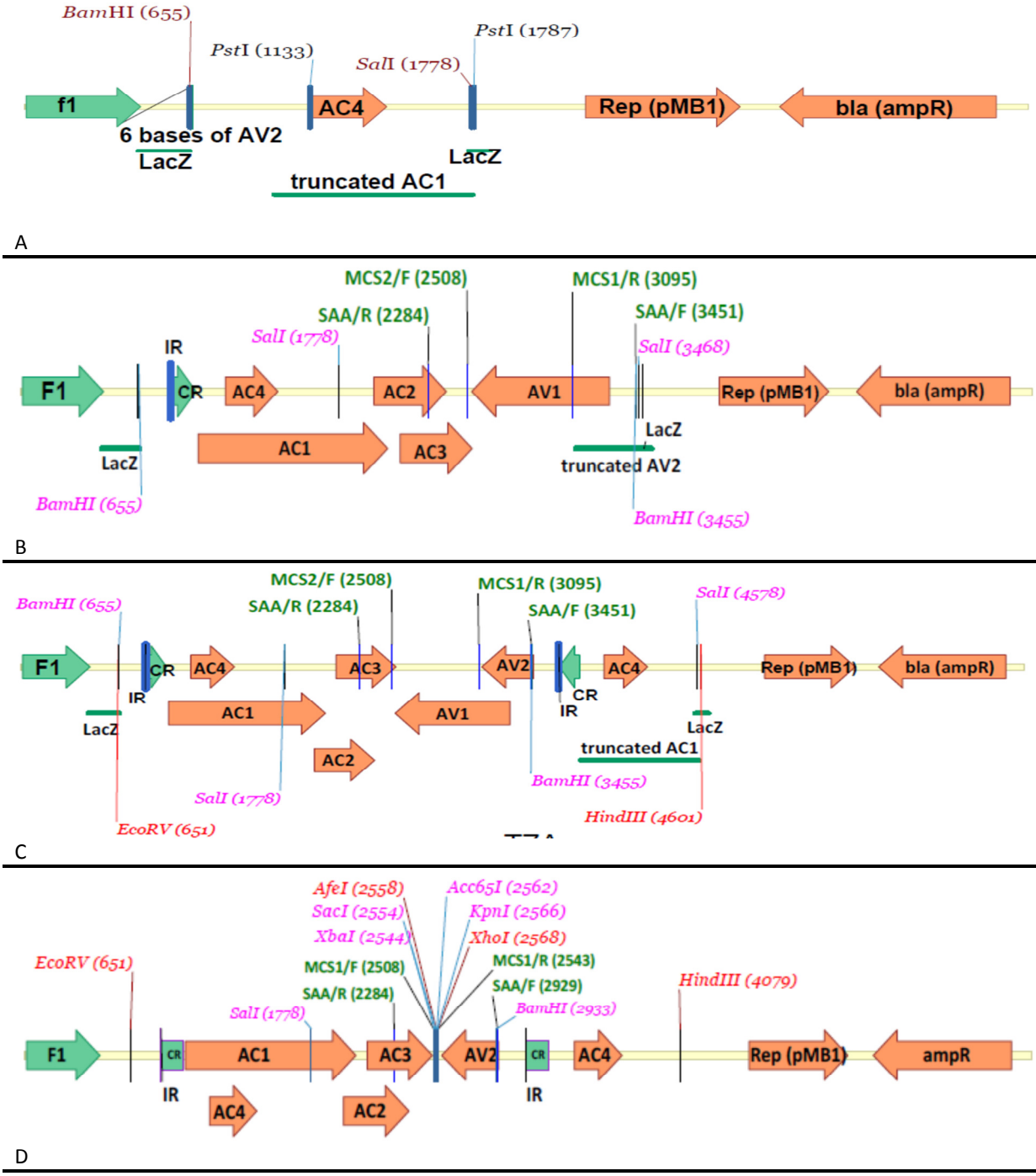

Figure 3-3: Diagrammatic representation of constructs designed in steps leading to SACMV-A vector
(A) PTZBS (B) pTZB2 (C) pTZA (D) pTZAΔCP. Orange arrows showing ORF; CR→ Common region; IR→ Intergenic region. MCS1/R, MCS2/F, SAA/F, SAA/R primers used to delete AV1 (CP). Primer binding sites and restriction site position are shown in brackets. Plasmid maps drawn using VectorNTI Advance 10 (Invitrogen, Carlsbad, USA).

A

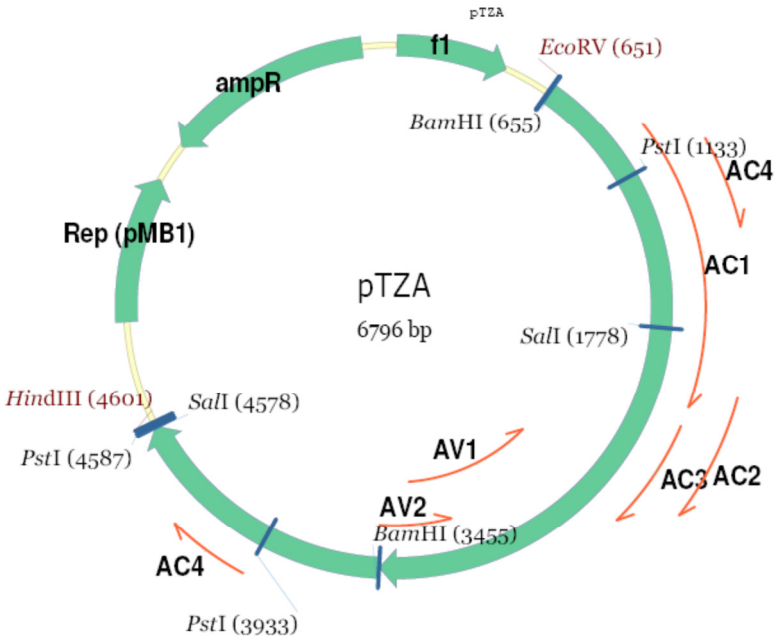

B

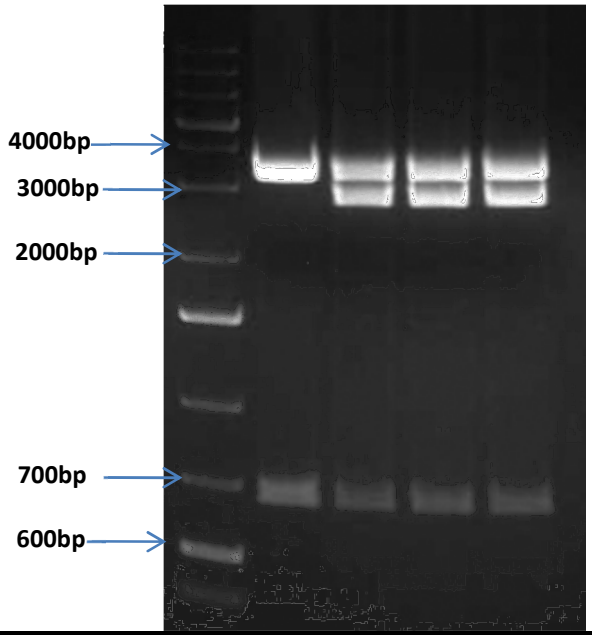

Figure 3-4: Screening of pTZA

Putative pTZA infectious clones were extracted using alkaline lysis and digested with *Pst*I which cuts pTZA 3 times at 1133 bp, 3933 bp and 4587 bp

(A) Cutting pTZA with *Pst*I would yield 3 fragments (B) of sizes 3342, 2800 and 654 bp. Plasmid map drawn using VectorNTI Advance 10 (Invitrogen, Carlsbad, USA).

(B) Four putative clones digested with *Pst*I were analyzed on 1X TAE, 1% agarose gel, with 1 µg/ml ethidium bromide. Positive banding pattern seen in lane 2-4. Molecular weight marker (MW) O'Generuler™ 1 Kb Plus (Fermentas International Inc., Burlington, Canada) DNA ladder (MW).

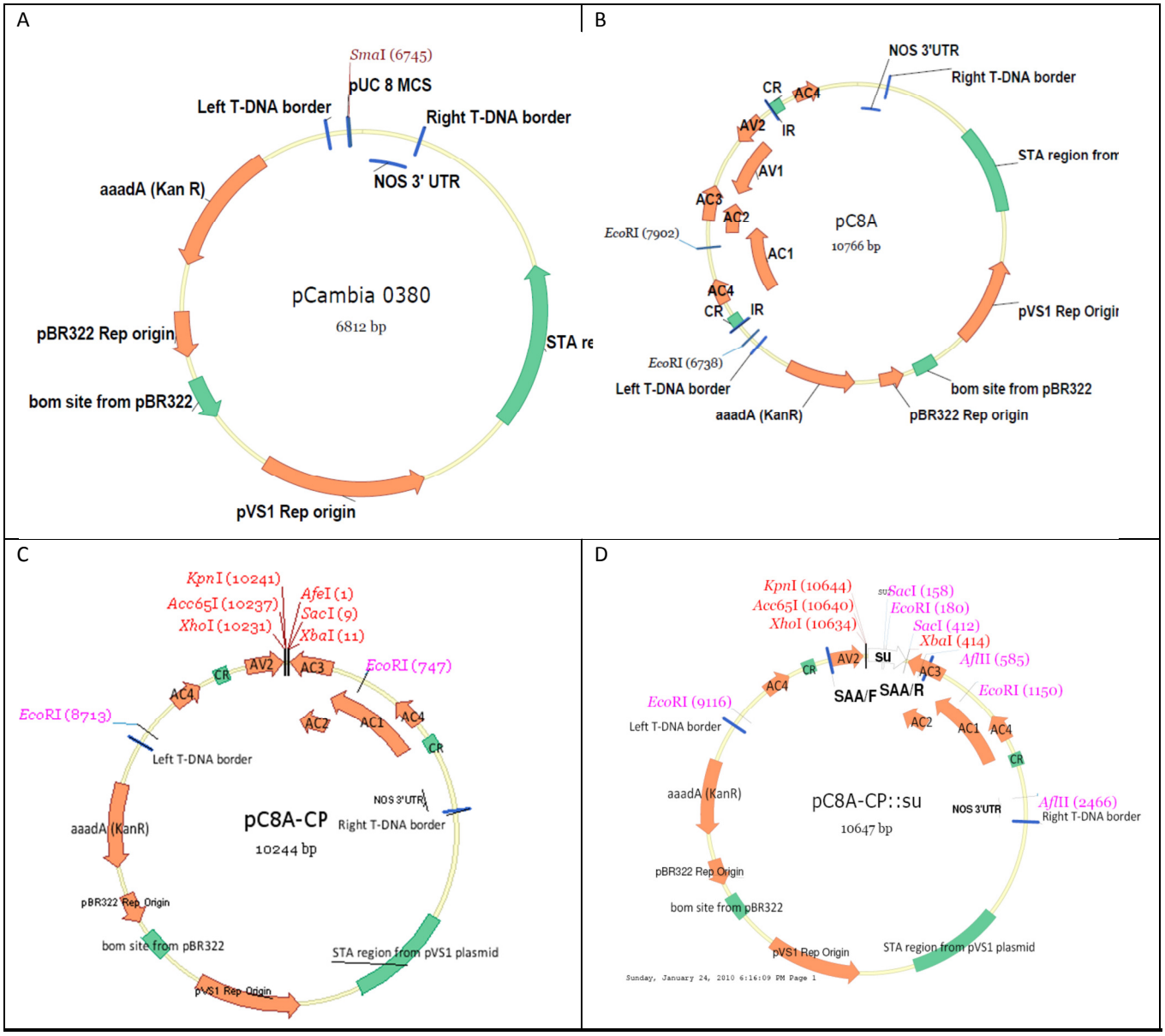

Figure 3-5: Maps of the different plasmids used for VIGS vector design

(A)-pCAMBIA0380 (Cambia) (B)-SACMV-A partial infectious clone (C)-SACMV-A VIGS vector (D)-*su* cloned into SACMV-A VIGS vector. The positions of the different restriction enzymes and primers used are indicated in these maps, to give an idea of the sizes expected fragments, unless otherwise stated. Plasmid maps were drawn using VectorNTI Advance 10.

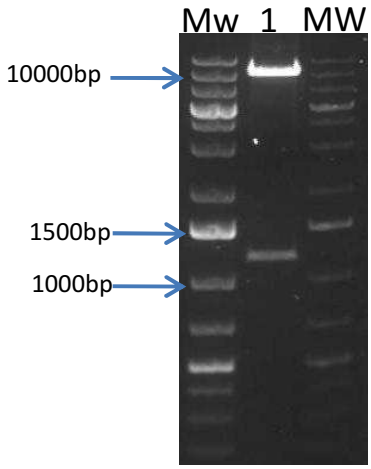

Figure 3-6: Screening of SACMV-A partial dimer
To verify the orientation of the SACMV-A partial dimer in pCAMBIA0380, pC8A was digested with *EcoR*I which cuts pC8A at 6378 bp and 7902 bp yielding 2 fragments of 1164 bp and 9602 bp (lane 1). Gel electrophoresis was carried out in 1XTAE 1% agarose with 1 µg/ml ethidium bromide with, O'Generuler^{TM} 1 Kb Plus (Fermentas International Inc., Burlington, Canada) DNA ladder (MW) on each side of the sample lane.

3.3.3 Construction of SACMV-AΔCP (SACMV-A VIGS)

Using pTZA (Figure 3-3C; Figure 3-4A), 2 sets of primers were designed to allow for the replacement of AV1 ORF with a MCS (Table 3-1). Primers SAA/F and SAA/R were designed to bind, respectively, at 164-187 bp and 1331-1354 bp of SACMV-A. Primers MCS1/R and MCS2/F were designed to bind respectively at 521-543 bp and 1096-1130 bp of SACMV-A. A 30 bp fragment bearing restriction sites for enzymes *Xba*I, *Sac*I, *Afe*I, *Acc65*I/*Kpn*I and *Xho*I (Table 3-1) was added to primers MCS1 and MCS2. The sequence was inserted in opposite orientation for the MCS primers to allow for fragment assembly using polymerase (Stemmer et al. 1995). Primers were designed to replace the region 543 bp-1096 bp from SACMV-A with an MCS bearing the 5 different restriction enzymes. Assembly PCR was carried out in two steps. The first step resulted in amplification of the region between 164 bp-543 bp, using primers SAA/F and MCS1 and the region between 1096-1354 bp using primers MCS2 and SAA/R.

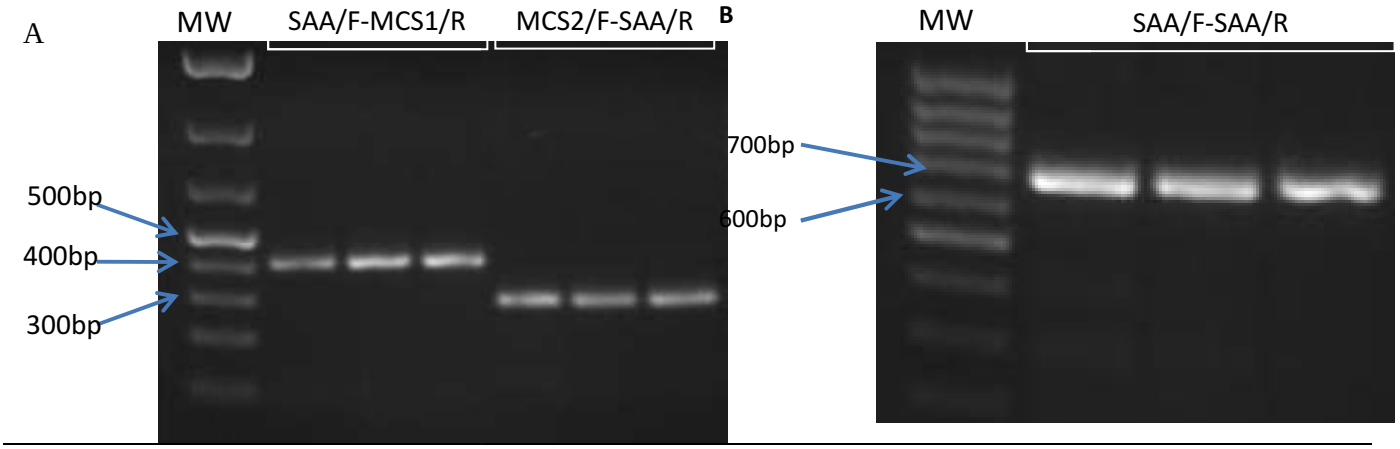

Figure 3-7: Amplification of fragments SAA/F-SAA/R using assembly PCR
Gel electrophoresis was carried out in 1XTAE 4% agarose with 1 µg/ml ethidium bromide. Molecular weight marker (MW) O'Generuler™ 1 Kb Plus (Fermentas International Inc., Burlington, Canada) DNA ladder (MW) was used for (A) and O'GeneRuler™ 50 bp (Fermentas International Inc., Burlington, Canada) DNA Ladder for (B). Different primers combinations used are indicated above in each electrophoretic gel in (A) and (B). Using combination SAA/F-MCS1/R the fragment expected was of size 409 bp and the combination MCS2/F-SAA/R, 288 bp (A). Combining the fragments, as expected, an amplicon of 667 bp was obtained (B).

Table 3-1: Primers used to replace AV1 (CP) from SACMV-A with the *su* gene in *N. benthamiana*

Primer Name	Sequence
SAA/F	GCGTGTCAACATGTGGGATCCATT
SAA/R	ACCACAACATCAGCAAGGCATTGG
MCS1/R	TCTAGAGAGCTCAGCGCTGGTACCCTCGAGTTCACAGCCACGCGGAACATCAG XbaI Sac AfeI Acc65I XhoI KpnI
MCS2/F	CTCGAGGGTACCAGCCCTGAGCTCTCTAGAGCAGTAACAAATAAAAGGTTGAATTTATTGC XhoI Acc65I KpnI Afe SacI XbaI
Su-Fw	CTTCTACACCCTGTCTTCTCGCT
Su-Rv	CTCAACAACAAGTACACCCGAGTC

Based on the binding sites of SAA/F and R and MCS1 and 2 (Figure 3-3A) and including the 30 bp tail added to MCS1 and 2, amplicons of sizes 409 bp for SAA/F-MCS1 and 288 bp for MCS2-SAA/R were expected and obtained (Figure 3-7A). The 3′end of the amplicon SAA/F-MCS1 and the 5′end of the amplicon MCS2-SAA/F had overlapping MCS fragment in antisense

or sense orientation, respectively. The second step involved using amplicons SAA/F-MCS1 and MCS2/SAA/R (Figure 3-7A) as template with primers SAA/F and SAA/R. As the amplicons had a 30 bp overlapping fragment, their amplification using SAA/F and SAA/R primers was expected to give a 667 bp amplicon. An amplicon of the predicted size was obtained as shown in the electrophoretic gel in Figure 3-7B.

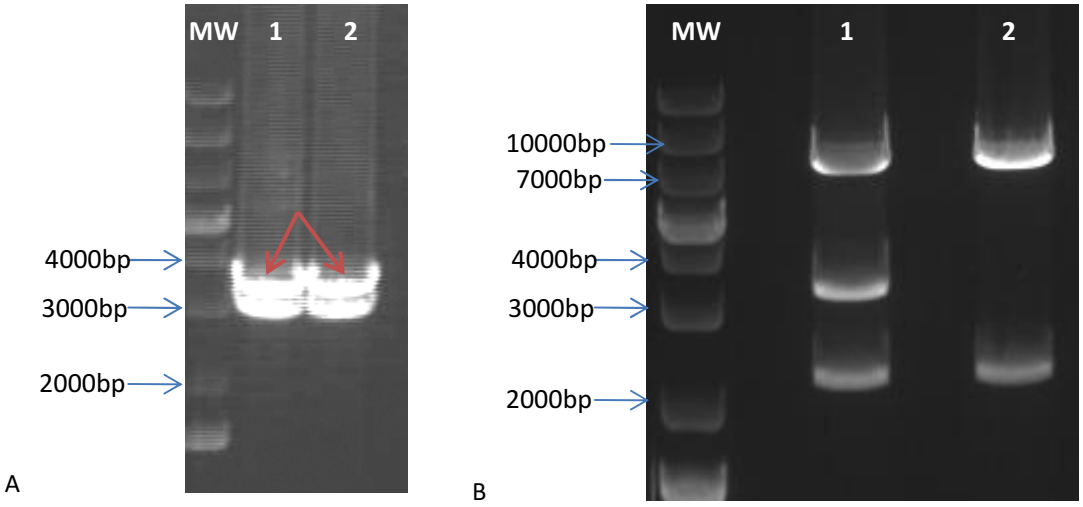

Figure 3-8: Screening of pTZAΔCP and SACMV-AΔCP
pTZAΔCP infectious clones were extracted using alkaline lysis and digested with *Hind*III and *EcoR*V which each cuts pTZAΔCP once at position 651 bp and 4079 bp. (A) shows *Hind*III and *EcoR*V restriction product and red arrows show the desired 3428 bp subcloned into pCAMBIA0380 both lane1 and 2 were loaded with the same sample. (B) *EcoR*I restriction digestion ion of pCAMBIA0380 carrying SACMV-A VIGS. *EcoR*I digests SACMV-AΔCP twice at 747 bp and 8713 bp, yielding 2 fragments of 7966 bp and 2278 bp. Positive banding pattern observed in lane 1. Gel electrophoresis was carried out in 1XTAE 4% agarose with 1 µg/ml ethidium bromide with, O'Generuler^{TM} 1 Kb Plus (Fermentas International Inc., Burlington, Canada) DNA ladder (MW).

SAA/F-SAA/R amplicon was digested using *Bsp1407*I and *BspT*I and subcloned into pTZA that had been digested with the same enzymes. The recombinant plasmid, named pTZAΔCP (Figure 3-3D), was digested with *Hind*III and *EcoR*V (Figure 3-8A) to transfer the partial dimer with CP deletion from a pTZ57R-based vector to the binary pCAMBIA0380. Based on the plasmid map of pTZAΔCP (Figure 3-3B), restriction digestion ion using *EcoR*I and *Hind*III should yield a fragment of about 3428 bp containing the partial-dimer fragment and a vector backbone of about 2800 bp, approximately the size of pTZ57R. The 3428 bp from Figure 3-8A was subcloned into pCAMBIA0380 and the resulting recombinant vector was named SACMV-AΔCP. Similarly to the construction of the SACMV-A infectious clone, the *EcoR*V- *Hind*III fragment from

pTZAΔCP was blunt end-cloned into pCAMBIA0380 and cloning in this way could have resulted in 2 possible orientations. To confirm orientation of insertion of the *EcoR*V – *Hind*III from pTZAΔCP into pCAMBIA0380, pC8A was digested with *EcoR*I, which would give different banding pattern, depending on the orientation of the insert. Based on the bandings obtained (Figure 3-6), the plasmid map for SACMV-AΔCP, the designed VIGS vector, was predicted to be as shown in (Figure 3-5C).

3.3.4 Insertion of Su-fragment

Su-Fw and Su-Rv were designed to amplify the region 49-1250 bp of the *su*-gene of *N. tabacum*. These primers were used in a 2 step RT-PCR and the PCR amplicons were ligated into pTZ57R/T. The recombinant vector was digested with *Eco32*I (Fermentas International Inc., Burlington, Canada) which cuts *su*-gene at 761 bp and 1164 bp, yielding a 403 bp fragment. SACMV-AΔCP was digested using *Eco47*III/*Afe*I, a blunt end restriction enzyme whose restriction site was inserted into the designed VIGS vector. The 403 bp su fragment was blunt-end ligated into linear SACMV-AΔCP and the recombinant vector was named SACMV-A::*su* (Figure 3-5D). To confirm insertion of *su* into SACMV-AΔCP, PCR was performed to screen putative clones using primers SAA/F-SAA/R. Based on the plasmid map in Figure 3-5D, an amplicon of 1072 bp was expected and obtained (Figure 3-**9**). Each amplicon was digested with *BspT*I/*Afl*II and *EcoR*I (Figure 3-10) and the position of the restriction sites of each of these restriction enzymes are shown in Figure 3-11.

As shown in Figure 3-11, depending on the orientation of *su* insertion, restriction digestion ion using *EcoR*I and *Afl*II/*BspT*I on the amplicon obtained through amplification of putative SACMV-A::*su* clones should yield fragments of sizes 575 bp, 405 bp and 93 bp for orientation depicted in Figure 3-11A; whereas for orientation in Figure 3-11B, the fragments should be of size 616 bp, 363 bp and 93 bp.

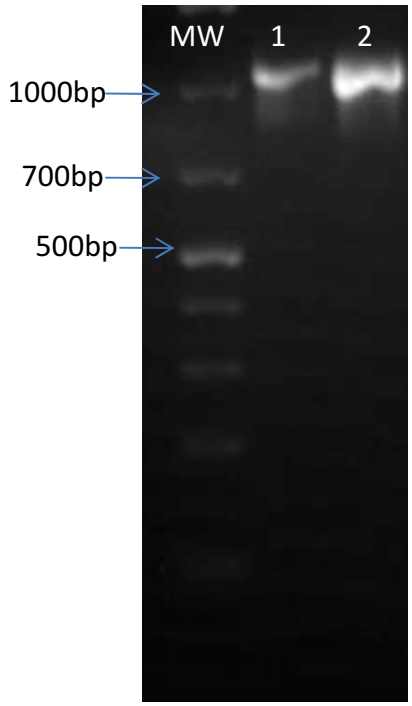

Figure 3-9: Amplification of SAA/F-SAA/R fragment of SACMV-A::su
Using primers SAA/F and SAA/R, the contained region in SACMV-A::*su.* PCR product (5 µl) was loaded on a 4% agarose gel using 1XTAE and 1 µg/ml of ethidium bromide. (MW) O'Generuler™ 1 Kb Plus (Fermentas International Inc., Burlington, Canada) DNA ladder.

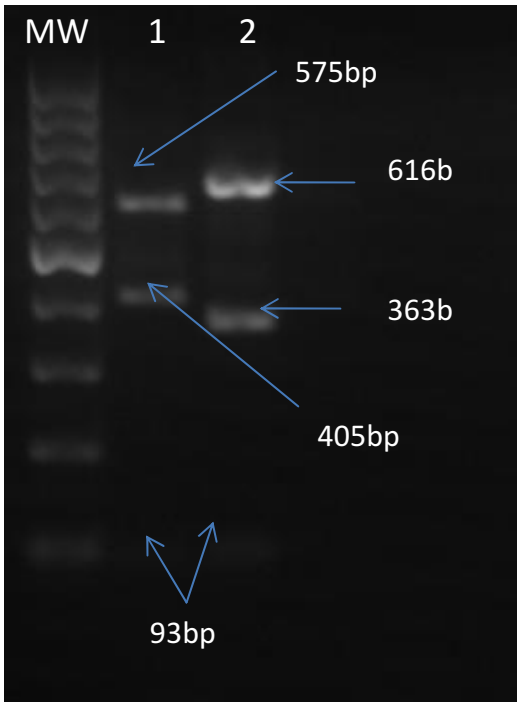

Figure 3-10: Restriction digestion of the SAA/F-SAA/R fragment of SACMV-A::su with EcoRI and AflII
PCR product SAA/F-SAA/R figment of SACMV-A::su was digested using *BspT*I and *EcoR*I. Sizes of the obtained fragment shown inside the electrophoretic gel. Restriction product was loaded 4% agarose gel using 1XTAE and 1 µg/ml of ethidium bromide. (MW) O'Generuler™ 100 bp (Fermentas International Inc., Burlington, Canada) DNA ladder.

Two clones were isolated corresponding to each of the above orientations and transformed separately into *A. tumefaciens* C58C1. To identify which orientation, sense or antisense, the orientation of the coding sequence of each clone was compared to the orientation of AV1 coding strand in non-modified SACMV-A. The clone bearing *su* insertion in an orientation similar to that of AV1 was noted as sense, because the AV1 ORF in SACMV-A is on the virion or sense strand. The other clone bearing *su* insertion in the opposite orientation was noted as antisense. The clone with the sense construct was named SACMV-A::*su*1 and the clone with the antisense construct SACMV-A::*su*2. Both clones were separately used in the experiments to silence *su* in *N. benthamiana*, results of which are depicted in section 3.4.5.

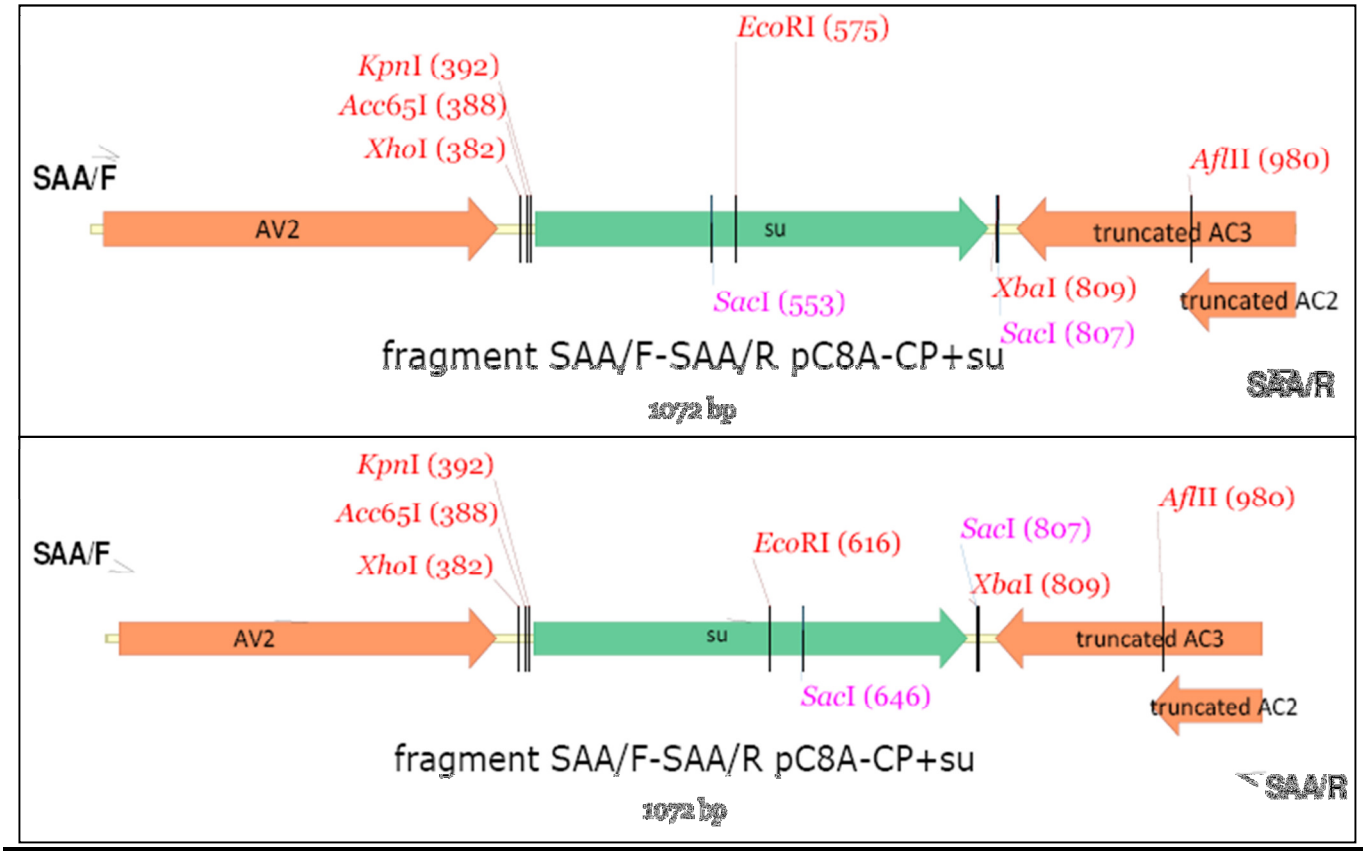

Figure 3-11: Diagrammatic representation of amplicons bearing the *su* gene insertion in different orientation.
The diagrams were drawn in order to predict the outcome of a digestion of SAA/F-SAA/R fragment of SACMV-A::su with *Afl*II/*BspT*I and *EcoR*I. Shown in the map are restriction sites inserted where AV1 has been deleted *Xho*I, *Acc65*I/*Kpn*I, *Sac*I, *and Xba*I. As the su fragment was clone into *Afe*I site of SACMV-AΔCP this fragment it is no longer available. Fragments maps were constructed using VectorNTI Advance 10 (Invitrogen, Carlsbad, USA).

3.3.5 Silencing of su-gene in N. benthamiana and cassava

Each of the SACMV-A::*su* clones mixed in equal part with SACMV-DNA B were used to agroinfiltrate *N. benthamiana* leaves of 4-6 weeks old *N. benthamiana* grown in a growth cabinet. *N. benthamiana* plants were also infiltrated with SACMV-AΔCP and SACMV-DNA B (Figure 3-12I) as a negative control for bleaching and as SACMV-A and SACMV-DNA B as infectivity positive control (Figure 3-12J). To assess the effect of the developmental age of the plant on silencing by the VIGS vector, SACMV-A::*su*1 and SACMV-DNA B and SACMV-A::*su*2 and SACMV-DNA B were used to silence *Su* in *N. benthamiana* older than 4 to 6 weeks that had passed the four to six leaf. To assess the capacity of a SACMV VIGS deficient lacking the movement proteins to silence endogenous genes, *N. benthamiana* plants were infected with SACMV-A::*su* clones only without SACMV-DNA B component. To evaluate the potential of

using SACMV-A VIGS to silence endogenous genes involved in disease resistance, *N. benthamiana* plants infected with SACMV-A::*su*2 clones were re-infected 7 days later with SACMV-A and SACMV-DNA B. Four plants were infected for each treatment, and infection in case of positive infection control was successful for each of the infected plants. Silencing was achieved in each of the infected plants with SACMV-A::*su* and SACMV-DNA B clones.

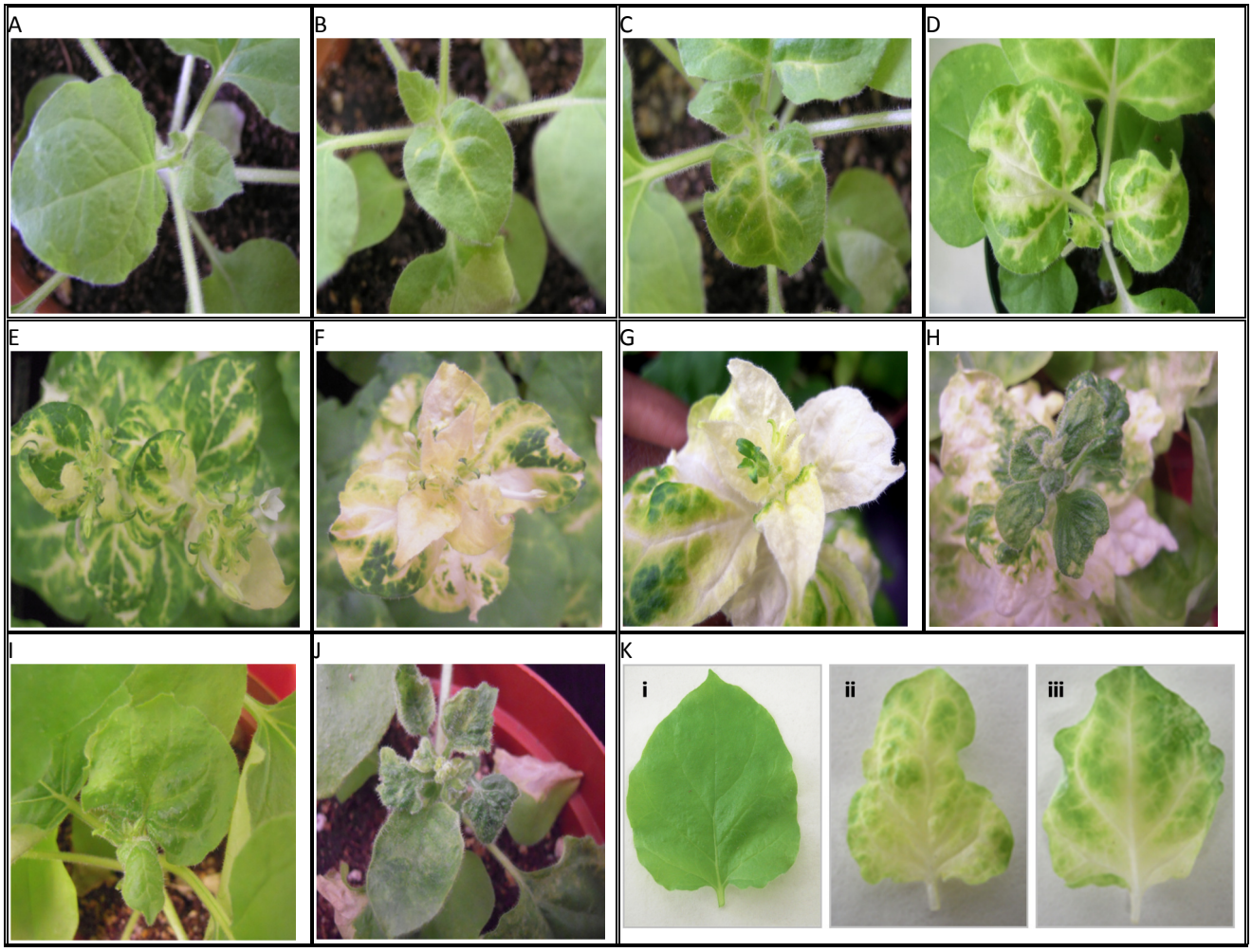

Figure 3-12: Silencing of *su*-gene from *N. Benthamiana*
N. benthamiana was infiltrated using the two SACMV-A::*su* clones. (A) healthy *N. benthamiana* (B) SACMV-A::*su*1 infected *N. benthamiana* at 12 dpi (C) SACMV-A::*su*2 infected *N. benthamiana* at 12 dpi(D) SACMV-A::*su*2 infected *N. benthamiana* at 21 dpi (E) SACMV-A::*su*2 infected *N. benthamiana* 35 dpi (F) SACMV-A::*su*1 infected *N. benthamiana* 35 dpi (G) SACMV-A::*su*2 infected *N. benthamiana* 35 dpi (H) SACMV-A::*su*2 infected *N. benthamiana* 35 dpi with delayed inoculation at 7 dpi (I) SACMV-A-VIGS infected *N. benthamiana* 35 dpi (J) SACMV-A infected *N. benthamiana* 35 dpi (K) degree of silencing variation in plants infected with the same construct i. wild type *N. benthamiana* leaves ii-iii SACMV::*su* infected leaves, showing different degrees of leaf whitening.

Leaf bleaching was observed on leaves at around 12 dpi for both SACMV-A::*su*1 and 2 (Figure 3-12B-C). The bleaching became more prominent at 21 dpi (Figure 3-12D) and by 35 dpi, leaves that were entirely bleached could be observed (Figure 3-12F). Although bleaching appeared at the same time in plants infected with SACMV-A::*su*1 and SACMV-A::*su*2, the initiation of silencing in SACMV-A::*su*1 infected plants at 12 dpi was less prominent (Figure 3-12B-C), but this was not observed later at 35 dpi (Figure 3-12F-G).

The degree of silencing obtained in plants infected by the same construct varied (Figure 3-12Kii and Kiii). The bleaching of the leaves was maintained in these plants throughout their lifespan (Not shown). The extent of silencing obtained in plants that were infected at the four to six leaf stage was different to plants that were infected after the four to six leaf stage (Figure 3-12D). When older plants were used for silencing, the observed bleaching was more variegated, with only few leaves of those plants being entirely bleached (Compare Figure 3-12D to Figure 3-12F, G or H). For both of these experiments, mild symptoms were observed when typical SACMV infection symptoms shown in the infectivity positive control (Figure 3-12J).

N. benthamiana infected with only SACMV-A::*su*1 and 2 were symptomless with no visible signs of silencing up to 2 months after infiltration (data not included). Plants that were infected with SACMV-A::*su*2 and SACMV-DNA B were re-infected 7days later with SACMV-A and B. Silencing or leaf bleaching in these plants was no longer visible at 35 dpi and these plants had green leaves emerging from previously white leaves (Figure 3-12H). Symptoms on these plants were similar to symptoms observed in infectivity positive control (Figure 3-12J).

Agroinfiltration was used to infect cassava with SACMV-A::*su*2 and SACMV-A and SACMV-AΔCP and SACMV-DNA B were used as negative control. White bleached spots were observed 8 weeks after infiltration (Figure 3-13A). Mild symptoms were observed in 2 of the 4 cassava plants agroinfiltrated SACMV-AΔCP and SACMV-DNA B (Figure 3-13B) and only 1 out of four cassava plants infected with SACMV-A*su*2 showed sign of silencing.

A B

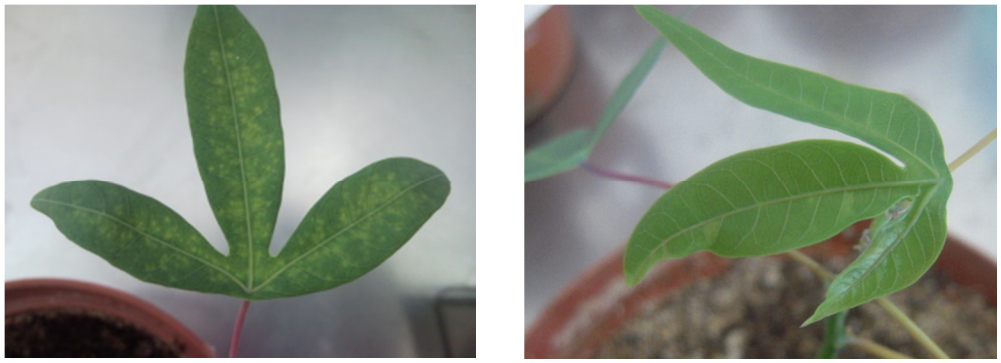

Figure 3-13: Silencing of su-gene from cassava T200
Cassava leaves were agroinfiltrated using TWEEN-20 as a surfactant and at 8 wpi patches of whitening could be observed on leaves (A) SACMV-A::*su2* infected cassava (B) SACMV-AΔCP

3.4 DISCUSSION

Since the first account of the use of a geminiviruses based vector, *Tobacco yellow dwarf virus* (TYDV), to silence CHS gene in petunia (Atkinson et al. 1998), different geminivirus silencing vectors have been developed. Because geminiviruses infect major cash and subsistence crops such as legumes, tomato, maize and cassava (Varma and Malathi 2003; Aragão and Brasileiro 2002), loss of yield arising from these infections are of enormous economic value and the development of a fast functional characterization method that can assist in the revelation of plant defense mechanism in these crops is imperative.

The first VIGS vectors designed were based on RNA viruses. Transgenic plants carrying sequences of tobacco etch virus (TEV) recovered from TEV infection through a VIGS mechanism (Lindbo et al. 1993) and PVX and TMV carrying PDS gene were used to silence PDS in *N. benthamiana* (Ruiz et al. 1998; Kumagai et al. 1995). RNA virus encodes proteins for their replication and for the transcription machinery. They replicate in the cytoplasm through an RNA-dependent intermediate, this allows not only their transcriptome but also their genome to be targeted by VIGS, hence the silencing potential is seen not to be stable (Bisaro 2006; Robertson 2004). In this research, a VIGS vector was designed based on the begomoviruses SACMV-A, which was used to successfully silence *su*-gene in *N. benthamiana* and cassava.

Begomoviruses consists generally of 2 ssDNA molecules of about 2.3-2.9 kb in size. Although begomoviruses infect different plant species, they share commonalities in their genomic sequences. Conserved sequence across known begomoviruses allows for the design of universal degenerate primers allowing the isolation of either component, DNA-A and DNA-B through PCR from infected plant leaves (Rojas et al. 1993; Briddon and Markham 1994). Although this practice has been instrumental in diagnosing new viruses, it requires optimization from one plant species to another and the outcome is dependent on the binding sites of the primers used for amplification, which could render molecular manipulations laborious. In this study, a different approach was taken.

To design the SACMV-A VIGS vector, full-length SACMV-DNA A was isolated from infected *N. benthamiana* using φ29 DNA polymerase mediated rolling circle amplification (RCA). φ29 amplifies with high-fidelity circular DNA templates (plasmids, phages, RNA and DNA virus) and when primed with random hexamers, yields dsDNA concatemers (Dean et al. 2001; Johne et al. 2009). RCA using φ29 has been used for isolation of geminiviruses (Inoue-Nagata et al. 2004; Knierim and Maiss 2007; Shepherd et al. 2008); it eliminates the need to design universal degenerate primers for each of the genome component. Routine infections have been carried out in our laboratory using SACMV infectious clones, in *A. tumefaciens* C58C1 (Berrie et al. 2001). However these infectious clones were constructed with two tandem repeats of SACMV-A monomers digested with *Sal*I and cloned into pBIN19. Infectious clones constructed in this way contained 2 copies of the AV1 gene which made the AV1 deletion experiments challenging.

In this research infectious dimer clones of SACMV-DNA A, named SACMV-A, were designed so that it would contain only one copy of the AV. These infectious clones facilitated the experiments needed to delete the AV1 gene in order to design SACMV-A VIGS. Both SACMV-A and SACMV-A VIGS designed contained 2 copies of the nonanucleotide TAATATT/AC, to allow for replication release, as infectious clones of geminiviruses cloned in a head to tail fashion require two copies of the nonanucleotide as nicking occurs within this sequence during replication resulting in release of a full length single copy virus (Stenger et al. 1991; Heyraud-Nitschke et al. 1993).

In the designed SACMV-A VIGS, 568 bp at the 3′ end of AV1 was replaced with an MCS containing different restriction sites, without disrupting the ORF of AV2 and AC3 found flanking AV1 (Figure 3-3A-B). To validate the ability of our VIGS vector to silence endogenous genes, a 403 bp fragment from *N. tabacum su* gene was subcloned into the VIGS vector, and used as a visual reporter. Various other visual reporters have been used to attest for designed VIGS vectors functionality in *N. benthamiana,* however the limited knowledge available on cassava transcriptome as described in Chapter 2 led us to choose the *N. tabacum* ortholog which was successfully used to silence *su* in cassava (Fofana et al. 2004). *Su*-gene (*Chl* I) is one of the three subunits that make up magnesium chelatase, an enzyme involved in chlorophyll production. Magnesium chelatase catalyzes the reaction in which protoporphyrin chelates

magnesium, the first step in chlorophyll synthesis (Walker and Weinstein 1991; Kruse et al. 1997; Jensen et al. 1996). Disruption of any of the three magnesium chelatase subunits, *Chl I, Chl D, Chl H,* disrupts the functioning of the enzyme, resulting in loss of function-like phenotype (Kruse et al. 1997; Jensen et al. 1996). Null mutations of *Chl I* have been shown to produce various degree of bleaching, from variegation to complete whitening of leaves, a condition found to be lethal in plants seedlings (Fitzmaurice et al. 1999).

Because the 403 bp of *N. tabacum su* was ligated in the VIGS vector (SACMV-AΔCP) through blunt end cloning, 2 possible outcomes for orientation of *su* insertion were expected. 2 clones were identified to have *su* insertion in opposite orientation, SACMV-A::*su*1 and SACMV-A::*su*2. Begomoviruses replicate in the nucleus where they assume a dsDNA template for replication and transcription. Their genome encodes for 2 genes in the virion strand (AV1 and AV2) and 4 genes on the complimentary strand (AC1-4). To identify the orientation of insertion of *su* in each of these clones, the orientation of *su* insertion was compared to orientation of AV1, found on the virion sense of SACMV-A. In relation to AV1, SACMV-A::*su*1 contained partial *su*-gene sequence in the sense orientation and SACMV-A::*su*2 contained the partial *su*-gene sequence in the antisense orientation

By 35 dpi, extensive silencing could be observed in *N. benthamiana* infected by SACMV-A::*su*1 and SACMV-A::*su*2 coupled with SACMV-DNA B (Figure 3-12F,G). Overall, both constructs resulted in mild symptoms compared to SACMV-A and SACMV-DNA B infected samples (Figure 3-12I). Although no difference in the level of silencing achieved could be seen by 35 dpi, at around 12 dpi, the antisense construct SACMV-A::*su*2 produced more pronounced silencing than SACMV-A::*su*1. Antisense, sense and inverted repeat constructs have been used to silence endogenous (Napoli et al. 1990; Jorgensen et al. 1996) as well as viral genes (Chellappan et al. 2004; Zhang et al. 2005) with varying degree of efficiency, (Thakur 2003; Wang and Metzlaff 2005; Waterhouse et al. 1998; Jorgensen et al. 1996). Silencing induced using sense constructs, commonly known as co-suppression, has been shown to occur through TGS mechanism by methylation of regulatory DNA regions (Bender 2004). Antisense constructs induce silencing mainly post-transcriptionally where antisense transcripts anneal to matching “sense” mRNA in the cell, resulting in dsRNA structures targeted by the RNA silencing machinery (Thakur 2003;

Wang and Metzlaff 2005). Constructs containing both sense and antisense sequences in inverted repeats or hairpin structures have been shown to be more efficient than sense or antisense constructs alone (Waterhouse et al. 1998). Inverted sequences, when expressed, fold back on themselves, forming dsRNA hairpins, which are subsequently targeted by the RNA silencing machinery (Smith et al. 2000). Because inverted repeat strategies do not need to recognize a target to trigger the RNA silencing machinery, they have been shown to be more efficient than antisense and sense strategies (Wang and Metzlaff 2005; Smith et al. 2000; Brodersen and Voinnet 2006; Wesley et al. 2001).

In this experiment, initiation of silencing at 12 dpi favored the antisense approach. Nonetheless, by 35 dpi, the extent of silencing was similar in plants infected by constructs in both sense and antisense orientation (Figure 3-12F, G). Although extensive silencing was achieved, there was no uniformity across the silenced plants silencing. At 35 dpi, in plants silenced using SACMV-A::*su* 1 and 2, there was a difference in silencing in leaves as some leaves appeared entirely bleached and others had spots of green. The same phenomenon is depicted in Figure 3-12Kii and Figure 3-12Kiii that shows that the extent of silencing in leaves infected by the same construct varied. Lack of uniformity in silencing produced from VIGS vector has been recorded previously and listed as one of the disadvantages of VIGS (Burch-smith et al. 2004). It would be interesting to compare silencing triggered by a hairpin construct contained in a VIGS vector and observe whether VIGS carried out in this manner would result in a decrease in leaf to leaf variation.

In cassava, silencing was only observed at 8 weeks post inoculation. The bleaching was not extensive as was the case with *N. benthamiana.* ACMV-VIGS has been successfully used to silence *su* in cassava using a fragment *N. tabacum* (Fofana et al. 2004). For ACMV-VIGS cassava plants were infected by particle bombardment which has been shown to produce better infection in cassava than agroinfiltration. Unlike *N. benthamiana,* leaves of cassava cannot be infiltrated as easily. Despite the addition of Tween-20 to act as a surfactant, the efficiency of infection in cassava was lower than in *N. benthamiana.* The use of VIGS in cassava will need to be improved to identify the appropriate method for virus infection.

Most geminiviruses VIGS vectors are designed using begomoviruses rather than monopartite viruses. As begomoviruses have genes expressed on DNA-B involved entirely on movement proteins, the CP (AV1) can be removed without affecting movement of the virus throughout the plant. Recently, a VIGS vector was designed on the monopartite virus BCTV, by removing the R1 (V1) gene which is responsible for viral encapsidation and movements. Although deficient in the main viral movement protein, the silencing effect was able to spread systematically (Golenberg et al. 2009). Other reports have indicated that VIGS signals can move beyond organs infected by the virus (Peele et al. 2001). Attempts to infect *N. benthamiana* with SACMV-A::*su* without SACMV-B, yielded negative results. In a 2008 review, Kalantidis et al., reported that movement of endogenous silencing was tightly regulated compared to transgenes silencing, and this could be the reason why no silencing was achieved in this case with a VIGS vector with no CP, no MP and no NSP. Although the BCTV VIGS was dispossessed of V1, V3 has been noted to have movement protein activity (Golenberg et al. 2009; Hormuzdi and Bisaro 1993), and this could be the reason why the results obtained here differ from those obtained with BCTV VIGS.

For plants such as cassava that are recalcitrant to transformation, VIGS has become the reverse genetics method of choice as it allows for quick functional characterization through a "null-mutation" like approach. The challenge with silencing defense related genes often arises when the virus under investigation is the one on which the VIGS vector is based. The symptoms produced by the VIGS vector alone, although mild, can often not be uncoupled from the effect that silencing of putative defense related genes has. Most VIGS based approaches used for characterization of genes participating in disease resistance involve silencing the genes with a VIGS vector based on a different virus to the virus under investigation (Purkayastha and Dasgupta 2009; Lu et al. 2003; Asai and Yoshioka 2009).

Cassava is not susceptible to "model" viruses such as PVX or TEV, used in VIGS studies and since the SACMV VIGS vector was designed to be used in our laboratory in functional studies of defense genes in response to SACMV, it was decided to test what would happen if a *su*-gene silenced tobacco was challenged with SACMV. Seven days after agroinfiltration of *N. benthamiana* with the SACMV-A::*su*2, the source leaves of the same plants were challenged with infectious dimers of SACMV-A and B. Silenced (bleached) leaves were obtained, with

prominent symptoms of stunting of the plant and increase in curling of leaves at 35 dpi (Figure 3-12H). As these plants aged, they recovered from the silencing; with newly emerging leaves exhibiting little or no visible silencing effects (Figure 3-12H). This decrease in silencing could have arisen as a result of an increase in viral titer that resulted in an increase expression of geminivirus inhibitors of gene silencing.

Geminiviruses encode for strong inhibitors of gene silencing as a mechanism to evade being targeted by the host's silencing machinery. With the AV1 gene being deleted from the SACMV-A VIGS vector, a decrease in viral accumulation occurred shown by attenuation of symptoms observed in plants infected with SACMV-AΔCP and SACMV-A::*su* clones (Figure 3-12F, G, I) compared to plants infected with SACMV-A (Figure 3-12J). The decrease in viral load eventually resulted in a decrease in production of viral silencing inhibitors. By inserting 7 days later a non-modified virus (SACMV-A) in SACMV-A::*su* infected plants not only boosted viral load, but also increased the expression of inhibitors of silencing. The increase in expression of silencing suppressor could have resulted in the suppression in infected cells of RNA silencing against viral proteins including the inserted *su* fragment. This is most probably the reason why *su* silencing was suppressed and emerging leaves appeared white.

Our results provide proof on the functionality of the SACMV-DNA A based vector, SACMV-AΔCP, to silence endogenous genes in *N. benthamiana.* Factors like temperature and size of the pots in which plants are grown do influence the outcome of a VIGS experiment (Robertson 2004). These factors were not tested in this research. One factor that was tested however was the dependency of the silencing outcome on the developmental stage of the plant at the time of infection. Infection of mature plants that were past the four to six leaf stage produced less extensive silencing (Figure 3-12E). The less severe silencing produced in mature plants was also observed in *Arabidopsis* infected past the four to six leaf stage (Turnage et al. 2002). Environmental variable is an important factor for the success of VIGS experiments and will need to be tested for every VIGS system and kept in check to maximize VIGS induced silencing.

CHAPTER 4.FUNCTIONAL CHARACTERISATION OF NbNOA1 USING VIGS

4.1 INTRODUCTION

Plant survival is persistently threatened by pests and pathogens such as fungi, bacteria and viruses. Pathogens mode of attack and the pathways they each elicit may differ from one to the other, however, there is a crosstalk existing between them. Beneath all pathogen specific pathways induced, lies an innate immunity response, responsible for containing pathogens to infected cells through the HR and alerting non-infected cells on the foreign invasion through the SAR. Two branches of innate immunity have been identified: pathogen associated molecules pattern (PAMP) triggered immunity and effector triggered immunity (Jones and Dangl 2006). Viral infection relates more to effector triggered immunity as they do not carry PAMPs capable of triggering an immune response. For a successful infection to occur the interaction between host encoded resistance (R) genes has to be "compatible" with the viral effector or *avr* gene. Incompatible interactions do not result in infection. Downstream of the R-*avr* interaction lies the HR which encompasses a signaling cascade that results in programmed cell death (PCD) or necrosis (Hussain et al. 2007).

Geminivirus genes have been identified as targets of plant defense response. Several MP and NSP genes have been identified as avr determinants (Garrido-Ramirez et al. 2000; Hussain et al. 2005; Zhou et al. 2007). Rep protein of ACMV and *Tomato yellow leaf curl virus-China* (TYLCV-C) as well as the PTGS suppressor domain at the C-terminal of the ToLCJV-A AV2 protein were found to be elicitors of plant HR response (Jin et al. 2008; van Wezel et al. 2002). Besides inducing HR, geminiviruses have evolved ways to suppress HR induction. TrAP of ToLCNDV was identified as a suppressor of HR induced PCD (Hussain et al. 2007) and AC4 from ACMV was found to counter Rep induced HR (Jin et al. 2008). At the center of the signaling cascade leading to PCD lies a signaling molecule, NO, whose involvement in plant defense responses is gradually being discovered (Leitner et al. 2009).

The properties of NO allows this highly reactive molecule to modulate ROS and Ca^{2+} accumulation, expression and post-translational modification of defense related proteins as well as transcriptional activity in a cell, events that together are required for PCD induction (Soosaar et al. 2005; Mur et al. 2006; Leitner et al. 2009). Despite being ubiquitously expressed in plants, the major source of NO production has not yet been deciphered. AtNOA1/AtNOS1 from *Arabidopsis thaliana* was previously predicted as the much anticipated plant NOS (Guo et al. 2003). Nitric oxide synthases are the main NO producing enzymes in mammals. They catalyze the conversion of L-arginine to NO and L-citrulline (Mayer and Hemmens 1997; Moncada et al. 1989). Because they are centrally placed in NO synthesis in animals, the idea of a homolog with the same functional characteristics in plants has led researchers to look into AtNOA1/AtNOS1. After being originally reported as a NOS-like enzyme, the NO producing ability of AtNOA1/AtNOS1 and its mammalian homolog mtAtNOS1 could not be duplicated (Zemojtel et al. 2006). The protein sequence of AtNOA1/AtNOS1 revealed domains homologous to bacterial cyclic permuted GTPase but no NO producing domain or motif (Moreau et al. 2008; Zemojtel et al. 2004).

Although AtNOA1/AtNOS1 possesses no NO producing function, based on the fact that AtNOA1 mutants have a lower NO production with phenotypic traits that can be rescued by exogenous NO application, AtNOA1 is deemed to be in some way involved with NO accumulation, probably through a modification of the performance of plastids (Gas et al. 2009). It has been speculated that defective plastids present in *atnoa1* mutants could results in elevated levels of ROS that readily react with NO present in cells, resulting in a decrease in the presence of free NO (Gas et al. 2009; Leitner et al. 2009) Our interest in AtNOA1 lies mainly on its involvement in disease resistance, where down-regulation of AtNOA1 activity has been shown to render the plant more susceptible to invading pathogens (Kato et al. 2007; Zeier et al. 2004). Also through the indirect connection between AtNOA1 and NO production, mutations in *AtNOA*1 indirectly affect NO availability. The objective of this study was to use the SACMV-A VIGS (designed in Chapter 3) to silence *NbNOA*1, the *AtNOA*1 homolog in *N. benthamiana.*

4.2 MATERIALS AND METHODS

All nucleic acid quantification procedures were performed using the NanoDrop® ND-1000 spectrophotometer (NanoDrop Technologies, Wilmington, USA). All plasmid maps were derived using VectorNTI Advance 10. All primers were designed using the PrimerQuest package of the Scitools online tool available at Integrated DNA Technology (http://eu.idtdna.com/Home/Home.aspx) and synthesized by Inqaba Biotec (Pretoria, South Africa). BioDoc-It™ System, (UVP, Upland, USA) was used for agarose electrophoresis gel documentation and Microsoft PowerPoint was used to label the individual gel images.

4.2.1 Cloning of NbNOA1 fragment into SACMV-AΔCP

To identify a region of high similarity across NOA1 homologs that could be used to potentially silence NbNOA1 and homologs across different species, the sequence of NbNOA1 was aligned with its *A. thaliana* (AtNOA1) and *O. sativa* (OsNOA1) homologs and *Glycine max* EST (Accession number BE661621), a putative NOA, using ClustalX software (See 2.2.1 above). Primers were designed using the sequence with percentage similarity across the species. The region flanked by primers qNbNOAFw (AGGCGACATATACCTTCAACGCCA) and qNbNOARv (TGCTTGCCTCCAGAATAACCTCCA) was scanned to identify regions with a potential to produce siRNAs, using the siRNA scan computational tool (Xu et al. 2006).

N. benthamiana plants were grown as previously described in section 3.2.5.3. RNA was extracted using Tri Reagent (Sigma-Aldrich, St Louis, USA) from 4 weeks old. One µg of *N. benthamiana* total RNA was reversely transcribed using SuperScript® III Reverse Transcriptase (Invitrogen, Carlsbad, USA) according to the manufacturer's recommendations, using a gene specific primer qNbNOARv. The final reaction was carried out in a total volume of 20 µl and contained 1x First-Strand buffer, 10 µM DTT, 40 UU RiboLock™ RNase inhibitor (Fermentas International Inc., Burlington, Canada), 50 U Superscript III (Invitrogen, Carlsbad, USA), 0.1 µM qNbNOARv, 0.5 mM dNTPs and 1 µg of total RNA. Before being added to the reaction, RNA together with the gene specific primers and dNTPs were incubated at 65˚C for 5 min, to minimize RNA secondary structures. After incubation at 65˚C, the rest of the reagents were

added, the reaction mix was incubated at 50˚C for 2 hours and the reaction was stopped by incubating at 85˚C for 5 min. cDNA (2 µl) was used in the second step with PCR using Phusion™ Hot Start High-Fidelity DNA Polymerase (Finnzymes, Espoo, Finland) and primers qNbNOAFw and qNbNOARv. PCR was carried out for 30 cycles and the following cycling conditions were applied: initial denaturation 98ºC for 30 sec, denaturation 98ºC, 10 sec, annealing 63ºC for 10 sec and elongation at 72ºC for 15 sec and final elongation 72ºC for 10 min. The PCR reaction components were used as recommended by the manufacturer without the optional addition of dimethyl sulfoxide (DMSO). The blunt ended PCR product obtained was ligated in a 1:10 ratio (vector:insert) using T4 DNA ligase (Fermentas International Inc., Burlington, Canada) into SACMV-A VIGS, according to the manufacturer's protocol. Each ligation reaction (20 µl) was transformed into 100 µl DH5α competent cells (prepared as stipulated in section 3.2.2.1), which were plated on LB plates with 1.5% agar supplemented with 100 mg/L kanamycin. The plates were incubated at 37°C overnight. Recombination was confirmed by performing colony PCR, using primers SAA/F (Table 3-1) and qNbNOAFw which bind respectively at 7875-7898 bp and 8564-8587 bp of the recombined SACMV-A::*NbNOA*1. Positive recombinants were later transformed into *A. tumefaciens* C58C1.

4.2.2 Silencing of NbNOA1 in N. benthamiana

To silence NbNOA1 in *N. benthamiana, N. benthamiana* seeds were grown as described previously in section 3.2.5.3. *A. tumefaciens* cultures containing equal volumes of DNA-A equivalent plasmid (SACMV-A, SACMV-AΔCP and SACMV-A::NbNOA1) were used to infiltrate the 2 source leaves of *N. benthamiana* at four weeks in plantlets that had reached the four to six leaf stage, with a needless syringe. *N. benthamiana* plants were agroinfiltrated with SACMV-A/SACMV-B (positive infectivity control), SACMV-AΔCP/SACMV-B (VIGS vector, negative control), and SACMV-AΔCP::*NbNOA*1/SACMV-B (NbNOA1 silencing vector).

In a separate experiment, plants previously infiltrated with SACMV-AΔCP/SACMV-B (positive control for delayed experiment) and SACMV-AΔCP::NbNOA1/SACMV-B (NbNOA1 silencing) were re-infiltrated 7 days later with SACMV-A and SACMV-DNA B. This was done in order to study the proliferation of SACMV infection in *nbnoa*1 silenced plants. To

differentiate the delay experiments from the non-delay, they will be referred to as dSACMV-AΔCP/SACMV-B and dSACMV-A::*NbNOA*1. Four plants were used for each experiment and were monitored for 28 dpi. Leaf bleaching and distortion to be used for symptom severity rating was captured using Nikon Coolpix S600. The images were cropped and labeled using Microsoft PowerPoint.

Symptom severity on score was rated at 28 dpi on a six-point scale where 0 = no symptoms; 1 = mild chlorosis without leaf deformation; 2 = clear mosaic with or without slight leaf deformation; 3 = strong mosaic all over the leaflets with leaf deformation; 4 = as in 3 but with severe leaf deformation; and 5 = severe mosaic and severe reduction of leaf size (Chellappan et al. 2004).

4.2.3 Quantitative Real-time PCR amplification

4.2.3.1 RNA and DNA extraction from silenced plants

To quantify the level of expression in *N. benthamiana* infected with SACMV-AΔCP/SACMV-B, SACMV-AΔCP::NbNOA1/SACMV-B, dSACMV-AΔCP/SACMV-B and dSACMV-AΔCP::NbNOA1/SACMV-B, leaves were harvested from three independent plants as biological replicates at 14, 21 and 28 dpi in SACMV-AΔCP/SACMV-B, SACMV-AΔCP::NbNOA1/SACMV-B, SACMV-AΔCP/SACMV-B and SACMV-AΔCP::NbNOA1/SACMV-B.

RNA and DNA were extracted simultaneously using a modified procedure using Tri Reagent (Sigma-Aldrich, St Louis, USA). This was performed in order to relate the decrease in *NbNOA*1 expression to viral load. Between 50 and 100 mg of leaf tissue was homogenized in a microcentrifuge tube using a micropestle in the presence of liquid nitrogen. The ground tissue was resuspended in 1ml of Tri Reagent (Sigma-Aldrich, St Louis, USA) and incubated at room temperature for 5 min. Chloroform (200 µl) was added, the sample was mixed vigorously, left to stand for 5 min at room temperature and centrifuged at 12000 g for 15 min at 4°C. The aqueous layer was transferred into a new microcentrifuge tube and the organic phase saved for isolation of DNA. To the aqueous phase, 500 µl of isopropyl alcohol were added to precipitate RNA. The

samples were incubated at room temperature for 10 min and centrifuged at 12000 g for 10 min at 4°C. The supernatant was removed and 1ml of 75% ethanol (v/v) was added. The pellet was dislodged by brief vortexing and the sample was centrifuged at 7500 g for 5 min at 4°C. The RNA pellet was allowed to air dry for 10 min and resuspended in nuclease-free water. The extracted RNA was stored at -70°C. Extracted RNA (200 µg) was treated using RNase-free DNAse (Fermentas International Inc., Burlington, Canada) according to the manufacturer's recommendations. To prevent RNA degradation, 40 U of RNase inhibitor (Fermentas International Inc., Burlington, Canada) was included and the DNAse treatment was carried out for an hour, twice longer than the recommended time.

To isolate DNA, 500 µl of back extraction buffer (4 M guanidinium thiocyanate) was added to the interphase-organic phase mixture. The samples were mixed by inversion for 15 sec and incubated at room temperature for 15 min. The samples were centrifuged at 12000 *g* for 15 min at 4°C to separate the phases. The upper aqueous phase was transferred to a new microcentrifuge tube, followed by addition of 400 µl of isopropanol to precipitate DNA. The samples were mixed by inversion, incubated for 5 min at room temperature. DNA was pelleted by centrifugation at 12000 *g* for 5 min at 4°C. The supernatant was discarded and the pellet dislodged in 1ml of and 12ml of 75% ethanol (v/v) was added. The pellet was dislodged by brief vortexing and the sample was centrifuged at 7500 *g* for 5 min at 4°C. The pellet was allowed to air dry for 10 min and resuspended in 100 µl of 8 mM NaOH, 3 µl of 50 mM EDTA, 10 µl 0.1 M Hepes, and water up to 150 µl. The pellet was allowed to resuspend overnight at 4°C. The resuspended DNA was treated with 200 µg/L RNase A, incubated at 37ºC for an hour to allow for completion of RNase digestion. The extracted DNA was stored at -20ºC.

4.2.3.2 Construction of plasmid standard

In order to quantify *NbNOA*1 expression in SACMV-AΔCP, dSACMV-AΔCP, SACMV-AΔCP::*NbNOA*1 and dSACMV-AΔCP::*NbNOA*1 silenced plants, primers were designed to quantify *NbNOA*1 expression using real-time amplification. Primers qRT-Nb1F (GCGTTGCAACTTCATATGGTGCCT) and qRT-Nb1R (TTCCTGTCGGCGGTGTCAATAGAA) were designed to amplify region 1297-1384 bp of NbNOA1, yielding an 88 bp fragment. For relative quantification using real-time, the expression

of a target gene is related to the expression of an internal control gene, *Elongation Factor 1 Alpha* (*EF1-α*). *EF1-α* which has been shown to be stably expressed in our laboratory in response SACMV and has been used as a reference gene in other NbNOA1 silencing VIGS experiment (Kato et al. 2007) was selected as the reference gene. Primers Nb1Ef-1F (AACCCTTCTTGAGGCTCTTGACCA) and Nb1Ef-1R (TTGAGGACACCAGTTTCCACACGA) were designed to amplify the region 450 bp-560 bp 180 bp fragment from *EF1*-α (AY206004).

To determine the efficiency of each of the above primer sets, plasmid standard curves were constructed for qRT-Nb1 primers set. RNA was extracted using Tri Reagent method as described in section **Error! Reference source not found.**. *N. benthamiana* total RNA (1 µg) was reversely transcribed using SuperScript® III Reverse Transcriptase (Invitrogen, Carlsbad, USA) according to the manufacturer's recommendations, using qRT-Nb1R. The final reaction was carried out in a total volume of 20 µl and contained 1x First-Strand buffer, 10 µM DTT, 40 U RiboLock^{TM} RNase inhibitor (Fermentas International Inc., Burlington, Canada), 50 U Superscript III (Invitrogen, Carlsbad, USA), 0.1 µM qRT-Nb1R, 0.5 mM dNTPs and 1 µg of total RNA. The reaction was carried out as described in section **Error! Reference source not found.**.

cDNA (2 µl) was used in the second step using Recombinant Taq DNA polymerase (Fermentas International Inc., Burlington, Canada). The reaction mix consisted of the following: 1X Taq buffer, 200 µM of each dNTPs, 1 µM of each primer (qRT-Nb1F and R), 1.5 µM $MgCl_2$ and 0.25 U Taq DNA polymerase (Recombinant.). PCR was carried out for 30 cycles and the following cycling conditions were applied: initial denaturation 94ºC for 2 min, denaturation 94ºC, 1 min, annealing 63ºC for 30 sec and elongation at 68ºC for 45 sec and final elongation 68ºC for 7 min. positive amplification was confirmed by agarose electrophoresis on 1% agarose gel stained with 1 µg/ml ethidium bromide. Once amplification was confirmed, 4 µl of PCR product was ligated unto pTZ57R/T using the InsTAclone PCR cloning kit (Fermentas International Inc., Burlington, Canada) according to the manufacturer's recommendation. The ligated product was transformed into competent DH5α cells, which were plated on LB agar plates supplemented with 100 mg/L ampicillin, 100 µM IPTG and 20 mg/L X-gal. The plates were incubated at 37°C for no more than 16 h. The following day, white colonies containing

presumptive positive recombinant plasmids were screened using PCR amplification with primers qRT-Nb1 F and R as described above. Alkaline lysis was performed on positive colonies as described in section 3.2.2.2 and the extracted plasmid was diluted down to $1x10^{4}$-$1x10^{-1}$ pg.

qRT-Nb1 plasmid standard were amplified using qRT-Nb1F and R primers in duplicate by real-time PCR in the LightCycler ® 1.5 Realtime system (Roche Applied Science, Penzberg, Germany) using Maxima SYBR Green (Fermentas International Inc., Burlington, Canada). To 10 µl of Maxima SYBR green master mix was added qRT-Nb1 primers, to a final concentration of 0.3 µM each, 1 µl of plasmid standard and nuclease-free water to a total volume of 20 µl. Real-time PCR was run for 35 cycles. Initial denaturation and enzyme activation was carried out at 95ºC for 10 min, denaturation at 95ºC, 15 sec, annealing at 60ºC for 30 sec and elongation at 72ºC for 30 sec. pTZEF1 plasmid construct was kindly donated by F. van Schalk. They were constructed by ligating a 180 bp amplicon from a s step RT-PCR using the primers Nb1Ef1-F and R. pTZEF1 was diluted down to $1x10^{4}$-$1x10^{-1}$ pg to be used as plasmid standards. For standard curve construction, the real-time reaction and cycling conditions were used as for qRT-Nb1 plasmid standard. A standard curve was generated by LightCycler software version 3 and from the standard curve, the PCR efficiency (E) for each primer was calculated using

$$E = 10^{\frac{-1}{-slope}} \qquad \textbf{Equation 4-1}$$

4.2.3.3 Quantification of gene expression

To quantify *NbNOA*1 relative expression in respect to *EF1*-α , 1 µg RNA was extracted from non-treated (Healthy), SACMV-AΔCP, dSACMV-AΔCP, SACMV-AΔCP::*NbNOA*1 and dSACMV-AΔCP::*NbNOA*1 at 14, 21 and 28 dpi was reversely transcribed using iScript cDNA synthesis kit according to the manufacturer's recommendation. Expression values obtained from healthy samples were used as the calibrator.

Real-time PCR reactions were carried out in the LightCycler ® 1.5 Realtime system (Roche Applied Science, Penzberg, Germany) using Maxima SYBR Green (Fermentas International Inc., Burlington, Canada). To 10 µl of Maxima SYBR green master mix was added corresponding primers, depending on the reaction, to a final concentration of 0.3 µM, 2 µl of

reversely transcribed cDNA and nuclease-free water to a total volume of 20 µl. Real-time PCR was run for 35 cycles. Initial denaturation and enzyme activation was carried out at 95ºC for 10 min, denaturation at 95ºC, 15 sec, annealing at 60ºC for 30 sec and elongation at 72ºC for 30 sec. The reactions were set up in a way that in each run, only biological run at a time point was run. cDNA for each treatment was run in duplicate and in each run, both the reference gene and *NbNOA*1 was quantified simultaneously.

The corresponding C_q values were generated by LightCycler version 4. Using Excel, the relative expression ratios of NbNOA1 to EF1α were calculated using C_q values obtained from LightCycler version 4 and the formula:

$$Ratio = \frac{\left(E_{Target}\right)^{\Delta Cq_{target}(calibrator-sample)}}{\left(E_{ref}\right)^{\Delta Cq_{ref}(calibrator-sample)}} \qquad \textbf{Equation 4-2}$$

Where

E_x= PCR efficiency of primers for amplification of X

Target = NbNOA1

Ref= *EF1*-α

ΔC_{qx}(calibrator-sample) = difference in C_q values obtained from the calibrator (healthy) and C_q values for each treatment, namely SACMV-AΔCP, SACMV-A::*NbNOA*1, dSACMV-AΔCP and dSACMV-A::NbNOA1

Relative expression values obtained from Equation 4-2 for healthy samples were used as the calibrator.

4.2.4 Quantification of viral load using Real-time PCR

Real-time amplification was used to quantify the viral load in each extracted DNA sample. A standard curve was generated by amplification of a 150 bp fragment of AC4 in pTZA using primers RepF (ATGATGTCGGTCCTGGAT) and RepR (TCATTGATGACGTCGACC). To construct a standard curve, pTZA was linearized with *Kpn*I (Fermentas International Inc., Burlington, Canada) according to the manufacturer's recommendation. The linearized pTZA was

diluted in concentration ranging from $1x10^{-3}$-$1x10^{1}$ pg and run in duplicate using Maxima SYBR Green (Fermentas International Inc., Burlington, Canada) and the LightCycler ® 1.5 Realtime system (Roche Applied Science, Penzberg, Germany). To 10 µl of Maxima SYBR green master mix was added, RepF and RepR primers to a final concentration of 0.3 µM for each primer, 1 µl of plasmid standard and nuclease-free water to a total volume of 20 µl. Real-time PCR was run for 35 cycles. Initial denaturation and enzyme activation was carried out at 95ºC for 10 min, denaturation at 95ºC, 15 sec, annealing at 60ºC for 30 sec and elongation at 72ºC for 30 sec.

For quantification of viral load, DNA extracted using the Tri Reagent (Sigma-Aldrich, St Louis, USA) in section 4.2.2 method was diluted to concentration ranging from 30-100 ng/µl. Extracted DNA (2 µl) was run in duplicate using Maxima SYBR Green (Fermentas International Inc., Burlington, Canada) and the LightCycler ® 1.5 Realtime System (Roche Applied Science, Penzberg, Germany). To 10 µl of Maxima SYBR green master mix was added RepF and RepR primers to a final concentration of 0.3 µM for each primer, 2 µl of each diluted DNA and nuclease-free water to a total volume of 20 µl. Real-time PCR was run for 35 cycles. Initial denaturation and enzyme activation was carried out at 95ºC for 10 min, denaturation at 95ºC, 15 sec, annealing at 60ºC for 30 sec and elongation at 72ºC for 30 sec.

$$viral\ molecules = \frac{G\ DNA\ X\ * 6.022.10^{23}}{Length\ of\ plasmid\ standard\ (bp) * 660} \qquad \textbf{Equation 4-3}$$

$$Viral\ molecules\ per\ G\ of\ DNA = \frac{Copy\ number}{Amount\ of\ DNA\ used\ per\ reaction} \qquad \textbf{Equation 4-4}$$

Amount of molecules in pg was generated by the LightCycler software version 4 (Roche Applied Science, Penzberg, Germany) from the pTZA based standard curve. Using the pg values obtained from LightCycler software version 4 (Roche Applied Science, Penzberg, Germany), the viral molecules that they corresponded to was calculated using Equation 4-3. Equation 4-4 was used to calculate the viral molecules per gram of extracted DNA. The viral molecules calculated for each treatment was plotted on a logarithmic graph.

4.2.5 Statistical analysis

Two way analysis of variance (ANOVA) was carried out using GraphPad Prism 5.02 (GraphPad Software, Inc., San Diego, CA) on relative expression ratios obtained using Equation 4-1 and viral load obtained using Equation 4-4.

4.3 RESULTS

*4.3.1 Cloning of NbNOA*1

Table 4-1: *siRNA scan* results showing predicted siRNA found on the 308 bp sequence of NbNOA1.

Number	Fragment	siRNA AS (3' - 5')	Hits
1	query_seq (26 - 46)	GUCCGGCACCGACGUAGAAGU	0
2	query_seq (27 - 47)	UCCGGCACCGACGUAGAAGUU	0
3	query_seq (46 - 66)	UUGCCACAAUCGGUGUUAGUU	0
4	query_seq (48 - 68)	GCCACAAUCGGUGUUAGUUCU	0
5	query_seq (54 - 74)	AUCGGUGUUAGUUCUUCUUUU	0
6	query_seq (55 - 75)	UCGGUGUUAGUUCUUCUUUUU	0
7	query_seq (158 - 178)	CACCUACGAGGCCCAAUACAA	0
8	query_seq (177 - 197)	AAGUGGUCCUCUGUAUGCUAA	0
9	query_seq (180 - 200)	UGGUCCUCUGUAUGCUAAACU	0
10	query_seq (182 - 202)	GUCCUCUGUAUGCUAAACUUU	0
11	query_seq (183 - 203)	UCCUCUGUAUGCUAAACUUUU	0
12	query_seq (206 - 226)	UUCGUAGUGGUCGAAUCUUUU	0
13	query_seq (212 - 232)	GUGGUCGAAUCUUUUCAAGAA	0
14	query_seq (213 - 233)	UGGUCGAAUCUUUUCAAGAAA	0
15	query_seq (215 - 235)	GUCGAAUCUUUUCAAGAAACA	0
16	query_seq (251 - 271)	GACAGAGUACCCGUGUACUAA	0
17	query_seq (279 - 299)	AUCCACCUUUACCUCCAAUAA	0

To predict possible siRNA forming sequences within the region of *NbNOA*1 to be used as a VIGS silencing fragment, the sequence 219-527 bp of *NbNOA*1 (bordered by primers qNbNOAFw and qNbNOARv that bind respectively at 219-239 bp and 504-527 bp) was subjected to the publicly available siRNA scan tool (Xu et al. 2006). The results obtained are shown in Table 4-1. Data that were obtained from this online tool included the position of potential siRNA precursors in the sequence as well as possible off-targets. Each of the potential siRNA precursor corresponded to no hits, showing that these precursors would not target any other gene in *N. benthamiana*.

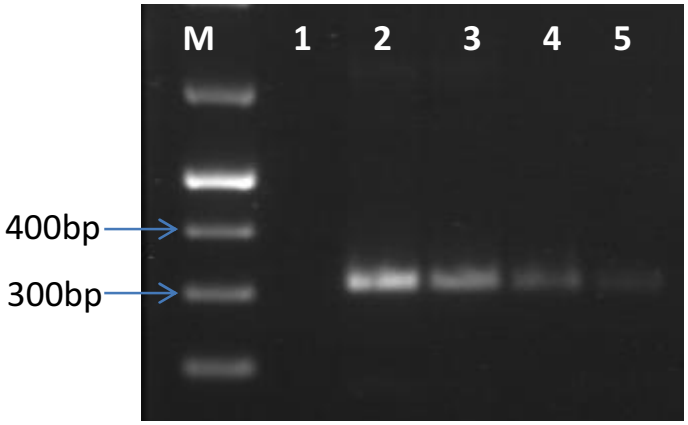

Figure 4-1: Amplification of a 308 bp fragment from *NbNOA*1
Reversely transcribed *N. benthamiana* cDNA was used to amplify the region 219-327 bp of *NbNOA*1. In lane 1 was loaded negative control and from lane2-5, PCR amplicon using different amount of cDNA template, 2 for lane 2 and 3 and 5 µl for lane 4 and 5. (MW), O'GeneRuler, DNA ladder 1 KbPlus. These samples were analyzed on 4% agarose gel, with 1 µg/ml ethidium bromide

Once the potential of this region to form siRNA precursors was confirmed, the 308 bp fragment was isolated through a two-step reverse transcription PCR (Figure 4-1). The amplified fragment was subcloned into SACMV-A VIGS vector (SACMV-AΔCP) through blunt end ligation. Because insertion using blunt end ligation is not directional, i.e. two insert orientations, sense or antisense did arise. Using VectorNTI, a presumptive plasmid map was drawn depicting the position of these primers expected for an antisense orientation (Figure 4-2). To screen for the orientation of the NbNOA1 fragment in SACMV-AΔCP, the recombined vector was subjected to PCR amplification using internal primer qNbNOAFw and an external primer SAA/F. According to this plasmid map, PCR on SACMV-AΔCP containing the 308 bp fragment inserted in the antisense would result in 712 bp amplicon (Figure 4-2). Of the resulting clones, 10 clones were screened using PCR with primers qNbNOAFw and SAA/F (Figure 4-3), and clone 8 that gave an amplicon that matched around 712 bp was selected.

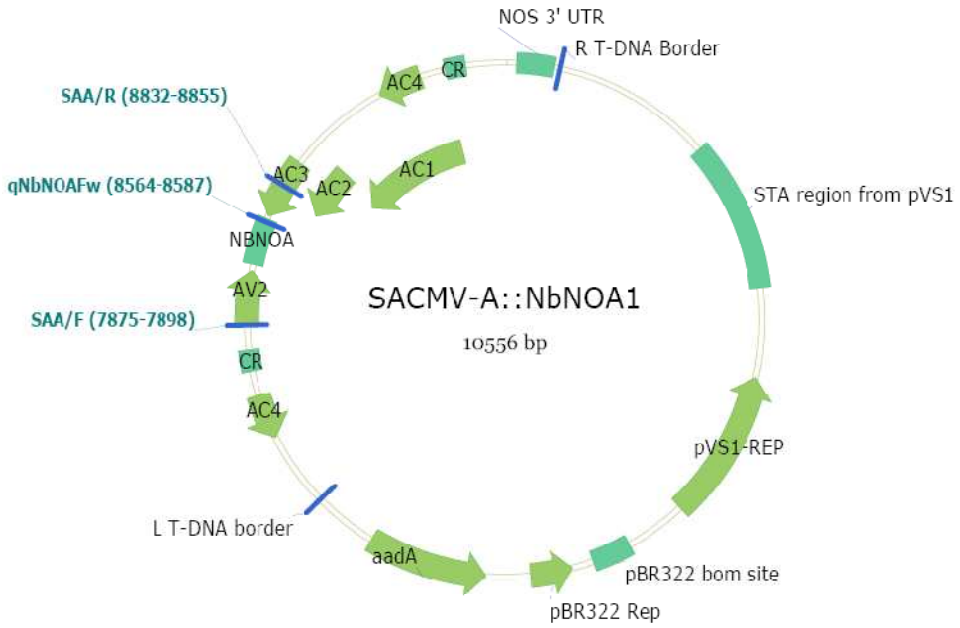

Figure 4-2: Plasmid map of SACMV-A::NbNOA1
Primers shown in teal with annealing site in brackets. The orientation of *NbNOA*1 insertion shown herein represents the predicted antisense insertion of the *NbNOA*1 308 bp fragment. Plasmid map drawn using VectorNTI Advance 10 (Invitrogen, Carlsbad, USA)

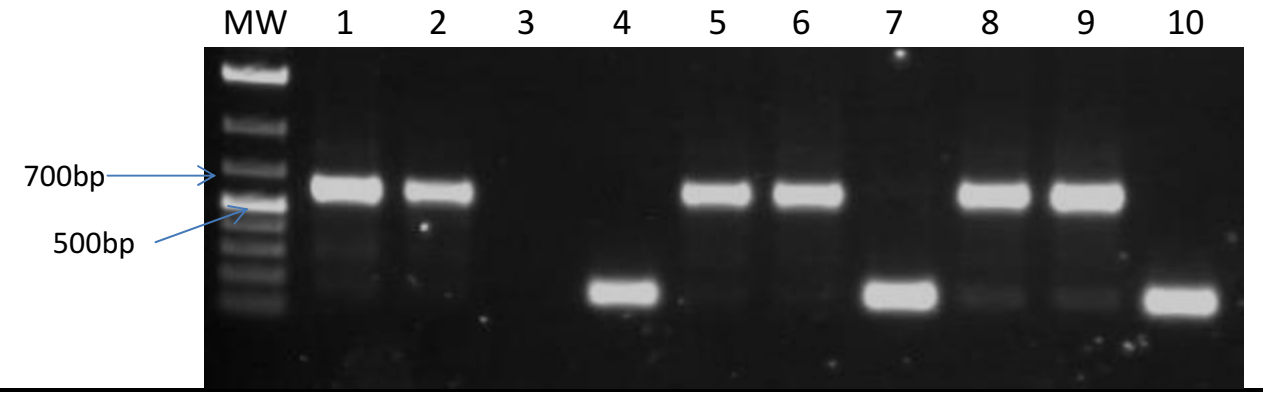

Figure 4-3: Colony PCR to identify a positive SACMV-A::*NbNOA*1.
Clones were screened to identify the orientation of the insert using primers SAA/F and qNbNOAFw, give a 712 bp amplicon. Clone 8 was selected (lane 8) and transformed into *A. tumefaciens* C58C1. (MW), O'GeneRuler, DNA ladder 1 KbPlus. These samples were analyzed on 4% agarose gel, with 1 µg/ml ethidium bromide

*4.3.2 Silencing of NbNOA*1

To silence *NbNOA*1, *N. benthamiana* plants at the four to six leaf stage were infiltrated with SACMV-A::*NbNOA*1 and also SACMV-A::*NbNOA*1 with SACMV-A and B 7 days later. In order to measure the extent of silencing, real-time amplification was performed on SACMV-A::*NbNOA*1, dSACMV-A::*NbNOA*1, SACMV-AΔCP and dSACMV-AΔCP extracted RNA

using primers for NbNOA1 (target) expression to EF1α (reference). Real-time PCR was also performed on RNA extracted from healthy samples so that these values could be used as the calibrator in Equation 4-2. To determine PCR efficiency for each primer set, qRT-Nb1 and Nb1Ef-1 was used to derive a standard curve from plasmid standard (Figure 4-4, Figure 4-5).

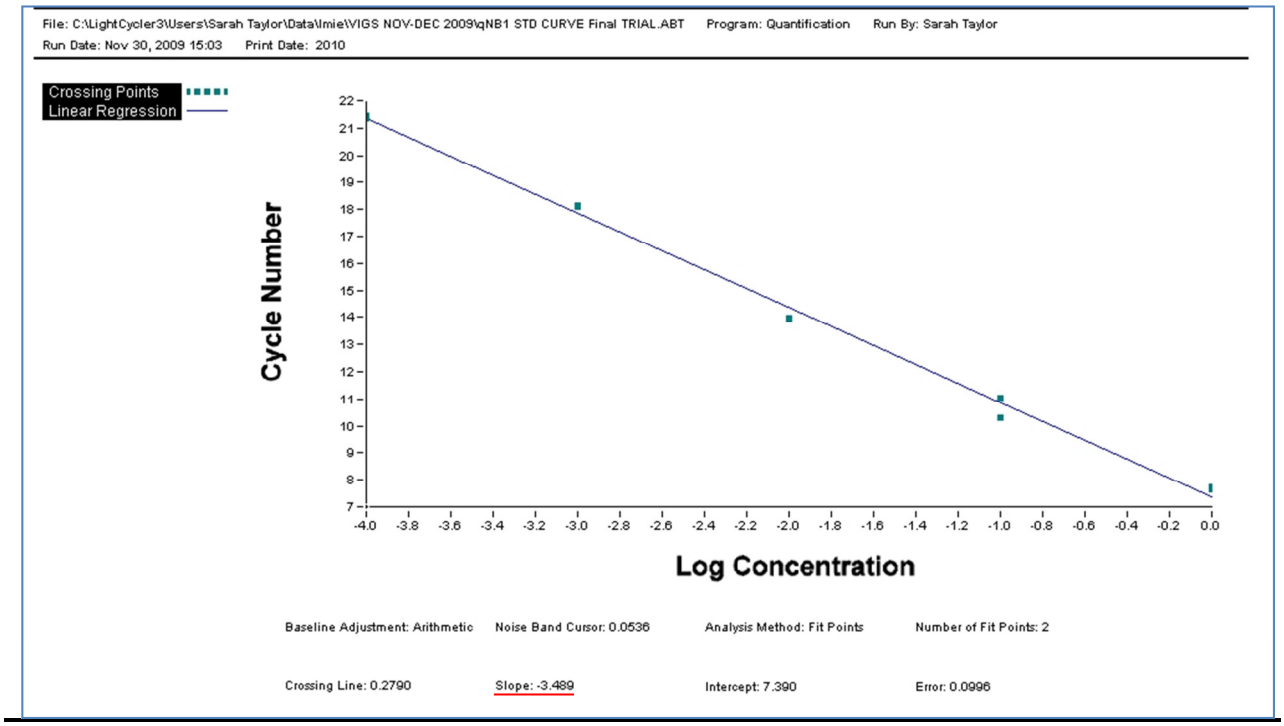

Figure 4-4: standard curve for serial dilutions of qRT-Nb1 plasmid standard
qRT-Nb1 plasmids standard were constructed by inserting amplicon obtained from amplification of the region bordered by qRT-Nb1 primers in *NbNOA*1. The plasmid standards were diluted to concentration ranging from 10000 pg to 0.1 pg. Standard curve was constructed using duplicate samples of plasmid standard. The standard curve was plotted in LightCycler Software version 3.0 in order to determine the efficiency of the primers based on the value of the slope. Slope (underlined in red) -3.489

Using the slope values obtained in Figure 4-4 and Figure 4-5, the efficiency of each primer set was calculated using Equation 4-1. For qRT-Nb1, the slope value was -3.489 (Figure 4-4) and using Equation 4-1, E_{NbNOA1} calculated to be 1.93. The slope value obtained from a standard curve using qNb1-EF1 primers (Figure 4-5) was -3.841 and using Equation 4-1, $E_{Ef1\alpha}$ calculated to be 1.82.

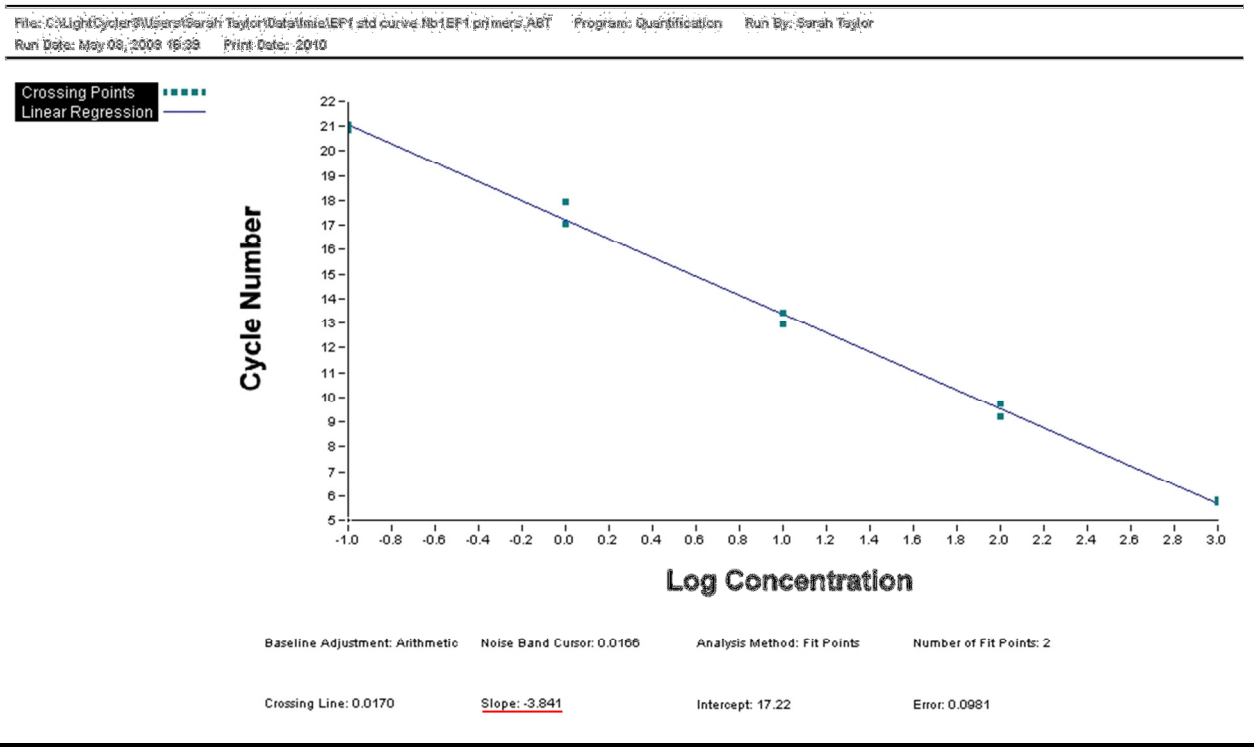

Figure 4-5: standard curve for serial dilutions of pTZEF1 plasmid standard
pTZEF1 plasmids standard were received from F. van Schalk. They were constructed by inserting amplicon obtained from amplification of the region bordered by qNb1-EF1 primers in *NbEF1α*. The plasmid standards were diluted to concentration ranging from 10000 pg to 0.1 pg. Standard curve was constructed using duplicate samples of pTZEF1 plasmid standard. The standard curve was plotted in LightCycler Software version 3.0 in order to determine the efficiency of the primers based on the value of the slope. Slope (underlined in red) -3.841.

Calculated E_{NbNOA1} and $E_{Ef1\alpha}$ were used in Equation 4-2 to calculate the relative expression ratio of *NbNOA*1 in relation to *Ef1α* in each treated sample and this value was compared to the relative expression of *NbNOA*1 in relation to *Ef1α* in healthy samples. Using Equation 4-2, the value of relative *NbNOA*1 expression in relation to *Ef1α* in the calibrator calculated to be 1. This is because $\Delta C_q = 0$ as the C_q values for the calibrator and the sample in this case will be the same. The different ratios obtained for each treatment were plotted (Figure 4-6, Figure 4-7). Two way ANOVA was performed on the relative level of expression of *NbNOA*1 in SACMV-A::*NbNOA*1 infected plants in respect to the expression in SACMV-AΔCP infected and found that the change in level of expression was significant ($P<0.05$) over the 3 time points studied and in terms of the treatment the plants were subjected to. Comparing *NbNOA*1 expression in delayed SACMV-A::*NbNOA*1 infection, the treatments did not account for significant change in level of expression.

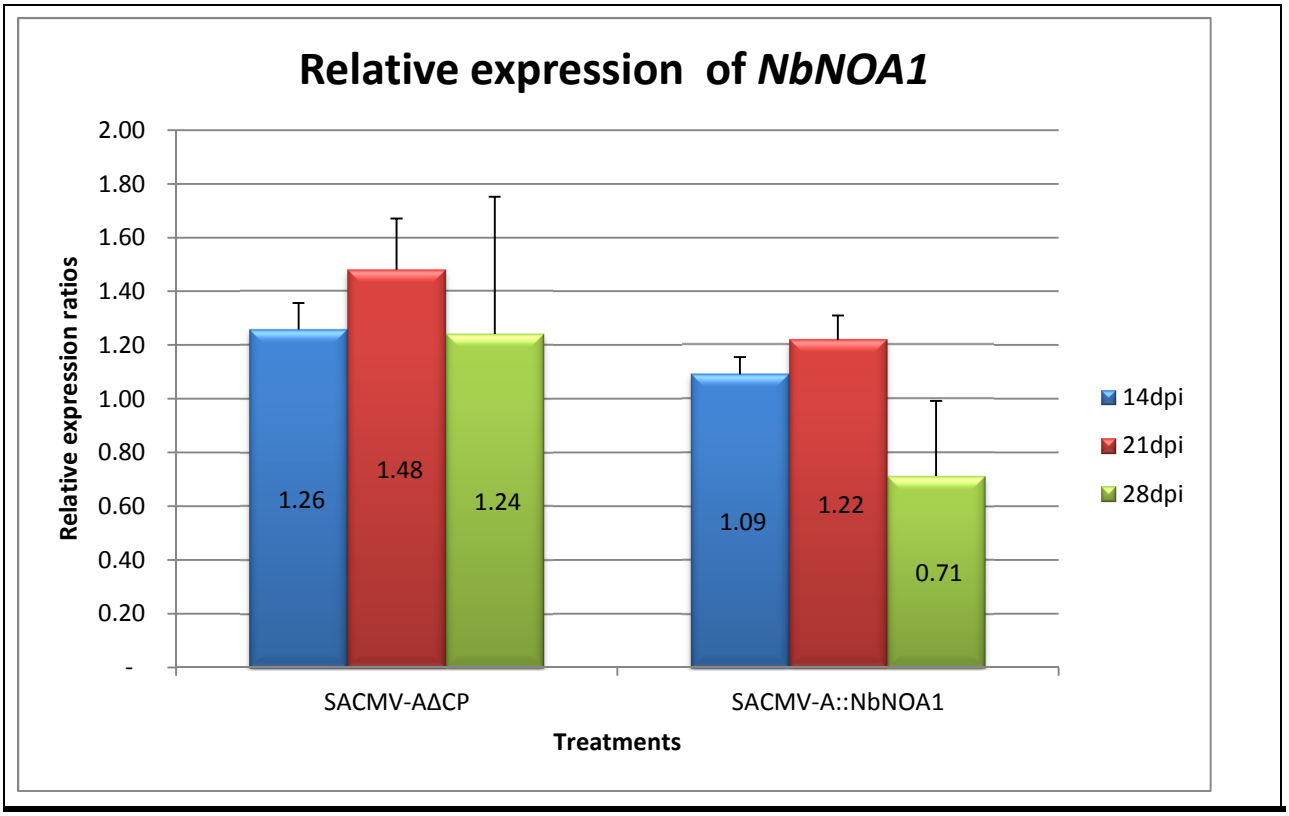

Figure 4-6: Relative expression of *NbNOA*1 in SACMV-AΔCP and in SACMV-A::*NbNOA*1 inoculated *N. benthamiana*

The value of NbNOA1 expression in healthy plant is constant at 1 because this was used as a calibrator. Error bars show standard error of the mean (SEM), n=3.

To compare the level of expression upon silencing using SACMV-A::*NbNOA*1, the relative expression values obtained for SACMV-A::*NbNOA*1 was compared to that of SACMV-AΔCP (Figure 4-6) and for the delayed experiments, the relative expression values obtained for dSACMV-A::*NbNOA*1 was compared to that of dSACMV-AΔCP (Figure 4-7).

At 14 dpi, there is a 13.5% [(1.09-1.26/1.26) X 100] decrease in *NbNOA*1 expression in plants infected with SACMV-A::*NbNOA*1 when compared to infection with the SACMV-AΔCP (Figure 4-6). When a similar treatment is applied followed with infection of SACMV-A and B 7 days after the first, plants initially treated with SACMV-A::*NbNOA*1 show an increase in expression (47%) when compared to dSACMV-AΔCP (Figure 4-7). At 21 dpi, a similar trend can be observed: an 17.5% decrease in expression in plants infected SACMV-A::*NbNOA*1 when compared to SACMV-AΔCP and a 21% increase in expression in dSACMV-A::NbNOA1 when compared to dSACMV-AΔCP. At 28 dpi, the expression of *NbNOA*1 in SACMV-A::*NbNOA*1

infected is further reduced by 43%. In dSACMV-AΔCP::*NbNOA*1, the expression is decreased by 25.5% when compared to dSACMV-AΔCP.

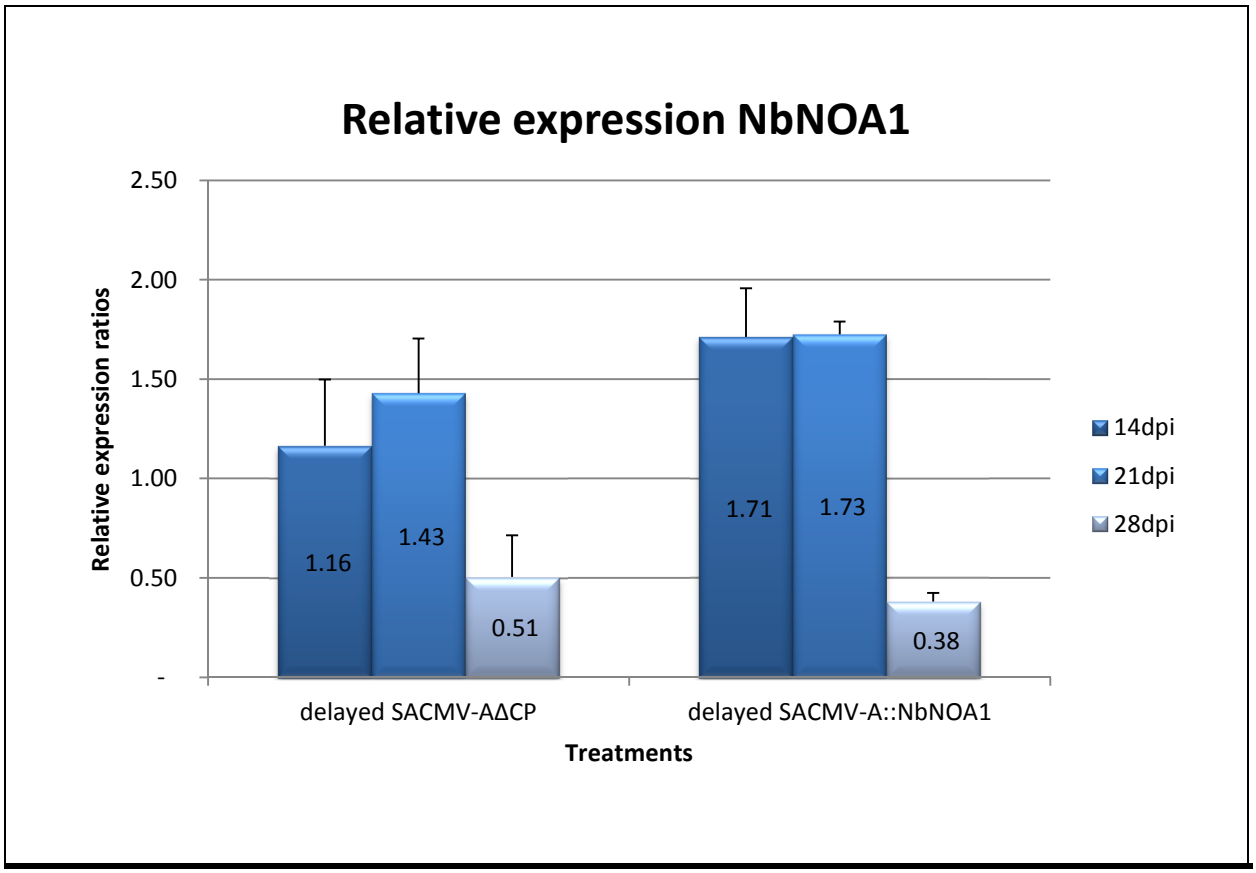

Figure 4-7: Relative expression of *NbNOA*1 in healthy untreated *N. benthamiana* and in SACMV-A::*NbNOA*1. *NbNOA*1 expression in healthy plants was used as a calibrator to which was compared the expression in delayed SACMV-AΔCP and SACMV-A::*NbNOA*1. Error bars show SEM, n=3.

Considering that the relative expression ratio of *NbNOA*1 in non-treated healthy plants was calculated to be 1 and this relative expression value was used as a calibrator. Comparing the relative expression of *NbNOA*1 in SACMV-AΔCP and dSACMV-AΔCP to that of *NbNOA*1 in non-treated healthy plants, *NbNOA*1 in both controls, SACMV-AΔCP and dSACMV-AΔCP, is higher at 14 and 21 dpi. At 28 dpi, *NbNOA*1 expression in dSACMV-AΔCP is lower than in healthy plants while in SACMV-AΔCP, it remains elevated.

4.3.3 Virus quantification

Based on the silencing results obtained above, using RT-PCR, the viral titer was quantified in response to modulation of *NbNOA*1 expression at the different time points. DNA was extracted simultaneously to RNA and diluted to between 30-100 ng/µl. A standard curve was constructed with different concentrations of pTZA ranging from $1x10^{-3}$-$1x10^{1}$ pg. In each run for viral titer quantification, one of the standards used to derive the standard curve was included in order to relate the C_P to amount of viral load in pg. The pg values obtained in the LightCycler software version 4 were converted to gram and used to calculate the copy number (Equation 4-3).

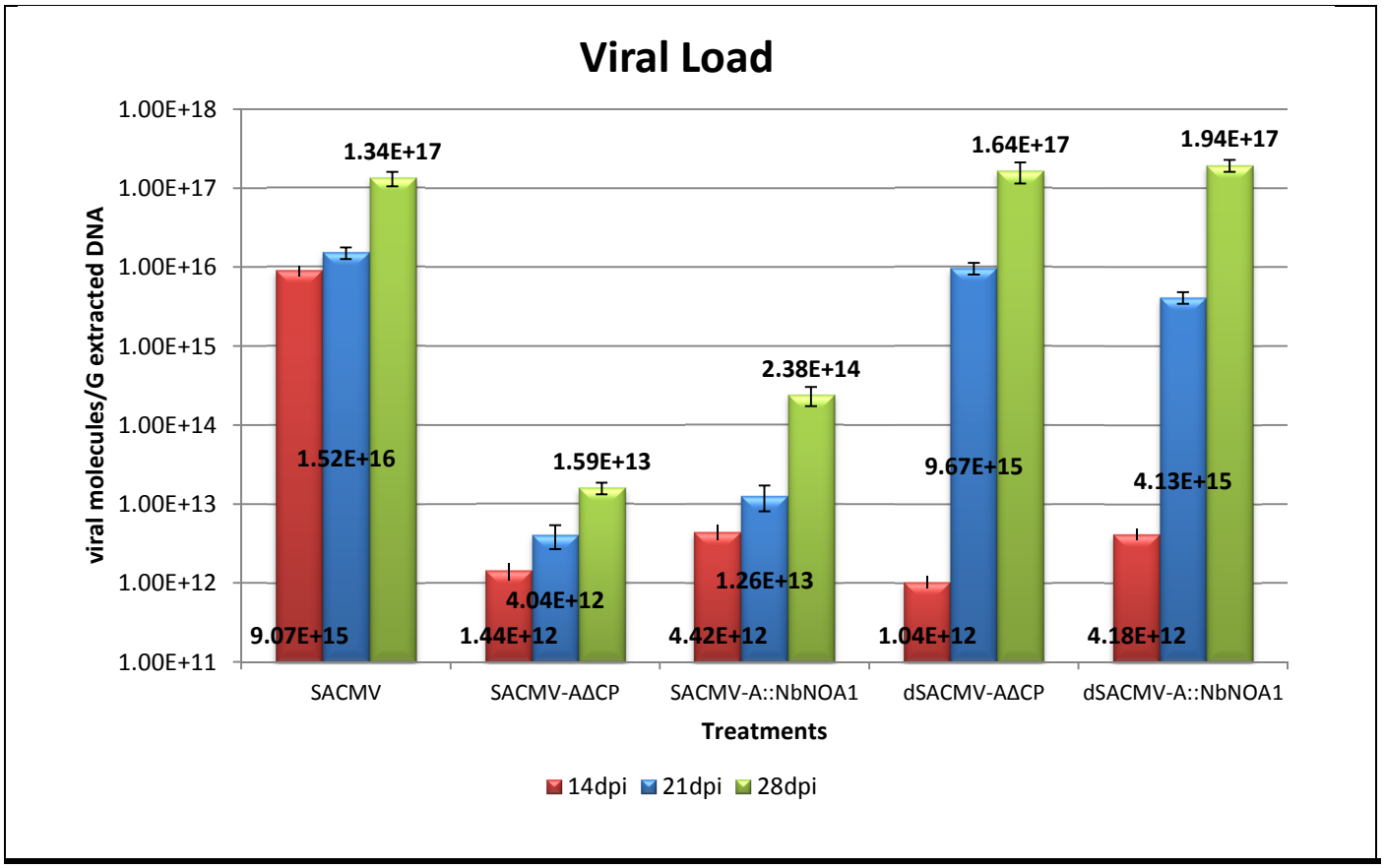

Figure 4-8: Analysis of viral load of SACMV in *N. benthamiana* infected with SACMV-A and B, SACMV-AΔCP, SACMV-A::*NbNOA*1, dSACMV-AΔCP and dSACMV-A::*NbNOA*1

The amount of SACMV DNA-A is expressed as viral molecules/g of extracted DNA were obtained using absolute real-time amplification. Y-axis is logarithmic scale. Error bars represent SEM. n=3

The copy number of viral molecules per gram of DNA was obtained using Equation 4-4. The copy number of viral molecules per gram of DNA values obtained was then plotted for each treatment and each time point under investigation (Figure 4-8). Viral load was quantified in SACMV-A and B infected plants in order to compare the viral titer in each treatment to the viral titer in SACMV-A and B infected *N. benthamiana.*

Looking at Figure 4-8, at 14 dpi, the viral load in SACMV-A::*NbNOA*1 infected plants was about three times higher than in SACMV-AΔCP. At 21 dpi, there was about a 4-fold increase in SACMV-A::*NbNOA*1 and SACMV-AΔCP compared to viral load in the same plants at 14 dpi. Looking at SACMV-A::*NbNOA*1 and comparing it to SACMV-AΔCP, the viral load was about three times higher in SACMV-A::*NbNOA*1 plants at 21 dpi than SACMV-AΔCP. At 28 dpi, there was a 20-fold increase in SACMV-A::*NbNOA*1 compared to viral load in the same plants at 21 dpi. In SACMV-AΔCP infected plants, there was about a 4-fold increase compared to viral load in the same plants at 21 dpi. Looking at SACMV::*NbNOA*1 and SACMV-AΔCP at 28 dpi, the viral load was 15 times higher in SACMV-A::*NbNOA*1.

Looking at delayed infection experiment, the viral load in dSACMV-A::*NbNOA*1 infected plants was about four times higher than in dSACMV-AΔCP at 14 dpi. At 21 dpi, there was a 1000-fold increase in dSACMV-A::*NbNOA*1 compared to viral load in the same plants at 14 dpi. In dSACMV-AΔCP infected plants, there was about a 9000-fold increase compared to viral load in the same plants at 14 dpi. Looking at dSACMV-A::*NbNOA*1 and comparing it to dSACMV-AΔCP, the viral load was halved in dSACMV-A::*NbNOA*1 plants at 21 dpi than dSACMV-AΔCP. At 28 dpi, there was a 50-fold increase in dSACMV-A::*NbNOA*1 compared to viral load in the same plants at 21 dpi. In dSACMV-AΔCP infected plants, there was about a 20-fold increase compared to viral load in the same plants at 21 dpi. Looking at dSACMV::*NbNOA*1 and dSACMV-AΔCP at 28 dpi, the viral load in both treatments was about the same, with viral load in dSACMV::*NbNOA*1 infected plants being 1.2-fold higher.

Comparing both experiments, non-delayed and delayed, to experiments in which plants were infected with SACMV-A and B, the viral titer in the non delayed experiments is much lower than viral titer in SACMV-A and B experiments. The highest viral load value, 2.38×10^{14}

obtained in SACMV::*A-NbNOA*1 infected plants was about 40 times lower than the lowest viral load recorded for SACMV-A and B, at 14 dpi. Looking at the delayed experiments, the viral load at 14 dpi is about 35 times lower than the viral load in SACMV-A and B, comparing the average viral load in dSACMV-AΔCP and dSACMV-A::*NbNOA*1 at 14 dpi to the viral load at 14 dpi for SACMV-A and B. At 21 dpi, the average viral load for the delay treatments is only about half of that in SACMV-A and B and by 28 dpi, these values are comparable.

ANOVA was performed on the values of viral titer, comparing the viral load of SACMV-AΔCP to that of SACMV-A::*NbNOA*1 and found that without the treatment, there is a 7% chance of randomly observing this change in viral load in an experiment of this size, the interaction is considered significant ($p < 0.1$). When comparing the viral load of dSACMV-AΔCP to that of dSACMV-A::*NbNOA*1, there is a 81% chance of randomly observing this difference in viral load in an experiment of this size. The effect is considered not significant.

4.3.4 Symptom evaluation

N. benthamiana plants infected with SACMV, SACMV-AΔCP, SACMV-A::*NbNOA*1, dSACMV-AΔCP and dSACMV-A::*NbNOA*1 were scored for symptoms severity. Looking at Table 4-2 and Figure 4-9, leaves infiltrated with SACMV-AΔCP generally had mild symptoms with slightly more pronounced symptoms observed for SACMV-A::*NbNOA*1 (Table 4-2). Leaves of plants infected for the delayed infection experiment, had more pronounced symptoms at 28 dpi. They scored between 4 and 5 and beside the size of leaves that seemed more reduced in SACMV-A and B, they were not much different, symptomatically than SACMV-A and B infected plants.

Table 4-2: Rating of leaf symptoms

Treatment	Mosaic	Leaf deformation	Chlorosis	Blistering	Score (0-5)
Healthy	0	0	0	0	0
SACMV-A and B	Se	Se	Se	Se	5
SACMV-AΔCP	0	0	M	M	1-2
SACMV-A::*NbNOA*1	M	M	S	M-S	2-3
dSACMV-AΔCP	Se	S	Se	S	4-5
dSACMV-A::*NbNOA*1	Se	S	Se	Se	4-5

Symptoms were scored as suggested in by a 2004 publication by (Chellappan et al. 2004). 0-no symptom, M= mild, S=strong, Se=severe

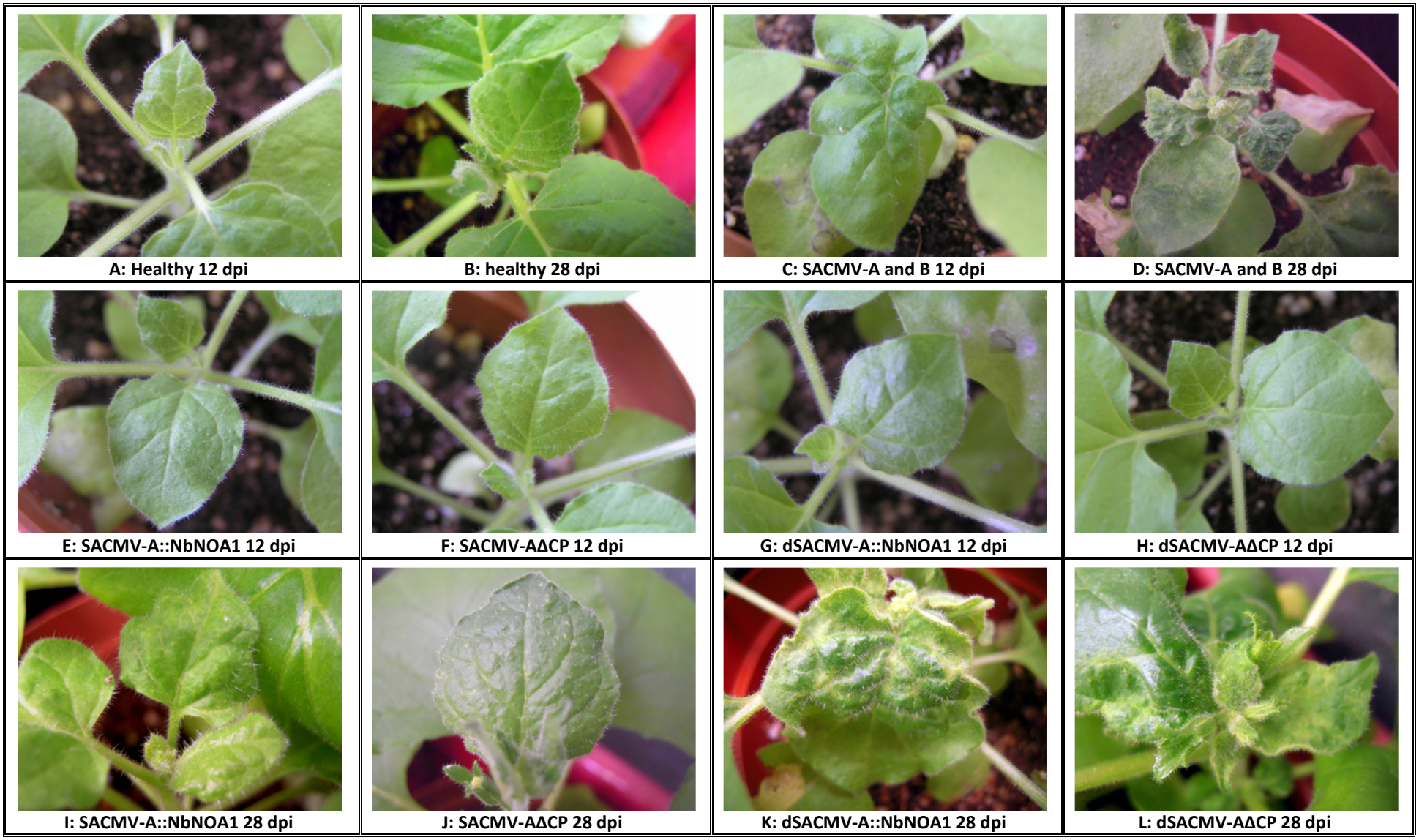

Figure 4-9: Symptoms development at 12 and 28 dpi.
Symptoms were observed at different time points and compared to that of healthy (A-B) and SACMV infected (C-D) at the different time points. The name of the corresponding treatments for each image is written at the bottom.

4.4 DISCUSSION

The development of VIGS technology has allowed functional characterization of different genes. especially genes involved in plant-pathogen interaction (Purkayastha and Dasgupta 2009). Disease resistance studies using VIGS involves silencing of the gene of interest with generally a TRV-based VIGS virus that has shown to induce more stable silencing effects than TMV or PVX-based virus (Ratcliff et al. 2001). Once silencing of the gene of interest has been established, the virus being studied is used to infect the plants, or in the case of non-host resistance studies, a pathogen to which the plant is not a natural host is used to infect the plants and disease symptoms are recorded. In this chapter, we report the silencing of *NbNOA*1 using SACMV-A VIGS designed in Chapter 3, and the potential effect that this silencing may have on SACMV accumulation in *N. benthamiana. NbNOA*1 was initially isolated from a cDNA library prepared from hyphal wall elicitor treated leaf tissues (Yoshioka et al. 2003). *NbNOA*1 has been previously reported to be involved in disease resistance against *Colletotrichum lagenarium* (Kato et al. 2007).

To identify the *NbNOA*1 sequence fragment to be used to silence *NbNOA*1 in *N. benthamiana*, sequences of *NbNOA*1 and homologs in *Arabidopsis*, rice and a partial putative *NOA*1 EST in *G. max* were aligned to identify the region with the highest nucleotide sequence similarity across these homologs. Because VIGS allows the silencing of homologous genes in different species, as seen in Chapter 3 where a VIGS vector carrying a fragment of *N. tabacum su* was used to successfully silence *su* in *N. benthamiana,* using a fragment that shares sequence similarity to *NOA*1 sequence in other plant species would allow the same vector to be used to silence NOA1 homologs in other plant species. The first plant *NOA*1 gene was identified in *Arabidopsis* (Guo et al. 2003), followed by *N. benthamiana* (Kato et al. 2007) and rice (Qiao et al. 2009). These proteins belong to novel family of GTPase and not much is known about their function (Moreau et al. 2008; Zemojtel et al. 2004). Mammalian NOA1 homologue localize in the mitochondrion (Zemojtel et al. 2004) while plants homologs localize in the mitochondrion (Guo and Crawford 2005) and recently have been localized in chloroplast (Moreau et al. 2008). For the purpose of this experiment, the possibility that these proteins could belong to a gene family where more than

one member could be present in a species could not be overlooked and by choosing a region with the highest similarity across different homologs, functional redundancy was avoided.

A 308 bp sequence fragment was selected from the "conserved" region and subjected to siRNA scan online tool (Xu et al. 2006). siRNA scan allows to minimize potential off-target PTGS, provides the identity and function of these potential off-targets found in a sequence and the efficiency estimation of potential siRNA in a given sequence. The veracity of the results obtained from the siRNA scan tool depends highly on the data available for the organism being investigated. Consequently, it can only be concluded that, based on what was known at the time of this investigation on the transcriptome of *N. benthamiana,* the 308 bp sequence gave no "*hits*" in siRNA scan (Table 4-1), and therefore this sequence would produce no unintended silencing in *N. benthamiana*.

Because the level of silencing achieved with VIGS vector between plants infected by the same construct is not uniform as shown in Chapter 3, RNA and DNA were simultaneously extracted from the same samples using a modified Tri Reagent method (Ambion 2005), in this way, the decrease in *NbNOA*1 expression could be directly compared to viral load. The acidity of Tri Reagent (Sigma-Aldrich, St Louis, USA) allows phase separation of RNA and DNA. At a pH of below 7 RNA is soluble in the aqueous phase and DNA is found in the lower interphase and organic phase containing DNA (Chomczynski and Sacchi 2006). The addition of the back extraction buffer to the interphase and organic phase alkalinized the lysate, allowing phase separation of DNA that solubilized in the aqueous phase and proteins that remained in the organic phase. The extracted RNA was used to quantify relative level of *NbNOA*1 in SACMV-AΔCP, SACMV-A::*NbNOA*1, dSACMV-AΔCP and dSACMV-A::*NbNOA*1 using the comparative C_q method with PCR efficiency correction (Pfaffl et al. 2002).

In the comparative C_q, the relative change in target gene expression in relation to internal control in treated samples is compared to the relative target gene expression in relation to internal control in untreated samples (Wong and Medrano 2005; Schmittgen and Livak 2008). Two separate experiments were carried out. In the first or non-delayed experiment, *N. Benthamiana* plants were infected with SACMV-A::*NbNOA*1 and SACMV-B as the experiment to silence

*NbNOA*1 and as a negative control, *N. Benthamiana* plants were infected with SACMV-AΔCP and SACMV-B as negative control. In the second or delayed experiment, *NbNOA*1 was silenced using SACMV-A::*NbNOA*1 and 7 days later these plants were infected with SACMV-A and SACMV-B. As a negative control, *N. benthamiana* were infected SACMV-AΔCP and 7 days later these plants were infected with SACMV-A and B.

The relative expression of *NbNOA*1 in SACMV-A::*NbNOA*1 and dSACMV-A::*NbNOA*1 was compared to the relative *NbNOA*1 expression in control plants. In order to relate the two experiments, relative expression of *NbNOA*1 at each time point in healthy plants was used as the calibrator and the value of *NbNOA*1 expression in healthy plants was calculated to be 1. The relative expression of *NbNOA1* in healthy plants was then used to obtain the relative expression ratios of *NbNOA*1 in SACMV-AΔCP, SACMV-A::*NbNOA*1, dSACMV-AΔCP and dSACMV-A::*NbNOA*1 (Figure 4-6 and Figure 4-7).

Although not under investigation, it was interesting to observe that expression of *NbNOA*1 in response to SACMV infection in SACMV-AΔCP and dSACMV-AΔCP was higher than expression of *NbNOA*1 in healthy plants. This was true for both experiments at 14 and 21 dpi. At 28 dpi however, expression of *NbNOA*1 in dSACMV-AΔCP infected plants was lower than expression in healthy and in SACMV-AΔCP, the expression of *NbNOA*1 remained higher. The fluctuation of *NbNOA*1 expression in both SACMV-AΔCP and dSACMV-AΔCP show that this gene is somehow affected by SACMV infection. What remains to be ascertained is the exact role in disease resistance, whether the increase in *NbNOA*1 expression during infection directed by the plants as a disease resistance response or is the increase in expression required by the virus in order to produce a successful infection. The expression of *NbNOA*1 in SACMV-A::*NbNOA*1 and dSACMV-A::*NbNOA*1 could not be compared to the expression of *NbNOA*1 in healthy plants because as these experiments were carried out with a purpose of decreasing *NbNOA*1 expression in comparison to SACMV-AΔCP and dSACMV-AΔCP infections, no conclusions could be drawn by relating them to *NbNOA*1 expression in healthy plants.

*NbNOA*1 expression in SACMV-A::*NbNOA*1 was lower than *NbNOA*1 expression in SACMV-AΔCP infected plants at 14, 21 and 28 dpi. Relating *NbNOA*1 silencing to viral load, looking at

Figure 4-6 and Figure 4-8, decrease in *NbNOA*1 expression at 14, 21 and 28 dpi in SACMV-A::*NbNOA*1 infected plants resulted in an increase in viral load at 14, 21 and 28 dpi when compared to viral load in dSACMV-AΔCP infected plants especially at 28 dpi where a 20-fold increase was observed (Figure 4-8). From these results it can be concluded that decrease in *NbNOA*1 increased the susceptibility of *N. benthamiana* to SACMV infection. Down-regulation in *NOA*1 expression has been previously linked with increase in pathogen susceptibility. In *N. benthamiana,* down-regulation of *NOA*1 through VIGS was reported to increase susceptibility of *N. benthamiana* to the fungal elicitor INF-1 (Kato et al. 2007) and in *Arabidopsis, atnoa1* mutants were shown to be highly susceptible to *P. syringae* (Zeidler et al. 2004).

The expression of *NbNOA*1 in dSACMV-A::*NbNOA*1 when compared to *NbNOA*1 expression in dSACMV-AΔCP did not follow a particular trend; at 14 and 21, expression of *NbNOA*1 in dSACMV-A::*NbNOA*1 was higher than *NbNOA*1 expression in dSACMV-AΔCP and at 28 dpi, the expression of *NbNOA*1 in dSACMV-A::*NbNOA*1 was lower than *NbNOA*1 expression in dSACMV-AΔCP. These results were expected as in Chapter 3, the silencing of *su* in plants that were infected with the SACMV-A::*su* was suppressed when 7 days later, SACMV-A and B was used to re-infect these plants. As this was observed previously, it was expected that dSACMV-A::*NbNOA*1 would result in suppression of *NbNOA*1 silencing. Comparing *NbNOA*1 expression to viral load in delayed experiments (Figure 4-7 and Figure 4-8) no conclusion could be drawn. At 14 dpi when the expression of *NbNOA*1 in dSACMV-A::*NbNOA*1 was higher than in dSACMV-AΔCP, the viral load in dSACMV-A::*NbNOA*1 was higher than in dSACMV-AΔCP. However, at 21 dpi, the viral load in dSACMV-A::*NbNOA*1 infected plants was lower than in dSACMV-AΔCP although, the expression of *NbNOA*1 in dSACMV-A::*NbNOA*1 was higher than in dSACMV-AΔCP. At 28 dpi, *NbNOA*1 expression in dSACMV-A::*NbNOA*1 was lower than in dSACMV-AΔCP with not much difference in viral load (1.64E+17 viral molecules per gram of extracted DNA for dSACMV-AΔCP and 1.94E+17 viral molecules per gram of extracted DNA for dSACMV-A::*NbNOA*1).

The viral load obtained through absolute real-time could be associated with symptoms observed on the infected leaves. Symptoms were slightly more severe in SACMV-*NbNOA*1 leaves when compared to SACMV-AΔCP leaves however, a difference between a score of 1-2 and one of 2-3

is not considered significant. Symptoms on leaves of delayed infections were more severe than those of SACMV-AΔCP and SACMV-*NbNOA*1 plants, almost as severe as leaves of *N. benthamiana* infected with SACMV-A and B. The milder symptoms observed in SACMV-*NbNOA*1 and SACMV-AΔCP could be associated with the low viral load recorded in these plants when compared to SACMV-A and B infected plants. Similarly the severe symptoms observed in dSACMV-*NbNOA*1 and dSACMV-AΔCP could be related to the higher viral load in these plants. The symptoms in dSACMV-*NbNOA*1 and dSACMV-AΔCP infected plants was severe but not as severe as SACMV-A and B infected plants although in terms of viral load, there was not much difference between the two sets and on average, leaves from both delayed infection had a slightly higher viral load than SACMV-A and B infected plants. The difference in symptoms can be attributed to the fact that in delayed plants, SACMV-A and B was inserted 7 days later than plants with SACMV-A and B (without the delay). This shows that relationship between viral load and symptoms is not a direct one and in comparing infectivity, both symptoms and viral load need to be recorded.

Because cassava is not susceptible to any of the model VIGS vector, TRV, PVX and TMV, the delayed experiments were carried out in an attempt to develop a Geminivirus-based VIGS system that would allow silencing pathogen related genes in *N. benthamiana* and cassava, which would assist in functional characterization of disease related genes. As mentioned previously, methodology of VIGS to silence pathogen related genes involves silencing the candidate gene with a VIGS vector, often TRV and later infecting with the virus of interest (TMV or PVX) that is different to VIGS vector VIGS (Purkayastha and Dasgupta 2009). Unfortunately, silencing *NbNOA*1 with a SACMV-A based VIGS vector and 7 days later infecting with SACMV-A and B did not result in silencing and therefore *NbNOA*1 silencing could not be related to viral load using this methodology.

Until *NbNOA*1 and its homologs are fully characterized in terms of their function, the effect that *nbnoa*1 silencing has on geminivirus viral load accumulation can only be speculative. NbNOA1 was recently identified as a cGTPase of the family YlqF/YawG family known to have nucleic acids and protein binding abilities (Sudhamsu et al. 2008; Moreau et al. 2008). GTP/GDP are involved in various processes in a cell, however the function of cGTPase in plants and mammals

has not yet been clarified. *YqeH*, the *NOA*1 homolog in *B. subtilis*, is involved in ribosome assembly and since *YqeH* can rescue phenotypes produced by *atnoa1* null mutation, the activity of YqeH could be said to mirror that of *AtNOA*1 (Sudhamsu et al. 2008). Because of their involvement in ribosomal assembly, one would expect that down-regulation of YqeH expression would result in obstruction to ribosome assembly to result in cell cycle arrest, however it has been shown that down-regulation in YqeH promotes chromosomal replication (Sudhamsu et al. 2008) highlighting a role in both ribosomal assembly and possibly cell cycle regulation. Assuming that down-regulation of *nbnoa*1 resulted in upregulation in chromosomal replication as is the case for *yqeh*, this would explain why down-regulation of *nbnoa*1 in *N. benthamiana* resulted in an increase in viral load as geminiviruses require infected cells to be actively replicating.

However, the fact that infection of SACMV in plants results in upregulation of *NbNOA*1 when compared to non-infected plants suggests a possible dual role for *NbNOA*1, which could work antagonistically to each other, depending on the cellular environment. GTP has been found to be essential for nuclear shuttling function of NSP and in intercellular trafficking of viral molecules (Ward and Lazarowitz 1999; Carvalho et al. 2008; Carvalho et al. 2008; Gafni 2002). *NbNOA*1 could play a major role in maintaining the GTP/GDP balance in the cell that would contribute to viral movement. This could explain why SACMV infection results in upregulation of *NbNOA*1 expression. However, the fact that down-regulation of *NbNOA*1 results in increase in viral load could imply that *NbNOA*1 could also play a different role in response to virus infection. Because overexpression of *AtNOA*1 in *A. thaliana* leads to an increase NO production (Guo et al. 2003; Crawford and Guo 2005), *atnoa1* null mutations in *Arabidopsis* as well as *NbNOA*1 silencing using VIGS in *N. benthamiana* result in decrease in NO, *NbNOA*1 and *AtNOA*1 involvement with NO cannot be overlooked, although no NOA1 homologs were shown to directly produce NO. The involvement of *NOA*1 in geminivirus disease resistance could also be as a result of NO accumulation.

Targets of NO protein modification include various transcription factors and proteins that participate in regulation of cell cycle. The cell cycle is usually targeted by geminiviruses during infection. Geminiviruses replicate their ssDNA genome through a dsDNA intermediate with the

help of the host's replication machinery, forcing dormant cells, in the G_0 stage of the cell cycle to re-enter the G_1 and replicate in the S phase without carrying on into mitosis, resulting in endoreduplication or genome duplication (Hanley-Bowdoin et al. 2004). The transition from the G_0 to the G_1 is initiated by Rep that modulates the activity of the retinoblastoma related (RBR) protein and elongation factor 2(EF2)-mediated suppression of the proliferating cell nuclear antigen (PCNA) whose activity can be affected by a nitric oxide burst (Durzan 2002). NO has been shown to induce the upregulation of the D-type cyclin the *CYCD3*;1 and suppression of *KRP*2 *(*kip related protein 2) of both promoting mitosis over endoreduplication (Verkest et al. 2005; Correa-Aragunde et al. 2006). Microarray analysis showed that the expression of *CYCD3;1* and *KRP2* remained constant in response to CalCuV infection in *A. thaliana* (Sozzani et al. 2008) as change in their activity favors initiation of mitosis rather than endocycle and this is detrimental to establishment of geminiviruses replication. The elucidation of the role of cGTPase in plants would allow answering the questions raised by this research, in terms of the involvement of *NbNOA*1 through either GTP/GDP or NO during geminivirus infection.

CHAPTER 5.CONCLUSIONS

Cassava is major source of starch in Africa with an industrial potential that is still underutilized. It is grown by small scale farmers mostly for consumption. In South Africa, cassava is mainly grown for use in the biofuel industry rather than consumption. Cassava infection by cassava mosaic geminiviruses results in high yield losses of up to 90% (Fauquet and Fargette 1990). *South African cassava mosaic virus* (SACMV) is endemic to South Africa, Madagascar, Swaziland and Zimbabwe (Ndunguru et al. 2005; Briddon et al. 2004). SACMV infection in the host triggers post-transcriptional gene silencing (PTGS), which target viral mRNA transcripts (Vanitharani et al. 2005). SACMV encodes for PTGS suppressor that allows the virus to evade the host PTGS response as well as hypersensitive response (HR) suppressor that prevents the virus from triggering HR in the host. Nitric oxide (NO) has been identified as a major player in oxidative burst induced cell death during the HR. AtNOA1 has been associated with NO production in disease resistance as noa1 mutants in *Arabidopsis* and *N. benthamiana* have been shown to have increased in susceptibility to pathogen (Zeidler et al. 2004; Kato et al. 2007). In this study the ability of SACMV to trigger gene silencing in plants was utilized to silence *NbNOA*1 in *N. benthamiana* and study the resulting effect on virus proliferation, a method known as Virus induced gene silencing (VIGS) that has been extensively used in *N. benthamiana* for functional genomics (Robertson 2004; Carrillo-Tripp et al. 2006). In this study, the construction of the first SACMV VIGS vector is reported. The vector was designed on SACMV-DNA A, by replacing a portion the coat protein (AV1) gene sequence with a multiple cloning site (MCS) as the AV1 gene is not absolutely required for systemic movement by bipartite geminivirus. To attest functionality of the vector, a fragment of *N. tabacum su* was inserted into the SACMV VIGS vector and used to positively silence *su i*n N. *benthamiana* and cassava.

Although using Southern hybridization, nucleotide sequences with similarity to *AtNOA*1 were identified in cassava, attempts to isolate *AtNOA*1 homolog using primers designed to anneal specifically at the 5′ and the 3′ end of *AtNOA*1 in cassava were unsuccessful but resulted in positive amplification in *N. benthamiana.* It was concluded that there was possibly low or no sequence similarities in regions to which *AtNOA*1 primers could anneal and this was confirmed

later on as ESTs searches in the public EST database at GenBank revealed 2 ESTs whose translated nucleotides when aligned to NOA1 amino acid sequences from *Arabidopsis* and *N. benthamiana* revealed high sequence similarity, across the sequence but not at the 5′ end. As no NOA1 sequence in cassava was isolated, a fragment from *N. benthamiana NbNOA1* was subcloned into SACMV-A VIGS to silence *NbNOA*1 in *N. benthamiana.*

Silencing in of *NbNOA*1 in *N. benthamiana* was quantified using relative real-time quantification and was compared to viral load to determine whether silencing of *NbNOA*1 had any influence on SACMV replication and susceptibility of *N. benthamiana* to the virus. *N. benthamiana* plants were infected with a VIGS vector carrying a partial sequence of *NbNOA*1. Using real-time amplification, the viral load in the silenced plants was quantified and compared to viral load in control plants infected SACMV-A VIGS vector only, to determine any difference in virus load between experiment and control. Silencing of *NbNOA*1 and its *AtNOA*1 homolog has been shown to increase susceptibility to pathogen infection in *N. benthamiana* and *Arabidopsis* respectively (Zeidler et al. 2004; Kato et al. 2007). Results from our study showed that decrease in *NbNOA*1 expression in *N. benthamiana* causes a significant increase in viral load at 14, 21 and 28 dpi. The highest increase in viral load was observed at 28 dpi, where the highest decrease in *NbNOA*1 (43%) resulted in a 20-fold increase in viral load. The fact that partial silencing of *NbNOA*1 resulted in increase in *N. benthamiana* susceptibility to SACMV infection suggests that *NbNOA*1 may play an indirect role in virus resistance in tobacco. This is the first report where *NbNOA*1 silencing has been carried out and the effect on geminivirus infection determined. This vector can be used for functional gene validation and characterization in SACMV susceptible plants such as cassava and *N. benthamiana.*

RNA viruses such as PVX, TRV and TMV have been used extensively in VIGS (Purkayastha and Dasgupta 2009). Silencing effected by RNA viruses has been shown not to be stable as their RNA genome is targeted by the host PTGS resulting in prevention of virus replication and consequently remission (Baulcombe 2004; Robertson 2004). VIGS using these RNA viruses for functional validation of plant genes involved in resistance and susceptibility involves silencing the candidate gene with a VIGS vector, often TRV and later infecting with the virus of interest that is different to VIGS vector VIGS (Purkayastha and Dasgupta 2009).

In this research, a different system was used because PVX, TRV and TMV do not infect cassava. Delayed infection experiments were carried out where *NbNOA1* in *N. benthamiana* was silenced using SACMV-A VIGS vector and 7 days after, the same plants were infected with SACMV-A and B. Delayed experiments carried out in this manner resulted in suppression of *NbNOA*1 silencing. We speculate that the decrease in *NbNOA*1 expression was a result of increase in SACMV viral load. As geminivirus encode strong silencer of gene expression such as AC2 and AC4 (Bisaro 2006; Rajeswaran et al. 2007; Fondong et al. 2007), it is probable that increase in viral load caused by infection of SACMV-A and B 7 days after silencing of *NbNOA*1 in delayed experiments, resulted in increase in silencing suppressor that caused suppression of viral gene silencing as well as suppression in *NbNOA*1 silencing. For validation of genes involved in disease resistance in *N. benthamiana* and cassava, it may be prudent to use a different virus unrelated to SACMV (and other cassava begomoviruses), as a VIGS vector, preferably one which will not silence any endogenous R genes in cassava or the model *N. benthamiana* plant. A cassava-infecting RNA virus that does not potentially silence host PTGS mechanisms and would not obscure effects of the target virus under study, namely SACMV, will be a challenge to find.

To understand the link between *NbNOA*1 and virus disease, light will need to be shed on the function of *NbNOA*1. At present *NbNOA*1 is known to have GTP hydrolysis function and is shown to be involved indirectly with NO (Moreau et al. 2008; Zemojtel et al. 2004). Through its involvement with GTP/GDP and NO regulation in the cell, the list of processes it could be involved with is endless. In this research we speculate that the link between *NbNOA*1 and geminivirus lies possibly through *NbNOA*1 involvement with chromosome replication as well as through NO mediated regulation of cell cycle proteins. Down-regulation of *YqeH* expression, the NOA1 functional homologue in *B. subtilis,* results in increase in chromosomal replication (Sudhamsu et al. 2008) and NO regulates expression of *CYCD3*;1 and *KRP*2 *(*kip related protein 2), involved in promoting mitosis in plants (Verkest et al. 2005; Correa-Aragunde et al. 2006). *NbNOA*1 could also be indirectly involved in responses to geminivirus infection through its GTPase function. Shuttling of geminiviruses genomic molecules replicating in the cytoplasm to the nucleus mediated by nuclear shuttling protein (BC1) requires GTP/GDP (Carvalho, Machado, et al. 2008). Because of its GTP hydrolysis properties, down-regulation of *NbNOA*1 in

N. benthamiana could have resulted in disruption in the GTP/GDP balance in favor of GTP, affecting nuclear shuttling.

In conclusion, the results of this study have proven to be most useful in designing further experiments to study SACMV interactions with the natural host cassava and in the model host *N. benthamiana.* More work is needed to elucidate the role of *NbNOA1* and the homologs that are beginning to be discovered in many plants, The recent sequencing of the cassava genome (http://www.phytozome.net/cassava.php#) and pending sequencing of several other genomes, and functional genomic studies in host plants for geminiviruses such as *N. benthamiana* and *Arabidopsis thaliana*, will shed more light on mechanisms of resistance and susceptibility to viral pathogens.

CHAPTER 6. REFERENCES

Ambion. **2005**. TRI Reagent ® DNA / Protein Isolation. *Technical Resources* **version 05**: 1-7.

Aragão FJ, Brasileiro AC. **2002**. Positive, negative and marker-free strategies for transgenic plant selection. *Brazilian Journal of Plant Physiology* **14**: 1-10.

Asai S, Yoshioka H. **2009**. Nitric Oxide as a Partner of Reactive Oxygen Species Participates in Disease Resistance to Necrotrophic Pathogen Botrytis cinerea in Nicotiana benthamiana. *Molecular Plant-Microbe Interactions* **22**: 619-629.

Atkinson RG, Bieleski LR, Gleave AP, Janssen B, Morris BA. **1998**. Post-transcriptional silencing of chalcone synthase in petunia using a geminivirus-based episomal vector. *The Plant Journal* **15**: 593-604.

Barroso JB, Corpas FJ, Carreras A, Sandalio LM, Valderrama R, Palma JM, Lupiáñez JA, del Río LA. **1999**. Localization of Nitric-oxide Synthase in Plant Peroxisomes. *The Journal of Biological Chemistry* **274**: 36729 -36733.

Baulcombe DC. **2004**. RNA silencing in plants. *Nature* **431**: 356-63.

Belenghi B, Acconcia F, Trovato M, Perazzolli M, Bocedi A, Polticelli F, Ascenzi P, Delledonne M. **2003**. AtCYS1, a cystatin from Arabidopsis thaliana, suppresses hypersensitive cell death. *European Journal of Biochemistry* **270**: 2593-2604.

Bender J. **2004**. DNA methylation and epigenetics. *Annual review of plant biology* **55**: 41-68.

Berrie LC, Palmer K, Rybicki EP, Hiyadat SH, Maxwell DP, Rey ME. **1997**. A new isolate of African cassava mosaic virus in South Africa. *African journal of root and tuber crops* **2**: 49-52.

Berrie L, Rybicki EP, Rey M. **2001**. Complete nucleotide sequence and host range of South African cassava mosaic virus: further evidence for recombination amongst begomoviruses. *Journal of General Virology* **82**: 53-58.

Besson-Bard A, Astier J, Rasul S, Dubreuil-maurizi C, Wawer I, Dubreuil-Maurizi C, Jeandroz S, Wendehenne D. **2009**. Current view of nitric oxide-responsive genes in plants. *Plant Science* **177**: 302-309.

Bisaro DM. **2006**. Silencing suppression by geminivirus proteins. *Virology* **344**: 158-168.

Blevins T, Rajeswaran R, Shivaprasad PV, Beknazariants D, Si-ammour A, Park H, Vazquez F, Robertson DN, Meins Jr F, Hohn T, Pooggin MM. **2006**. Four plant Dicers mediate viral small RNA biogenesis and DNA virus induced silencing. *Nucleic Acids Research* **34**: 6233-46.

Borsani O, Zhu J, Verslues PE, Sunkar R, Zhu J. **2005**. Endogenous siRNAs derived from a pair of natural cis-antisense transcripts regulate salt tolerance in Arabidopsis. *Cell* **123**: 1279-91.

Briddon RW, Markham PG. **1994**. Universal primers for the PCR amplification of dicot-infecting geminiviruses. *Molecular biotechnology* **1**: 202-205.

Briddon RW, Robertson I, Markham PG, Stanley J. **2004**. Occurrence of South African cassava mosaic virus (SACMV) in Zimbabwe. *Plant Pathology* **53**: 233.

Brodersen P, Voinnet O. **2006**. The diversity of RNA silencing pathways in plants. *Trends in Genetics* **22**: 268-280.

Burch-smith TM, Anderson JC, Martin GB, Dinesh-Kumar SP. **2004**. Applications and advantages of virus-induced gene silencing for gene function studies in plants. *The Plant Journal* **39**: 734-746.

Cai X, Wang C, Xu Y, Xu Q, Zheng Z, Zhou X. **2007**. Efficient gene silencing induction in tomato by a viral satellite DNA vector. *Virus Research* **125**: 169-75.

Calvert LA, Thresh JM. **2002**. The Viruses and Virus Diseases of Cassava. In: Hillocks, RJ, Thresh, JM, Bellotti, AC, *Cassava: Biology, Production and Utilization*. CAB International 2002, 237-260.

Calvert LA, Cuervo M, Lozano I, Villareal N, Arroyave J. **2008**. Identification of Three Strains of a Virus Associated with Cassava Plants Affected by Frogskin Disease. *Journal of Phytopathology* **156**: 647-653.

Carrillo-Tripp J, Lozoya-Gloria E, Rivera-Bustamante RF. **2007**. Symptom Remission and Specific Resistance of Pepper Plants After Infection by Pepper golden mosaic virus. *Phytopathology* **97**: 51-9.

Carrillo-Tripp J, Shimada-Beltrán H, Rivera-Bustamante R. **2006**. Use of geminiviral vectors for functional genomics. *Current opinion in plant biology* **9**: 209-15.

Carvalho CM, Fontenelle MR, Florentino LH, Santos AA, Zerbini FM, Fontes EP. **2008**. A novel nucleocytoplasmic traffic GTPase identified as a functional target of the bipartite geminivirus nuclear shuttle protein. *The Plant Journal* **55**: 869-80.

Carvalho CM, Machado JP, Zerbini FM, Fontes EP. **2008**. NSP-interacting GTPase. A cytosolic protein as cofactor for nuclear shuttle proteins. *Plant Signaling and Behavior* **3**: 752-754.

Chellappan P, Masona MV, Vanitharani R, Taylor NJ, Fauquet CM. **2004**. Broad Spectrum Resistance to ssDNA Viruses Associated with Transgene-Induced Gene Silencing in Cassava. *Plant Molecular Biology* **56**: 601-611.

Chellappan P, Vanitharani R, Ogbe F, Fauquet CM. **2005**. Effect of Temperature on Geminivirus-Induced RNA Silencing in Plants. *Plant Physiology* **138**: 1828-1841.

Chomczynski P, Sacchi N. **2006**. The single-step method of RNA isolation by acid guanidinium thiocyanate-phenol-chloroform extraction: twenty-something years on. *Nature protocols* **1**: 581-5.

Chowda-Reddy RV, Achenjang F, Felton C, Etarock MT, Anangfac M, Nugent P, Fondong VN. **2008**. Role of a geminivirus AV2 protein putative protein kinase C motif on subcellular localization and pathogenicity. *Virus Research* **135**: 115-24.

Clarke A, Desikan R, Hurst RD, Hancock JT, Neill SJ. **2000**. NO way back: nitric oxide and programmed cell death in Arabidopsis thaliana suspension cultures. *The Plant Journal* **24**: 667-677.

Cohn J, Sessa G, Martin GB. **2001**. Innate immunity in plants. *Current opinion in immunology* **13**: 55-62.

Corpas FJ, Palma JM, del Río LA, Barroso JB. **2009**. Evidence supporting the existence of L-arginine-dependent nitric oxide synthase activity in plants. *The New phytologist* **184**: 9-14.

Correa-Aragunde N, Graziano M, Chevalier C, Lamattina L. **2006**. Nitric oxide modulates the expression of cell cycle regulatory genes during lateral root formation in tomato. *Journal of experimental botany* **57**: 581-588.

Crawford NM, Guo F. **2005**. New insights into nitric oxide metabolism and regulatory functions. *Trends in Plant Science* **10**: 195-200.

Crawford NM, Galli M, Tischner R, Heimer Y, Okamoto M, Mack A. **2006**. Response to Zemojtel et al: Plant nitric oxide synthase: back to square one. *Trends in Plant Science* **11**: 526-527.

De-Jiang F, Xiang L, Song G, Hong-lin X, Xiao-li W, Jun-wang X, Zhen Z. **2004**. Virus-induced PVX Coat Protein Gene Silencing and Methylation in Transgenic Tobaccos. *Acta Botanica Sinica* **46**: 116-123.

Dean FB, Nelson JR, Giesler TL, Lasken RS. **2001**. Rapid amplification of plasmid and phage DNA using Phi 29 DNA polymerase and multiply-primed rolling circle amplification. *Genome research* **11**: 1095-9.

Delledonne M, Xia Y, Dixon RA, Lamb C. **1998**. Nitric oxide functions as a signal in plant disease resistance. *Nature* **394**: 585-588.

Dlakić M. **2006**. DUF283 domain of Dicer proteins has a double-stranded RNA-binding fold. *Bioinformatics* **22**: 2711-2714.

Dong Z, Han M, Fedoroff N. **2008**. The RNA-binding proteins HYL1 and SE promote accurate in vitro processing of pri-miRNA by DCL1. *Proceedings of the National Academy of Sciences of the United States of America* **105**: 9970-9975.

Doyle J, Doyle JL. **1987**. A rapid DNA isolation procedure for small quantities of fresh leaf tissue. *Phytochemical Bulletin* **19**: 11-15.

Durner J, Klessig DF. **1999**. Nitric oxide as a signal in plants. *Current Opinion in Plant Biology* **2**: 369-374.

Durner J, Wendehenne D, Klessig DF. **1998**. Defense gene induction in tobacco by nitric oxide, cyclic GMP, and cyclic ADP-ribose. *Proceedings of the National Academy of Sciences of the United States of America* **95**: 10328-33.

Durrant WE, Dong X. **2004**. Systemic acquired resistance. *Annual review of phytopathology* **42**: 185-209.

Durzan D. **2002**. Stress-induced nitric oxide and adaptive plasticity in conifers. *Journal of Forest Science* **48**: 281-291.

Ekpechi OL. **1973**. Endemic goiter and high cassava diets in eastern Nigeria. In: Nestel, B, MacIntyre, R, *Proceedings of an Interdisciplinary Workshop*. London, England: International development centre, 139-145.

Elmer JS, Sunter G, Gardiner WE, Brand L, Browning CK, Bisaro DM, Rogers SG. **1988**. Agrobacterium-mediated inoculation of plants with tomato golden mosaic virus DNAs. *Plant Molecular Biology* **10**: 225-234.

Fargette D, Roberts IM, Harrison BD. **1991**. Particle purification and properties of cassava Ivorian bacilliform virus. *Annals of Applied Biology* **119**: 303-312.

Fauquet CM, Fargette D. **1990**. African Cassava Mosaic Virus: Etiology, Epidemiology, and Control. *Plant Disease* **74**: 404-411.

Fauquet CM, Stanley J. **2003**. Geminivirus classification and nomenclature: progress and problems. *Annals of Applied Biology* **142**: 165-189.

Fauquet CM, Briddon RW, Brown JK, Moriones E, Stanley J, Zerbini FM, Zhou X. **2008**. Geminivirus strain demarcation and nomenclature. *Archives of Virology* **153**: 783-821.

Fitzmaurice WP, Nguyen LV, Wernsman EA, Thompson WF, Conkling MA. **1999**. Transposon Tagging of the Sulfur Gene of Tobacco Using Engineered Maize Ac Ds Elements. *Genetics* **153**: 1919-1928.

Florentino LH, Santos AA, Zerbini FM, Fontes EP. **2008**. Begomoviruses: molecular cloning and identification of replication origin. *Methods in molecular biology (Clifton, N.J.)* **451**: 145-66.

Flores-Pérez U, Sauret-Güeto S, Gas E, Jarvis P, Rodríguez-Concepción M. **2008**. A mutant impaired in the production of plastome-encoded proteins uncovers a mechanism for the homeostasis of isoprenoid biosynthetic enzymes in Arabidopsis plastids. *The Plant Cell* **20**: 1303-15.

Fofana IB, Sangaré A, Collier R, Taylor CG, Fauquet CM. **2004**. A geminivirus-induced gene silencing system for gene function validation in cassava. *Plant Molecular Biology* **56**: 613-24.

Foissner I, Wendehenne D, Langebartels C, Durner J. **2000**. In vivo imaging of an elicitor-induced nitric oxide burst in tobacco. *The Plant Journal* **23**: 817-824.

Fondong VN, Reddy RV, Lu C, Hankoua B, Felton C, Czymmek K, Achenjang F. **2007**. The consensus N-myristoylation motif of a geminivirus AC4 protein is required for membrane binding and pathogenicity. *Molecular Plant-Microbe Interactions* **20**: 380-91.

Fontes EP, Eagle PA, Sipe PS, Luckow VA, Hanley-Bowdoin LK. **1994**. Interaction between a geminivirus replication protein and origin DNA is essential for viral replication. *The Journal of Biological Chemistry* **269**: 8459-65.

Food and Agriculture Organization. **2006**. Starch market adds value to cassava. *Agriculture, Biosecurity, Nutrition and Consumer Protection Department*.

Frischmuth T, Stanley J. **1991**. African cassava mosaic virus DI DNA interferes with the replication of both genomic components. *Virology* **183**: 539-544.

Gafni Y. **2002**. The role of host and viral proteins in intra- and inter-cellular trafficking of geminiviruses. *Physiological and Molecular Plant Pathology* **60**: 231-241.

Garcia-Brugger A, Lamotte O, Vandelle E, Bourque S, Lecourieux D, Poinssot B, Wendehenne D, Pugin A. **2006**. Early signaling events induced by elicitors of plant defenses. *Molecular Plant-Microbe Interactions* **19**: 711-24.

Garrido-Ramirez ER, Sudarshana MR, Lucas WJ, Gilbertson RL. **2000**. Bean dwarf mosaic virus BV1 Protein Is a Determinant of the Hypersensitive Response and Avirulence in Phaseolus vulgaris. *Molecular Plant-Microbe Interactions* **13**: 1184-1194.

Gas E, Flores-Pérez U, Sauret-Güeto S, Rodríguez-Concepción M. **2009**. Hunting for plant nitric oxide synthase provides new evidence of a central role for plastids in nitric oxide metabolism. *The Plant Cell* **21**: 18-23.

Gasciolli V, Mallory AC, Bartel DP, Vaucheret H. **2005**. Partially redundant functions of Arabidopsis DICER-like enzymes and a role for DCL4 in producing trans-acting siRNAs. *Current biology* **15**: 1494-500.

Golenberg EM, Sather DN, Hancock LC, Buckley KJ, Villafranco NM, Bisaro DM. **2009**. Development of a gene silencing DNA vector derived from a broad host range geminivirus. *Plant Methods* **5**: 9.

Goodin MM, Zaitlin D, Naidu RA, Lommel SA. **2008**. Nicotiana benthamiana: its history and future as a model for plant-pathogen interactions. *Molecular Plant-Microbe Interactions* **21**: 1015-26.

Gopal P, Pravin Kumar P, Sinilal B, Jose J, Kasin Yadunandam A, Usha R. **2007**. Differential roles of C4 and betaC1 in mediating suppression of post-transcriptional gene silencing: evidence for transactivation by the C2 of Bhendi yellow vein mosaic virus, a monopartite Begomovirus. *Virus Research* **123**: 9-18.

Guo F, Crawford NM. **2005**. Arabidopsis nitric oxide synthase1 is targeted to mitochondria and protects against oxidative damage and dark-induced senescence. *The Plant Cell* **17**: 3436-50.

Guo F, Okamoto M, Crawford NM. **2003**. Identification of a plant nitric oxide synthase gene involved in hormonal signaling. *Science (New York, N.Y.)* **302**: 100-3.

Gutierrez C. **2000**. DNA replication and cell cycle in plants: learning from geminiviruses. *The EMBO Journal* **19**: 792-799.

Gutierrez C. **2002**. Strategies for geminivirus DNA replication and cell cycle interference. *Physiological and Molecular Plant Pathology* **60**: 219-230.

Hahn SK, Howland AK, Terry ER. **1980**. Correlated mosaic and resistance of cassava to bacterial blight diseases. *Euphytica* **29**: 305-311.

Hahn SK, Terry ER, Leuschner K. **1980**. Breeding cassava for resistance to cassava mosaic disease. *Euphytica* **29**: 673-683.

Hanley-Bowdoin LK, Settlage SB, Robertson DN. **2004**. Reprogramming plant gene expression: a prerequisite to geminivirus DNA replication. *Molecular Plant Pathology* **5**: 149-56.

Harrison BD. **2002**. Begomovirus coat protein: serology, variation and functions. *Physiological and Molecular Plant Pathology* **60**: 257-271.

Harrison R. **2002**. Structure and function of xanthine oxidoreductase: where are we now? *Free radical biology and medicine* **33**: 774-97.

Herr AJ, Baulcombe DC. **2004**. RNA silencing pathways in plants. *Cold Spring Harbor symposia on quantitative biology* **69**: 363-70.

Heyraud-Nitschke F, Matzeit V, Schaefer S, Schell J, Gronenborn B. **1993**. The conserved nonanucleotide motif of the geminivirus stem-loop sequence promotes replicational release of virus molecules from redundant copies. *Biochimie* **75**: 605-615.

Hillocks RJ, Wydra K. **2002**. Bacterial , Fungal and Nematode. In: Hillocks, RJ, Thresh, JM, Bellotti, AC, *Cassava: Biology, Production and utilization*. CAB International, 261-280.

Himber C, Dunoyer P, Moissiard G, Ritzenthaler C, Voinnet O. **2003**. Transitivity-dependent and -independent cell-to-cell movement of RNA silencing. *The EMBO Journal* **22**: 4523-33.

Hong Y, Stanley J, Wezel RV. **2003**. Novel System for the Simultaneous Analysis of Geminivirus DNA Replication and Plant Interactions in *Nicotiana benthamiana*. *Journal of Virology* **77**: 13315-13322.

Hormuzdi SG, Bisaro DM. **1993**. Genetic analysis of beet curly top virus: evidence for three virion sense genes involved in movement and regulation of single- and double-stranded DNA levels. *Virology* **193**: 900-9.

Huang C, Xie Y, Zhou X. **2009**. Efficient virus-induced gene silencing in plants using a modified geminivirus DNA1 component. *Plant biotechnology journal* **7**: 254-65.

Hussain M, Mansoor S, Iram S, Fatima AN, Zafar Y. **2005**. The nuclear shuttle protein of Tomato leaf curl New Delhi virus is a pathogenicity determinant. *Journal of Virology* **79**: 4434-4439.

Hussain M, Mansoor S, Iram S, Zafar Y, Briddon RW. **2007**. The Hypersensitive Response to Tomato leaf curl New Delhi virus Nuclear Shuttle Protein Is Inhibited by Transcriptional Activator Protein. *Molecular Plant-Microbe Interactions* **20**: 1581-1588.

Inoue-Nagata AK, Albuquerque LC, Rocha WB, Nagata T. **2004**. A simple method for cloning the complete begomovirus genome using the bacteriophage φ29 DNA polymerase. *Journal of Virological Methods* **116**: 209-211.

Jensen PE, Willows RD, Petersen BL, Vothknecht UC, Stummann BM, Kannangara CG, von Wettstein D, Henningsen KW. **1996**. Structural genes for Mg-chelatase subunits in barley: Xantha-f, -g and -h. *Molecular and general genetics* **250**: 383-94.

Jin M, Li C, Shi Y, Ryabov E, Huang J, Wu Z, Fan Z, Hong Y. **2008**. A single amino acid change in a geminiviral Rep protein differentiates between triggering a plant defense response and initiating viral DNA replication. *Journal of General Virology* **89**: 2636-41.

Johne R, Müller H, Rector A, van Ranst M, Stevens H. **2009**. Rolling-circle amplification of viral DNA genomes using phi29 polymerase. *Trends in Microbiology* **17**: 205-11.

Jones JD, Dangl JL. **2006**. The plant immune system. *Nature* **444**: 323-9.

Jones L, Thomas CL, Maule AJ. **1998**. De novo methylation and co-suppression induced by a cytoplasmically replicating plant RNA virus. *EMBO Journal* **17**: 6385-6393.

Jorgensen RA, Cluster PD, English J, Que Q, Napoli CA. **1996**. Chalcone synthase cosuppression phenotypes in petunia flowers: comparison of sense vs. antisense constructs and single-copy vs. complex T-DNA sequences. *Plant Molecular Biology* **31**: 957-973.

Kalantidis K, Schumacher HT, Alexiadis T, Helm JM. **2008**. RNA silencing movement in plants. *Biology of the cell* **100**: 13-26.

Kato H, Asai S, Yamamoto-Katou A, Yoshioka H, Doke N, Kawakita K. **2007**. Involvement of NbNOA1 in NO production and defense responses in INF1-treated Nicotiana benthamiana. *Journal of General Plant Pathology* **74**: 15-23.

Kjemtrup S, Sampson KS, Peele CG, Nguyen LV, Conkling MA, Thompson WF, Robertson DN. **1998**. Gene silencing from plant DNA carried by a geminivirus. *The Plant Journal* **14**: 91-100.

Knierim D, Maiss E. **2007**. Application of Phi29 DNA polymerase in identification and full-length clone inoculation of tomato yellow leaf curl Thailand virus and tobacco leaf curl Thailand virus. *Archives of Virology* **152**: 941-54.

Kruse E, Mock H, Grimm B. **1997**. Isolation and characterization of tobacco (Nicotiana tabacum) cDNA clones encoding proteins involved in magnesium chelation into protoporphyrin IX. *Plant Molecular Biology* **35**: 1053-1056.

Kumagai MH, Donson J, Della-Cioppa G, Harvey D, Grill LK, Hanley-Bowdoin LK. **1995**. Cytoplasmic inhibition of carotenoid biosynthesis with virus-derived RNA. *Proceedings of the National Academy of Sciences of the United States of America* **92**: 1679-1683.

Kumakura N, Takeda A, Fujioka Y, Motose H, Takano R, Watanabe Y. **2009**. SGS3 and RDR6 interact and colocalize in cytoplasmic SGS3/RDR6-bodies. *FEBS letters* **583**: 1261-1266.

Lamotte O, Courtois C, Barnavon L, Pugin A, Wendehenne D. **2005**. Nitric oxide in plants: the biosynthesis and cell signaling properties of a fascinating molecule. *Planta* **221**: 1-4.

Latham JR, Saunders K, Pinner MS, Stanley J. **1997**. Induction of plant cell division by beet curly top virus gene C4. *The Plant Journal* **11**: 1273-1283.

Lazarowitz SG, Wu LC, Rogers SG, Elmer JS. **1992**. Sequence-Specific interaction with the Vira1 ALI Protein identifies a Geminivirus DNA Replication Origin. *The Plant Cell* **4**: 799-809.

Leitner M, Vandelle E, Gaupels F, Bellin D, Delledonne M. **2009**. NO signals in the haze Nitric oxide signaling in plant defense. *Current Opinion in Plant Biology* **12**: 451-458.

Lindbo JA, Fitzmaurice WP, Della-Cioppa G. **2001**. Virus-mediated reprogramming of gene expression in plants. *Current opinion in plant biology* **4**: 181-5.

Lindbo JA, Silva-Rosales L, Proebsting WM, Dougherty WG. **1993**. Induction of a Highly Specific Antiviral State in Transgenic Plants: implications for Regulation of Gene Expression and Virus Resistance. *The Plant Cell* **5**: 1749-1759.

Liu Y, Schiff M, Czymmek K, Levine B, Haven N. **2005**. Autophagy regulates programmed cell death during the plant innate immune response. *Cell* **121**: 567-77.

Lu R, Malcuit I, Moffett P, Ruiz MT, Peart J, Wu A, Rathjen JP, Day L, Baulcombe DC. **2003**. High throughput virus-induced gene silencing implicates heat shock protein 90 in plant disease resistance. *EMBO Journal* **22**: 5690-5699.

Luttrell WE. **2009**. Cyanogen bromide. *Journal of Chemical Health and Safety* **16**: 29-30.

Mansoor S, Khan SH, Bashir A, Saeed M, Zafar Y, Malik KA, Briddon RW. **1999**. Identification of a novel circular single-stranded DNA associated with cotton leaf curl disease in Pakistan. *Virology* **259**: 190-199.

Matzke M, Kanno T, Daxinger L, Huettel B, Matzke AJ. **2009**. RNA-mediated chromatin-based silencing in plants. *Current opinion in cell biology* **21**: 367-76.

Mayer B, Hemmens B. **1997**. Biosynthesis and action of nitric oxide in mammalian cells. *Trends in biochemical sciences* **22**: 477-481.

Mette MF, Aufsatz W, Winden VD, J. M, M.a, Matzke AJ. **2000**. Transcriptional silencing and promoter methylation triggered by double-stranded RNA. *The EMBO Journal* **19**: 5194-5201.

Metzlaff M, O'dell M, Cluster P, Flavell R. **1997**. RNA-Mediated RNA Degradation and Chalcone Synthase A Silencing in Petunia. *Cell* **88**: 845–854.

Modolo LV, Cunha FQ, Braga R, Salgado I. **2002**. Nitric oxide synthase-mediated phytoalexin accumulation in soybean cotyledons in response to the Diaporthe phaseolorum f. sp. meridionalis elicitor. *Plant Physiology* **130**: 1288.

Moncada S, Palmer RM, Higgs EA. **1989**. Biosynthesis A Pathway For Of Nitric Oxide From L-Arginine The Regulation Of Cell Function And Communication. *Biochemical Pharmacology* **38**: 1709-1715.

Montagnac JA, Davis CR, Tanumihardjo SA. **2009**. Processing Techniques to Reduce Toxicity and Antinutrients of Cassava for Use as a Staple Food. *Comprehensive Reviews in Food Science and Food Safety* **8**: 17-27.

Moreau M, Lee GI, Wang Y, Crane BR, Klessig DF. **2008**. AtNOS/AtNOA1 is a functional Arabidopsis thaliana cGTPase and not a nitric-oxide synthase. *The Journal of Biological Chemistry* **283**: 32957-67.

Muangsan N, Beclin C, Vaucheret H, Robertson DN. **2004**. Geminivirus VIGS of endogenous genes requires SGS2/SDE1 and SGS3 and defines a new branch in the genetic pathway for silencing in plants. *The Plant Journal* **38**: 1004-1014.

Mur LA, Carver TL, Prats E. **2006**. NO way to live; the various roles of nitric oxide in plant-pathogen interactions. *Journal of Experimental Botany* **57**: 489-505.

Mur LA, Kenton P, Lloyd AJ, Ougham H, Prats E. **2008**. The hypersensitive response; the centenary is upon us but how much do we know? *Journal of experimental botany* **59**: 501-20.

Murashige T, Skoog F. **1962**. A Revised Medium for Rapid Growth and Bio Assays with Tobacco Tissue Cultures. *Physiologia Plantarum* **15**: 473-497.

Nagar S, Pedersen TJ, Carrick KM, Hanley-Bowdoin LK, Robertson DN. **1995**. A Geminivirus lnduces Expression of a Host DNA Synthesis Protein in Terminally Differentiated Plant Cells. *The Plant Cell* **7**: 705-719.

Nagaraj SH, Gasser RB, Ranganathan S. **2007**. A hitchhiker's guide to expressed sequence tag (EST) analysis. *Briefings in bioinformatics* **8**: 6-21.

Napoli CA, Lemieux C, Jorgensen RA. **1990**. Introduction of a Chimeric Chalcone Synthase Gene into Petunia Results in Reversible Co-Suppression of Homologous Genes in trans. *The Plant Cell* **2**: 279-289.

Nawaz-ul-rehman MS, Fauquet CM. **2009**. Evolution of geminiviruses and their satellites. *FEBS Letters* **583**: 1825-1832.

Ndunguru J, Legg JP, Aveling TA, Thompson G, Fauquet CM. **2005**. Molecular biodiversity of cassava begomoviruses in Tanzania: evolution of cassava geminiviruses in Africa and evidence for East Africa being a center of diversity of cassava geminiviruses. *Virology Journal* **2**: 21.

Neill SJ, Desikan R, Clarke A, Hancock J. **2002**. Nitric oxide is a novel component of abscisic acid signaling in stomatal guard cells. *Plant Physiology* **128**: 13-16.

Neill SJ, Desikan R, Hancock JT. **2003**. Nitric oxide signalling in plants. *The New Phytologist* **159**: 11-35.

Nestel B. **1973**. Current utilization and future potential for cassava. In: Nestel, B, MacIntyre, R, *Proceedings of an Interdisciplinary Workshop*. London: International development centre, 11-26.

Okigbo BN. **1980**. Nutritional implications of projects giving high priority to the production of staples of low nutritive quality: The Case for Cassava (Manihot esculenta, Crantz) in the Humid Tropics of West Africa. *Africa* **4**: Accessed 08.09.09.

Osuntokun B. **1973**. Ataxic neuropathy associated with high cassava diets. In: Nestel, B, MacIntyre, R, *Proceedings of an Interdisciplinary Workshop*. London: International development centre, 127-138.

Padidam M, Beachy RN, Fauquet CM. **1996**. The role of AV2 ("precoat") and coat protein in viral replication and movement in tomato leaf curl geminivirus. *Virology* **224**: 390-404.

Pandey P, Choudhury NR, Mukherjee SK. **2009**. A geminiviral amplicon (VA) derived from Tomato leaf curl virus (ToLCV) can replicate in a wide variety of plant species and also acts as a VIGS vector. *Virology Journal* **6**: 152.

Parani M, Rudrabhatla S, Myers R, Weirich H, Smith B, Leaman DW, Goldman SL. **2004**. Microarray analysis of nitric oxide responsive transcripts in Arabidopsis. *Plant biotechnology journal* **2**: 359-66.

Park W, Li J, Song R, Messing J, Chen X. **2002**. CARPEL FACTORY, a Dicer homolog, and HEN1, a novel protein, act in microRNA metabolism in Arabidopsis thaliana. *Current biology* **12**: 1484-95.

Patil BL, Dasgupta I. **2006**. Defective interfering DNAs of plant viruses. *Crit. Rev. Plant Sci* **25**: 47-64.

Peele CG, Jordan CV, Muangsan N, Turnage MA, Egelkrout E, Eagle PA, Hanley-Bowdoin LK, Robertson DN. **2001**. Silencing of a meristematic gene using geminivirus-derived vectors. *The Plant Journal* **27**: 357-366.

Peragine A, Yoshikawa M, Wu G, Albrecht HL, Poethig RS. **2004**. SGS3 and SGS2/SDE1/RDR6 are required for juvenile development and the production of trans-acting siRNAs in Arabidopsis. *Genes and development* **18**: 2368-79.

Pfaffl MW, Horgan G, Dempfle L. **2002**. Relative expression software tool (REST (C)) for group-wise comparison and statistical analysis of relative expression results in real-time PCR. *Nucleic Acids Research* **30**: e36.

Polverari A, Molesini B, Pezzotti M, Buonaurio R, Marte M, Delledonne M. **2003**. Nitric Oxide-Mediated Transcriptional Changes in Arabidopsis thaliana. *Molecular Plant-Microbe Interactions* **16**: 1094-1105.

Porebski S, Bailey LG, Baum BR. **1997**. Modification of a CTAB DNA extraction protocol for plants containing high polysaccharide and polyphenol components. *Plant Molecular Biology Reporter* **15**: 8-15.

Prats E, Mur LA, Sanderson R, Carver TL. **2005**. Nitric oxide contributes both to papilla-based resistance and the hypersensitive response in barley attacked by Blumeria graminis f. sp. hordei. *Molecular Plant Pathology* **6**: 65-78.

Purkayastha A, Dasgupta I. **2009**. Virus-induced gene silencing: a versatile tool for discovery of gene functions in plants. *Plant Physiology and Biochemistry* **47**: 967-76.

Qian Y, Mugiira RB, Zhou X. **2006**. A modified viral satellite DNA-based gene silencing vector is effective in association with heterologous begomoviruses. *Virus Research* **118**: 136-42.

Qiao W, Xiao S, Yu L, Fan L. **2009**. Expression of a rice gene OsNOA1 re-establishes nitric oxide synthesis and stress-related gene expression for salt tolerance in Arabidopsis nitric oxide-associated 1 mutant Atnoa1. *Environmental and Experimental Botany* **65**: 90-98.

Qin S, Ward B, Lazarowitz S. **1998**. The bipartite geminivirus coat protein aids BR1 function in viral movement by affecting the accumulation of viral single-stranded DNA. *Journal of Virology* **72**: 9247-9256.

Qu F, Ye X, Morris TJ. **2008**. Arabidopsis DRB4, AGO1, AGO7, and RDR6 participate in a DCL4-initiated antiviral RNA silencing pathway negatively regulated by DCL1. *Proceedings of the National Academy of Sciences of the United States of America* **105**: 14732-7.

Rajeswaran R, Sunitha S, Shivaprasad PV, Pooggin MM, Hohn T, Veluthambi K. **2007**. The mungbean yellow mosaic begomovirus transcriptional activator protein transactivates the viral promoter-driven transgene and causes toxicity in transgenic tobacco plants. *Molecular Plant-Microbe Interactions* **20**: 1545-54.

Ratcliff FG, Harrison BD, Baulcombe DC. **1997**. A similarity between viral defense and gene silencing in plants. *Science (New York, N.Y.)* **276**: 1558-1560.

Ratcliff FG, Macfarlane SA, Baulcombe DC. **1999**. Gene Silencing without DNA: RNA-Mediated Cross-Protection between Viruses. *The Plant Cell* **11**: 1207-1215.

Ratcliff FG, Martin-hernandez AM, Baulcombe DC. **2001**. Tobacco rattle virus as a vector for analysis of gene function by silencing. *The Plant Journal* **25**: 237-245.

Ravindran G, Ravindran V. **1988**. Changes in the nutritional composition of cassava (Manihot esculenta Crantz) leaves during maturity. *Food Chemistry* **27**: 299-309.

Ribeiro Jr EA, Cunha FQ, Tamashiro WM, Martins IS. **1999**. Growth phase-dependent subcellular localization of nitric oxide synthase in maize cells. *FEBS letters* **445**: 283-6.

Roberts IM, Robinson DJ, Harrison BD. **1984**. Serological Relationships and Genome Homologies among Geminiviruses. *Journal of General Virology* **65**: 1723-1730.

Robertson DN. **2004**. VIGS vectors for gene silencing: many targets, many tools. *Annual review of plant biology* **55**: 495-519.

Rojas MR, Gilbertson RL, Russell DR, Maxwell DP. **1993**. Use of degenerate primers in the polymerase chain reaction to detect whitefly-transmitted geminivirus. *Plant Disease* **77**: 340-347.

Ruiz MT, Voinnet O, Baulcombe DC. **1998**. Initiation and Maintenance of Virus-Induced Gene Silencing Gene Silencing. *The Plant Cell* **10**: 937-946.

Rybicki EP. **1994**. A phylogenetic and evolutionary justification for three genera of Geminiviridae. *Archives of Virology* **139**: 49-77.

Sakurai T, Rodr F, Seki M, Toyoda A, Ishiwata A, Tohme J, Sakaki Y, Shinozaki K, Ishitani M. **2007**. Sequencing analysis of 20000 full length cDNA clones from cassava reveals a lineage specific expansions in gene families related to stress response. *BMC Plant Biology* **7**.

Sambrook J, Fritsch E, Maniatis T. **1989**. *Molecular cloning: a laboratory manual*. New York: Cold Spring Harbor Laboratory Press.

Sanford J, Johnston S. **1985**. The concept of parasite-derived resistance: Deriving resistance genes from the parasite's own genome. *Journal of Theoretical Biology* **113**: 395-405.

Saunders K, Bedford ID, Briddon RW, Markham PG, Wong SM, Stanley J. **2000**. A unique virus complex causes Ageratum yellow vein disease. *Proceedings of the National Academy of Sciences of the United States of America* **97**: 6890-6895.

Saunders K, Norman A, Gucciardo S, Stanley J. **2004**. The DNA B satellite component associated with ageratum yellow vein disease encodes an essential pathogenicity protein (BC1). *Virology* **324**: 37-47.

Schauer SE, Jacobsen SE, Meinke DW, Ray A. **2002**. DICER-LIKE1: Blind men and elephants in Arabidopsis development. *Trends in Plant Science* **7**: 487-491.

Schmittgen TD, Livak KJ. **2008**. Analyzing real-time PCR data by the comparative CT method. *Nature Protocols* **3**: 1101-1108.

Selth LA, Randles JW, Rezaian MA. **2004**. Host responses to transient expression of individual genes encoded by Tomato leaf curl virus. *Molecular Plant-Microbe Interactions* **17**: 27-33.

Senthil-Kumar M, Hema R, Anand A, Kang L, Udayakumar M, Mysore KS. **2007**. A systematic study to determine the extent of gene silencing in Nicotiana benthamiana and other Solanaceae species when heterologous gene sequences are used for virus-induced gene silencing. *The New phytologist* **176**: 782-91.

Shao Y, Zhu HL, Tian HQ, Wang XG, Lin XJ, Zhu BZ, Xie YH, Luo YB. **2008**. Virus-Induced Gene Silencing in Plant Species. *Russian Journal of Plant Physiology* **55**: 168-174.

Sharma P, Ikegami M. **2010**. Tomato leaf curl Java virus V2 protein is a determinant of virulence, hypersensitive response and suppression of posttranscriptional gene silencing. *Virology* **396**: 85-93.

Shepherd DN, Martin DP, Lefeuvre P, Owor BE, Rybicki EP, Varsani A. **2008**. A protocol for the rapid isolation of full geminivirus genomes from dried plant tissue. *Journal of Virological Methods* **149**: 97-102.

Shivaprasad PV, Akbergenov R, Trinks D, Rajeswaran R, Veluthambi K, Hohn T, Pooggin MM. **2005**. Promoters, transcripts, and regulatory proteins of Mungbean yellow mosaic geminivirus. *Journal of Virology* **79**: 8149-63.

Sijen T, Vijn I, Recbocho A, Blokland RV, Roelofs D, Mol JN, Kootere JM. **2001**. Transcriptional and posttranscriptional gene silencing are mechanistically related. *Current Biology* **11**: 436-440.

Siritunga D, Sayre R. **2004**. Engineering cyanogen synthesis and turnover in cassava (Manihot esculenta). *Plant Molecular Biology* **56**: 661-669.

Smith LM, Pontes O, Searle I, Yelina N, Yousafzai FK, Herr AJ, Pikaard CS, Baulcombe DC. **2007**. An SNF2 protein associated with nuclear RNA silencing and the spread of a silencing signal between cells in Arabidopsis. *The Plant Cell* **19**: 1507-21.

Smith NA, Singh SP, Wang M, Stoutjesdijk PA, Green AG, Waterhouse PM. **2000**. Total silencing by intron-spliced hairpin RNAs. *Nature* **407**: 319-320.

Song F, Goodman RM. **2001**. Activity of Nitric Oxide Is Dependent On, But Is Partially Required for Function of, Salicylic Acid in the Signaling Pathway in Tobacco Systemic Acquired Resistance. *Molecular Plant-Microbe Interactions* **14**: 1458-1462.

Soosaar JL, Burch-smith TM, Dinesh-kumar SP. **2005**. Mechanisms of plant resistance to viruses. *Nature reviews. Microbiology* **3**: 789-798.

Sozzani R, Lee T, Chu T, Cella R, Hanley-Bowdoin LK. **2008**. Global Analysis of Arabidopsis Gene Expression Uncovers a Complex Array of Changes Impacting Pathogen Response and Cell Cycle during Geminivirus Infection. *Plant Physiology* **148**: 436-454.

Stanley J, Townsend R. **1985**. Characterisation of DNA forms associated with cassava latent virus infection. *Nucleic Acids Research* **13**: 2189-2206.

Stemmer WP, Crameri a, Ha KD, Brennan TM, Heyneker HL. **1995**. Single-step assembly of a gene and entire plasmid from large numbers of oligodeoxyribonucleotides. *Gene* **164**: 49-53.

Stenger DC, Revington GN, Stevenson MC, Bisaro DM. **1991**. Replicational release of geminivirus genomes from tandemly repeated copies: evidence for rolling-circle replication of a plant viral DNA. *Proceedings of the National Academy of Sciences of the United States of America* **88**: 8029-8033.

Stöhr C, Strube F, Marx G, Ullrich W, Rockel P. **2001**. A plasma membrane-bound enzyme of tobacco roots catalyses the formation of nitric oxide from nitrite. *Planta* **212**: 835-841.

Sudhamsu J, Lee GI, Klessig DF, Crane BR. **2008**. The structure of YqeH. An AtNOS1/AtNOA1 ortholog that couples GTP hydrolysis to molecular recognition. *The Journal of Biological Chemistry* **283**: 32968-76.

Sunter G, Bisaro DM, Hertitz MD, Hormuzdi SG, Brough CL. **1990**. Genetic analysis of tomato golden mosaic virus: ORF AL2 is required for coat protein accumulation while ORFAL3 is necessary for efficient DNA replication. *Virology* **179**: 69-77.

Tao X, Zhou X. **2004**. A modified viral satellite DNA that suppresses gene expression in plants. *The Plant Journal* **38**: 850-60.

Taylor N, Chavarriaga P, Raemakers K, Siritunga D. **2004**. Development and application of transgenic technologies in cassava. *Plant Molecular Biology* **56**: 671-688.

Tewe OO. **2004**. An overview of cassava in sub-saharan africa. In: Lutaladio, N, *Cassava for livestock feed in sub-Saharan Africa*. Ibadan, Nigeria: Food and agricultural organisation, 1-5.

Thakur A. **2003**. RNA interference revolution. *Electronic Journal of Biotechnology* **6**.

Trinks D, Rajeswaran R, Shivaprasad PV, Akbergenov R, Oakeley EJ, Veluthambi K, Hohn T, Pooggin MM. **2005**. Suppression of RNA silencing by a geminivirus nuclear protein, AC2, correlates with transactivation of host genes. *Journal of Virology* **79**: 2517-2527.

Turnage MA, Muangsan N, Peele CG, Robertson DN. **2002**. Geminivirus-based vectors for gene silencing in Arabidopsis. *The Plant Journal* **30**: 107-14.

Tuttle JR, Idris AM, Brown JK, Haigler CH, Robertson DN. **2008**. Geminivirus-Mediated Gene Silencing from Cotton Leaf Crumple Virus Is Enhanced by Low Temperature in Cotton. *Plant Physiology* **148**: 41-50.

Tylleskär T, Banea M, Bikangi N, Cooke R, Poulter NH, Rosling H. **1992**. Cassava cyanogens and konzo, an upper motoneuron disease found in Africa. *The Lancet* **339**: 208-211.

Unseld S, Hohnle M, Ringel M, Frischmuth T. **2001**. Subcellular Targeting of the Coat Protein of African Cassava Mosaic Geminivirus. *Virology* **383**: 373-383.

Unver T, Budak H. **2009**. Virus-Induced Gene Silencing, a Post Transcriptional Gene Silencing Method. *International journal of plant genomics* **2009**: Article ID 198680.

Vaistij FE, Jones L. **2009**. Compromised Virus-Induced Gene Silencing in RDR6-Deficient Plants. *Plant Physiology* **149**: 1399-1407.

Van Kammen A. **1997**. Virus-induced gene silencing in infected and transgenic plants. *Trends in Plant Science* **2**: 409-411.

Vanitharani R, Chellappan P, Pita JS, Fauquet CM. **2004**. Differential roles of AC2 and AC4 of cassava geminiviruses in mediating synergism and suppression of posttranscriptional gene silencing. *Journal of Virology* **78**: 9487-9498.

Vanitharani R, Chellappan P, Fauquet CM. **2005**. Geminiviruses and RNA silencing. *Trends in Plant Science* **10**: 144–151.

Varma A, Malathi V. **2003**. Emerging geminivirus problems: a serious threat to crop production. *Annals of Applied Biology* **142**: 145–164.

Vaucheret H. **2008**. Plant ARGONAUTES. *Trends in Plant Science* **13**: 350-8.

Vazquez F, Vaucheret H, Rajagopalan R, Lepers C, Gasciolli V, Mallory AC, Hilbert J, Bartel DP, Crété P. **2004**. Endogenous trans-acting siRNAs regulate the accumulation of Arabidopsis mRNAs. *Molecular cell* **16**: 69-79.

Verkest A, Manes CD, Vercruysse S, Maes S, Van Der Schueren E, Beeckman T, Genschik P, Kuiper M, Inzé D, De Veylder L. **2005**. The cyclin-dependent kinase inhibitor KRP2 controls the onset of the endoreduplication cycle during Arabidopsis leaf development through inhibition of mitotic CDKA;1 kinase complexes. *The Plant Cell* **17**: 1723-36.

Walker CJ, Weinstein JO. **1991**. In vitro assay of the chlorophyll biosynthetic enzyme Mg-chelatase: Resolution of the activity into soluble and membrane- bound fractions. *Proceedings of the National Academy of Sciences of the United States of America* **88**: 5789-5793.

Wang M, Metzlaff M. **2005**. RNA silencing and antiviral defense in plants. *Current Opinion in Plant Biology* **8**: 216-222.

Ward BM, Lazarowitz SG. **1999**. Nuclear export in plants. Use of geminivirus movement proteins for a cell-based export assay. *The Plant Cell* **11**: 1267-76.

Wassenegger M, Heimes S, Riedel L, Sanger HL. **1994**. RNA-directed de novo methylation of genomic sequences in plants. *Cell* **76**: 567-576.

Waterhouse PM, Graham MW, Ming-Bo W. **1998**. Virus resistance and gene silencing in plants can be induced by simultaneous expression of sense and antisense RNA. *Proceedings of the National Academy of Sciences of the United States of America* **95**: 13959-13964.

Wendehenne D, Durner J, Klessig DF. **2004**. Nitric oxide: a new player in plant signalling and defense responses. *Current opinion in plant biology* **7**: 449-55.

Wendehenne D, Pugin A, Klessig D, Durner J. **2001**. Nitric oxide: comparative synthesis and signaling in animal and plant cells. *Trends in Plant Science* **6**: 177-183.

Wesley SV, Helliwell Ca, Smith NA, Wang MB, Rouse DT, Liu Q, Gooding PS, Singh SP, Abbott D, Stoutjesdijk Pa, Robinson SP, Gleave aP, Green aG, Waterhouse PM. **2001**. Construct design for efficient, effective and high-throughput gene silencing in plants. *The Plant Journal* **27**: 581-90.

Wezel RV, Dong X, Liu H, Tien P, Stanley J, Hong Y. **2002**. Mutation of three cysteine residues in Tomato yellow leaf curl virus-China C2 protein causes dysfunction in pathogenesis and posttranscriptional gene-silencing suppression. *Molecular Plant-Microbe Interactions* **15**: 203-8.

White W, Arias-Garzon D, McMahon J, Sayre R. **1998**. Cyanogenesis in cassava. The role of hydroxynitrile lyase in root cyanide production. *Plant Physiology* **116**: 1219-25.

Wong ML, Medrano JF. **2005**. Real-time PCR for mRNA quantitation. *The Plant Cell* **39**: 1-11.

Wu F, Yu L, Cao W, Mao Y, Liu Z, He Y. **2007**. The N-terminal double-stranded RNA binding domains of Arabidopsis HYPONASTIC LEAVES1 are sufficient for pre-microRNA processing. *The Plant Cell* **19**: 914-25.

Wydra K, Verdier V. **2002**. Occurrence of cassava diseases in relation to environmental, agronomic and plant characteristics. *Science* **93**: 211-226.

Xie Z, Allen E, Wilken A, Carrington JC. **2005**. DICER-LIKE 4 functions in trans-acting small interfering RNA biogenesis and vegetative phase change in Arabidopsis thaliana. *Proceedings of the National Academy of Sciences of the United States of America* **102**: 12984-9.

Xu P, Zhang Y, Kang L, Roossinck MJ, Mysore KS, Division PB, Samuel T, Noble R. **2006**. Computational Estimation and Experimental Verification of Off-Target Silencing during Posttranscriptional Gene Silencing in Plants. *Plant Physiology* **142**: 429-440.

Yang Z, Ebright YW, Yu B, Chen X. **2006**. HEN1 recognizes 21-24 nt small RNA duplexes and deposits a methyl group onto the 2' OH of the 3' terminal nucleotide. *Nucleic Acids Research* **34**: 667-75.

Yoshioka H, Numata N, Nakajima K, Katou S, Kawakita K, Rowland O, Jones JD, Doke N. **2003**. Nicotiana benthamiana gp91 phox Homologs NbrbohA and NbrbohB Participate in H2O2 Accumulation and Resistance to Phytophthora infestans. *The Plant Cell* **15**: 706-718.

Zaninotto F, La Camera S, Polverari A, Delledonne M. **2006**. Cross talk between reactive nitrogen and oxygen species during the hypersensitive disease resistance response. *Plant Physiology* **141**: 379-83.

Zeidler D, Zähringer U, Gerber I, Dubery I, Hartung T, Bors W, Hutzler P, Durner J. **2004**. Innate immunity in Arabidopsis thaliana: lipopolysaccharides activate nitric oxide synthase (NOS) and induce defense genes. *Proceedings of the National Academy of Sciences of the United States of America* **101**: 15811-6.

Zeier J, Delledonne M, Mishina T, Severi E, Sonoda M, Lamb C. **2004**. Genetic Elucidation of Nitric Oxide Signaling in Incompatible Plant-Pathogen Interactions. *Plant Physiology* **136**: 2875-2886.

Zemojtel T, Fröhlich A, Palmieri MC, Kolanczyk M, Mikula I, Wyrwicz LS, Wanker EE, Mundlos S, Vingron M, Martasek P, Durner J. **2006**. Plant nitric oxide synthase: a never-ending story? *Trends in Plant Science* **11**: 524-5; author reply 526-8.

Zemojtel T, Penzkofer T, Dandekar T, Schultz JC. **2004**. A novel conserved family of nitric oxide synthase? *Trends in biochemical sciences* **29**: 224-226.

Zhang P, Vanderschuren H, Fütterer J, Gruissem W. **2005**. Resistance to cassava mosaic disease in transgenic cassava expressing antisense RNAs targeting virus replication genes. *Plant biotechnology journal* **3**: 385-97.

Zhou Y, Garrido-Ramirez ER, Sudarshana MR, Yendluri S, Gilbertson RL. **2007**. The N-terminus of the Begomovirus nuclear shuttle protein (BV1) determines virulence or avirulence in Phaseolus vulgaris. *Molecular Plant-Microbe Interactions* **20**: 1523-34.

Zhu J. **2008**. Reconstituting plant miRNA biogenesis. *Proceedings of the National Academy of Sciences of the United States of America* **105**: 9851-2.

van Der Krol AR, Mur LA, Beld M, Mol JN, Stuitje AR. **1990**. Number of Gene Copies May Lead to a Suppression of. *The Plant Cell* **2**: 291-299.

van Wezel R, Dong X, Blake P, Stanley J, Hong Y. **2002**. Differential roles of geminivirus Rep and AC4 (C4) in the induction of necrosis in Nicotiana benthamiana. *Molecular Plant Pathology* **3**: 461-71.